DEVELOPMENT OF A LIGHT-COMMERCIAL COMPRESSOR LOAD STAND TO MEASURE COMPRESSOR PERFORMANCE USING LOW-GWP REFRIGERANTS

By
DREW D. SCHMIDT
Bachelor of Science in Mechanical Engineering
Oklahoma State University
Stillwater, OK
2016

Submitted to the Faculty of the
Graduate College of the
Oklahoma State University
in partial fulfillment of
the requirements for
the Degree of
MASTER OF SCIENCE
December, 2018

DEVELOPMENT OF A LIGHT-COMMERCIAL COMPRESSOR LOAD STAND TO MEASURE COMPRESSOR PERFORMANCE USING LOW-GWP REFRIGERANTS

Thesis Approved:

Dr. Craig Bradshaw

Thesis Advisor

Dr. Christian Bach

Dr. Jeffrey Spitler

ACKNOWLEDGMENTS

Throughout the whole duration of this project, many faculty, students, and Oklahoma State employees graciously supported and assisted myself, giving their time and effort to help with the completion of the compressor load stand.

First, I would like to thank my parents for allowing me to have this opportunity, and for supporting me throughout my undergraduate and graduate career at Oklahoma State.

I would like to thank Drs Craig Bradshaw and Christian Bach for everything they have done. Their guidance and patience are greatly appreciated, and the success of this project is due to the time and mentor ship I have received from them over the past two and a half years. Dr. Bach is the reason I am in BETSRG, and I am always thankful I got to be a part of this amazing thermal systems research group. Dr. Bradshaw's support and trust in my work gave me the confidence to keep working even when difficult problems arose.

I would also like to thank the other graduate students in BETSRG that I have worked alongside with. Their willingness to give a helping hand, or to offer their opinions on problems never went unnoticed. The friendly and comforting work atmosphere I have found in my office made working with these guys a breeze.

The support of Gary Thacker and Gerry Battles is a huge reason the load stand was completed. I thank Gary for his advice, patience, and willingness to help with all the electrical and other various components on the load stand. I thank Gerry for his help with brazing, and for his help with the building chilled water lines. The

Acknowledgments reflect the views of the author and are not endorsed by committee members or Oklahoma State University.

guidance of Gary, Gerry, and Patrick Wheeler made possible the fast construction of the mezzanine.

I would also like to thank Jake Singleton with his assistance on the load stand. His help with every aspect of the load stand construction, and his work on the load stand wiring and controls are a huge reason the load stand works today. It was a privilege to be able to work alongside Jake everyday, and his countless hours put into this project has made it a success.

Lastly, I would like to thank Wayne Kiner and the Bioystems and Agricultural lab for their help with machining some flanges and copper fittings. I thank Gerrod Forquer and Facilites Management for their help brazing some difficult components.

Acknowledgments reflect the views of the author and are not endorsed by committee members or Oklahoma State University.

Name: DREW D. SCHMIDT

Date of Degree: DECEMBER, 2018

Title of Study: DEVELOPMENT OF A LIGHT-COMMERCIAL COMPRESSOR LOAD STAND TO MEASURE COMPRESSOR PERFORMANCE USING LOW-GWP REFRIGERANTS

Major Field: MECHANICAL ENGINEERING

Abstract: Popular hydrofluorocarbon refrigerants such as R134a and R410A are in the process of being phased out due to the high Global Warming Potential (GWP) of these fluids. A large variety of low-GWP refrigerants are being considered as replacements including R1234yf, R1234ze(E), R1234ze(D), R32, and blends of these with traditional refrigerants. As a result of high efficiency standards for HVAC&R equipment, the choice of refrigerant has a large impact on the design of a compressor to maximize its efficiency. Therefore, changing the most common refrigerants will require significant design changes to compressors and test environments that support re-design activities such as a hot-gas bypass compressor load stand. The hot-gas bypass style is a common system design to test compressors and is used for its many benefits, including rapid transition between testing conditions and low operational cost. A thermodynamic model of a hot-gas bypass cycle has been developed in Engineering Equation Solver (EES). Outputs from this model were used to select the components and tubing sizes in combination with ASHRAE guidelines. The design capacity for the load stand is a range of 10-80 tons (35-281 kW) compressor capacity. The large range in capacities desired created many design challenges to overcome including maintaining proper oil circulation and refrigerant velocity. The compressor load stand is capable of testing the performance of different compressors over a range of operating conditions. It also includes independent control over oil circulation/injection rate as well as a dedicated economizer circuit. These capabilities can then be used to optimize a wide spectrum of compressor types on low-GWP refrigerants. Ultimately, the load stand serves as a new addition to the thermal systems research infrastructure at Oklahoma State University. This allows for the continuation of research into new compressor technologies, as well as, for improvements in compressor efficiency in existing technologies.

TABLE OF CONTENTS

Chapter Page

LIST OF TABLES

LIST OF FIGURES

Figure Page

Figure Page

Figure Page

NOMENCLATURE

$\dot{m}$ ..... Refrigerant mass flow rate (kg hr^{-1})
h ..... Specific enthalpy (kJ kg^{-1})
$\dot{V}$ ..... Refrigerant volume flow rate (m^3 h^{-1})
n ..... Compressor rotational speed (rev min^{-1})
v_d ..... Volume displacement (cm^3 rev^{-1})
α ..... Kinetic energy coefficient
$\bar{V}$ ..... Average velocity (ft s^{-1})
$\bar{X}_i$ ..... Measured parameter average
δ ..... The change in parameter
$\dot{m}_c$ ..... Refrigerant mass flow rate through the condensers (kg hr^{-1})
$\dot{Q}_{hr}$ ..... Heat rejection from load stand (kW)
$\dot{W}$ ..... Compressor power (kW)
η ..... Efficiency
ω ..... Compressor rotational speed (Hz)
ρ ..... Density (kg m^{-3})
$\theta_{i'}$ ..... Relative sensitivity coefficient
b_R ..... Absolute systematic standard uncertainty of R
$b_{\bar{x}_i}$ ..... Systematic standard uncertainty of the measured parameter
Cv ..... Flow coefficient
D ..... Pipe diameter (ft)
f ..... Friction factor
g ..... Gravity (ft s^{-2})
h_l ..... Major loss (ft^2 s^{-2})
$h_{2,s}$ ..... Specific enthalpy of isentropic process (kJ kg^{-1})
h_{lm} ..... Minor loss
K ..... Loss coefficient
L ..... Pipe length (ft)
m_{oil} ..... Mass of oil (lbm)
$m_{ref,oil}$ .. Mass of refrigerant dissolved in oil (lbm)
P ..... Pressure
p ..... Pressure (psf)
R ..... Dependent variable of uncertainty equation (Result)
$S.G.$ ..... Specific gravity

T ..... Temperature
x_{oil} ..... Oil mass fraction

Subscripts/Superscripts
c ..... Condensing
is ..... Adiabatic
o, is ..... Overall isentropic
vol ..... Volumetric

CHAPTER I

INTRODUCTION

Recently, there has been a push to improve the efficiencies and reduce the environmental impact of HVAC&R systems. In 2016, 111 quadrillion BTUs of energy were used by the United States, 20 percent of this being consumed by commercial and residential HVAC&R systems (EIA (2018)), with 6% used by the compressors of these systems, on average (Roth et al. (2002); Kelso (2012)). The high energy consumption of compressors creates importance to improve the efficiencies of compressor technology to reduce their environmental footprint.

One way to reduce the environmental impact of HVAC&R systems is to reduce the use of HFC refrigerants and to switch to low-Global Warming Potential (GWP) refrigerants. In fact, the Kigali Amendment to the Montreal Protocol requires countries to reduce HFC use by 85% between 2019 and 2036. It is predicted by Dr. Guus Velders in Doniger (2016), that these changes alone will mitigate an increase in global surface temperature of 0.5°C. To realize this reduction in environmental impact, it is necessary to begin the switch to low-GWP refrigerants immediately.

Without designs specific to low-GWP refrigerants, recent studies suggest that many of the fluids dropped-in to current heat pump technologies would increase energy use through either thermodynamic disadvantages or a reduction in unit component efficiency, such as the compressor or heat exchangers (In et al. (2014)). This suggests necessary design, development, and modeling activities for various compressor technologies, supported by experimental data. Therefore, it is essential to develop testing environments to determine how compressors will perform using new refriger-

ants. Since there is a wide range of low-GWP refrigerants that could be used, data will need to be collected to measure compressor efficiency with each refrigerant. A hot-gas bypass compressor load stand has been constructed at Oklahoma State University for the purpose of performance testing a wide variety of compressors with a wide variety of refrigerants, including low-GWP variants, to characterize compressors and support design, development, and modeling activities. The load stand additionally includes features such as economization and independent lubricant management to allow a wide range of compressor applications to be simulated.

1.1 Literature Review

Many types of compressor test environments exist today for the purpose of measuring compressor performance. This performance is calculated using the enthalpy difference between the inlet and outlet of the compressor multiplied by the refrigerant mass flow rate through the compressor. Two of the main methods used for compressor testing are the calorimeter and the flowmeter types, which are distinguished by the method of which it determines the refrigerant mass flow rate. A calorimeter is able to determine refrigerant mass flow rate by means of performing a heat balance on a heat exchanger. ASHRAE-23.1 (2010) breaks up the calorimeter types into two sections: Evaporator calorimeters and Condenser calorimeters. The flowmeter type directly measures the refrigerant mass flow rate, and is divided into gaseous and liquid flowmeter types, with the hot-gas bypass style falling under the gaseous flowmeter type.

The calorimeter type is widely used today in the HVAC&R industry. Wujekand et al. (2014) studied the impact of refrigerant-lubricant mixture properties on compressor efficiencies. They tested a transcritical carbon dioxide compressor in a calorimeter using several different lubricants and oil circulation rates. The study found that accounting for the lubricant content inside the compressor effects the isentropic ef-

ficiency calculation. Tan et al. (2014) set out to validate the concept of a novel compressor mechanism called the Revolving Vane compressor. A calorimeter was used to validate the mathematical model, ultimately proving the novel mechanism can function reliably in a refrigeration compressor. Cuevas et al. (2010) conducted a study characterizing a scroll compressor operating beyond its well defined operating conditions achieving a very wide range of testing conditions. A secondary fluid calorimeter is used to validate a semi-empirical model. Shrestha et al. (2013) used a calorimeter to test compressor performance on R-410A alternatives, while Cogswell and Verma (2018) tested low GWP refrigerants on a novel compressor design.

All the works described above showcase the versatility and widespread use of the calorimeter type test method. However this type of test method has certain drawbacks and limitations. Duggan et al. (1988) identified the differences between the calorimeter and flowmeter type methods, listing many limitations of the calorimeter methods. For testing larger compressors, those over 30 kW, a calorimeter becomes very large and expensive with running costs about two-thirds higher than the flowmeter type. They also state that stabilization times are lower for the flowmeter type when compared to a calorimeter. Additionally, Marriott (1973) also comments on the lengthy stabilization time required with the calorimetric methods as compared to the flowmeter type method. He also states that the flowmeter type method simplifies the system as only one refrigerant phase change is required.

Moving on to the flowmeter type method, specifically the hot-gas bypass configuration, several other advantages are seen when compared to other types of compressor test set-ups such as a calorimeter. Sathe et al. (2008) describes many of these advantages, such as fewer components than a calorimeter, as well as easier construction and operation. The design also enables rapid movement between test conditions and offers enhanced stability of operating conditions as a result of the bypass and liquid expansion valve control scheme. An evaporator is not needed and smaller condensers

can be used due to most of the refrigerant flow being bypassed.

Experiments using hot-gas bypass compressor load stands have been done for several applications to develop new compressor technologies. Bradshaw et al. (2011) designed a load stand to test the performance of a custom-designed miniature linear compressor. They were able to control the temperature and pressure of the inlet and the pressure at discharge by controlling flowrates through the system using expansion valves. Similarly, the model of the novel rotating spool compressor developed by Bradshaw and Groll (2013) was validated using data from a hot-gas bypass style load stand testing a 5-ton (18 kW), R410A, spool compressor prototype with data presented in Orosz et al. (2014). As a follow-on study, a 40-ton (141 kW), R134a, spool compressor prototype was developed on a separate hot-gas bypass compressor load stand with data presented in Orosz et al. (2016). This experience with hot-gas bypass load stand design and operation to support compressor development lead to a series of best practices of hot-gas bypass load stand environments present by Bradshaw (2014) that this work has followed.

Additional considerations have been made to compressor load stands to include novel cycle modifications such as liquid, vapor, and oil injection. Gu and Mathison (2014) developed a load stand to test compressors with two vapor injection ports and therefore two pressures between the suction and discharge. They determined that lowering the condensing temperature would result in a lower quality of injection. Bell (2011) presented data from an oil injected scroll compressor using a modified hot-gas bypass load stand configuration. This study presented the potential improvements to compressor efficiency as a result of oil injection. To enable the ability to test these advanced cycle modifications the load stand developed in this work has been constructed to be able to test compressors installed in these simulated cycles.

1.2 Cycle Description

The hot-gas bypass style design is a common method used for compressor testing, due to the many advantages listed above. It has many similarities with the common four component vapor compression cycle used widely in the HVAC&R industry today. The hot-gas bypass style distinguishes itself from the normal vapor compression cycle by excluding the use of the evaporator, which is what gives it the ability for rapid movement between test conditions. Figure 1.1 shows a basic illustration of the hot-gas bypass cycle, with the corresponding log(p)-h diagram shown in Figure 1.2. The numbered state points in Figure 1.2 match the numbered locations in Figure 1.1.

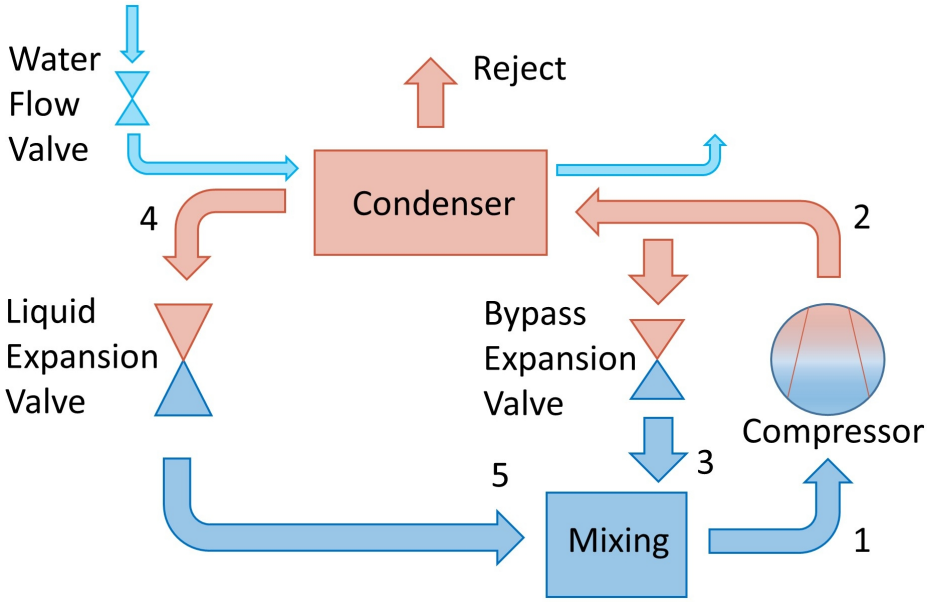

Figure 1.1: Illustration of a hot-gas bypass cycle

The cycle works by taking the discharge refrigerant gas exiting the compressor and separates the flow into two distinct paths. Most of the refrigerant mass flow bypasses the condenser, and is expanded back down to suction pressure. The remaining amount of mass flow is condensed and then throttled down to suction pressure. The two flows then mix together to create the desired condition at the inlet of the compressor. Manipulation of the expansion valves and water flow valve create a control scheme that allows for stable operating conditions.

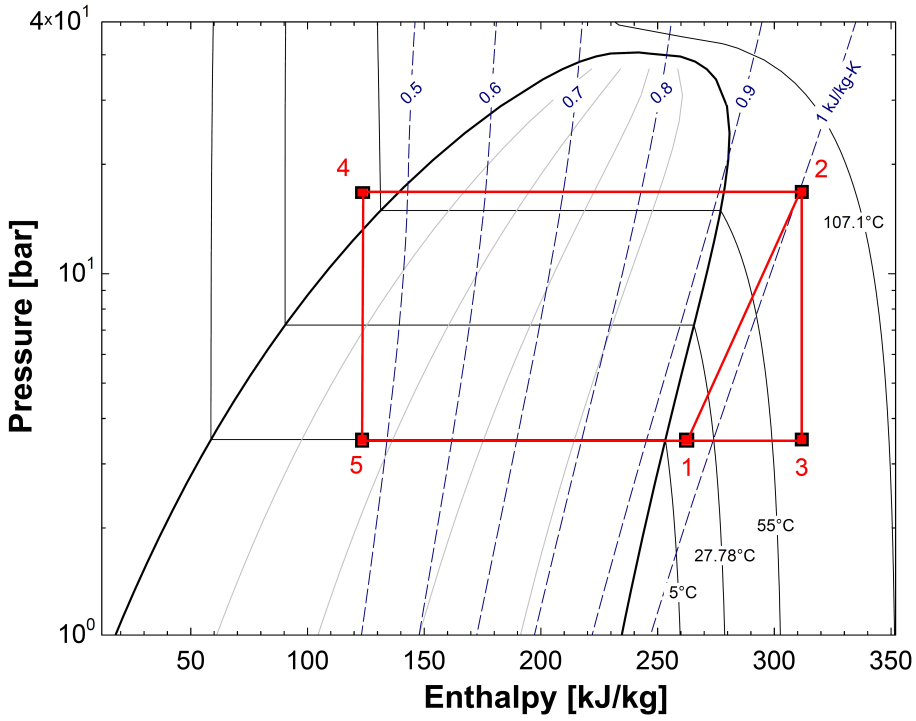

Figure 1.2: Pressure-enthalpy diagram for a hot-gas bypass system with R134a

Incorporated into this hot-gas bypass cycle is an economizer circuit to allow for liquid/vapor injection. This is common feature in screw compressors, thus expanding the types of conditions the stand is able to achieve. The economizer circuit operates with a similar working principle as the hot-gas bypass style described above. Figure 1.3 shows the same illustration of a hot-gas bypass cycle above, but with the added economizer feature.

The economizer circut works by taking a portion of the discharge mass flow and a portion of the liquid mass flow, expands them to suction pressure, and then mixes them to create the desired injection condition. Again, the manipulation of the bypass and liquid expansion valves on the economizer circuit allow for precise control of the injection condition. The numbered locations in Figure 1.3 match with the numbered state points in Figure 2.1. A more detailed explanation of the hot-gas bypass cycle with economization is found at the beginning of Chapter 3.

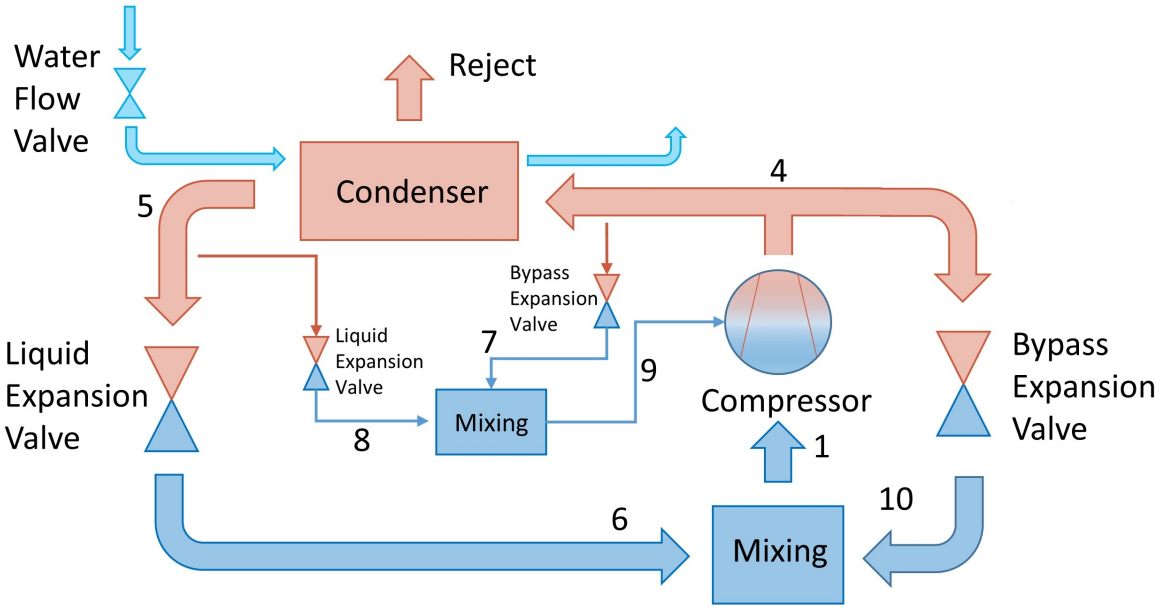

Figure 1.3: Illustration of a hot-gas bypass cycle with economization

1.3 Objective of Thesis

The objective of this thesis was to design and build a hot-gas bypass compressor load stand capable of testing light-commercial compressors. The load stand is meant to be a permanent part of the OSU thermal systems group research infrastructure, alongside the psychrometric chambers and wind tunnel. Given the initial scope of the project, this being a compressor capacity range that the load stand needed to be able to handle, I was tasked with the following objectives. First, I had to create a thermodynamic model of the load stand. Using this model, I was able to estimate tube sizes, component sizes, and instrumentation limits. I then created a 3D Solidworks model to visualize and design the tubing and component layout. With the help of Jake Singleton (undergraduate research assistant at the time), the load stand was then built from scratch in the high-bay of the ATRC lower basement (Room 042). Next, the instrumentation and control wiring was completed. The LabVIEW code controlling the stand was written by Jake with the help of Dr. Craig Bradshaw. The last objective was to get the load stand up and running with a 40-ton scroll compressor.

CHAPTER II

THERMODYNAMIC MODEL

2.1 Model Overview

A thermodynamic model of a hot-gas bypass system, including economization, was developed in Engineering Equation Solver (EES) (Klein and Alvarado (1992)) to represent the physical behavior of the load stand. Its purpose is to estimate the load stand system limitations, such as maximum head pressure, and to estimate important parameters, such as mass flow rates, that are needed when selecting and sizing components. The ultimate goal being for the model to provide a good estimation on the upper and lower performance bounds of the load stand so that the appropriate design choices are made. This model makes typical assumptions to calculate every thermodynamic state point in the cycle. This includes the compressor being modeled with a fixed adiabatic and volumetric efficiency of 0.7 and 0.9, respectively. All expansion valves are assumed isenthalpic, mixing is assumed adiabatic, and heat exchangers are assumed isobaric. Figure 2.1 shows the pressure-enthalpy diagram for the load stand as predicted by the thermodynamic model, including the economization circuit. Mass and energy balances, neglecting kinetic and potential energy, were used to calculate the ratio of flow split through the compressor bypass relative to the liquid line for both the main (2.1) and economizing (2.2) loops. Numbered subscripts correspond to Figures 1.3 and 2.1.

$$\frac{\dot{m}_{10}}{\dot{m}_6} = \frac{h_6 - h_1}{h_1 - h_{10}} \tag{2.1}$$

$$\frac{\dot{m}_7}{\dot{m}_8} = \frac{h_8 - h_9}{h_9 - h_7} \tag{2.2}$$

The model takes in various inputs from the user, and outputs the main cycle state points, as well as, various cycle parameters. The inputs are refrigerant type, amount of subcooling and superheat, assumed adiabatic compressor efficiency, assumed volumetric efficiency, evaporating temperature, condensing temperature, compressor volumetric displacement, and compressor speed. With these inputs, the model is able to output five main refrigerant state points throughout the load stand. These state points coincide with the suction condition, discharge condition, condensed liquid, expanded liquid, and expanded hot gas. The critical outputs that it calculates are volume flow rate, mass flow rate, velocity, heat rejection, compressor power, and cooling capacity. If the economizer is involved, then some extra inputs include the percent of total compressor volume used for economizing, and the injection temperature. Five more state points are required for the economizing loop, all at the intermediate injection pressure.

The following equations are used to calculate the critical outputs listed above for a non-economizing cycle. The refrigerant mass flow rate ($\dot{m}$) is defined as the product of the volume flow rate ($\dot{V}$) and suction density (ρ_s), where the volume flow rate is defined as the product of the compressor speed (n), compressor volume displacement (v_d), and the assumed volumetric efficiency (η_{vol}). Equation 2.3 calculates the mass flow rate, while equation 2.4 calculates the volume flow rate.

$$\dot{m} = \dot{V}\rho_s \tag{2.3}$$

$$\dot{V} = nv_d\eta_{vol} \tag{2.4}$$

The heat rejection ($\dot{Q}_{hr}$)and compressor power ($\dot{W}$) are found using the energy

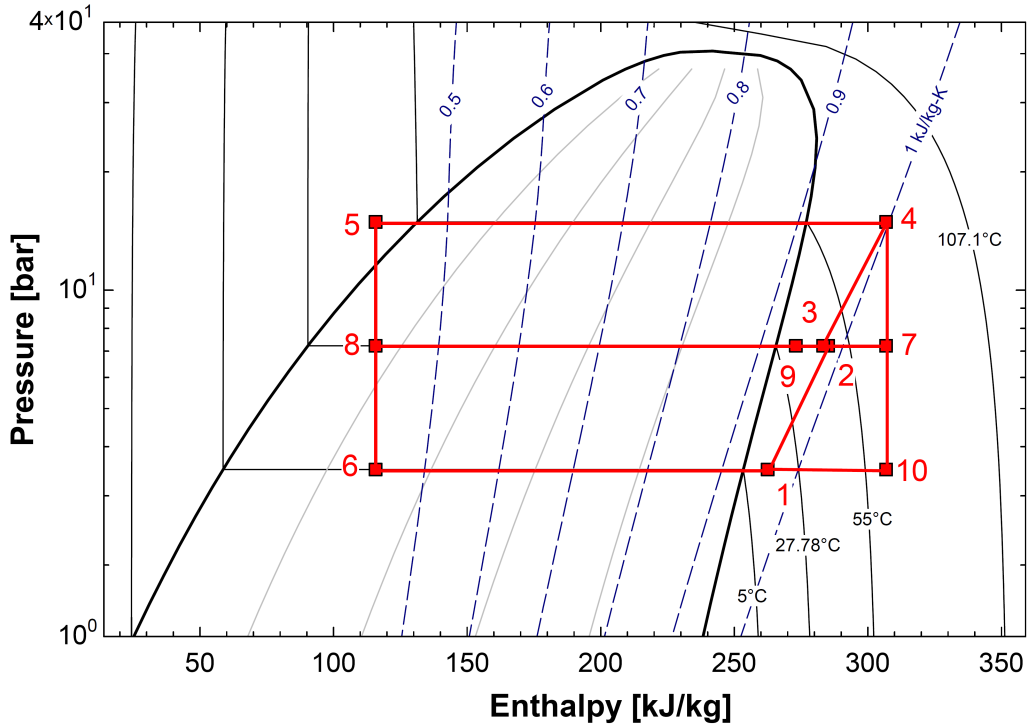

Figure 2.1: Pressure-enthalpy diagram of a hot-gas bypass system with economization

balances shown in equations 2.5 and 2.6. Both values are defined as the product of the mass flow rate through the component ($\dot{m}$) and the change of specific enthalpies (h) from the entrance to the exit of the component. Due to the nature of a hot-gas bypass system, these two equations are equal. The heat rejection in the condensers and subcooler is equal to the power used by the compressor. Numbered subscripts correspond to Figures 1.1 and 1.2.

$$\dot{Q}_{hr} = \dot{m}_c(h_2 - h_4) \tag{2.5}$$

$$\dot{W} = \dot{m}(h_2 - h_1) \tag{2.6}$$

2.1.1 State Point Description

Each cycle state point is set with two independent refrigerant property inputs, and utilizes the R134a fundamental equation of state developed by Tillner-Roth and Baehr (1994). State point 1 is set with the evaporation temperature and amount of superheat inputs, and with a saturation pressure corresponding to the evaporating temperature. State point 2 is set with an intermediate pressure equal to the square root of the product of the condensing and evaporating pressures. The second property input being the specific enthalpy found with equation 2.7 for adiabatic efficiency (η_{is}).

$$\eta_{is} = \frac{h_{2,s} - h_1}{h_2 - h_1} \tag{2.7}$$

The compressor adiabatic efficiency is assumed to be 0.7, and $h_{2,s}$ is found with the intermediate pressure and with the specific entropy at state 1. State point 3 is set with the intermediate pressure and with a specific enthalpy value found with the percent of total compressor volume used for economizing. State point 4 is set with the condensing temperature and with the specific enthalpy found in a similar fashion as described with state point 2. These four points represent the fixed isentropic compression process with vapor injection at an intermediate pressure. State point 5 is set with the condensing temperature and amount of subcooling inputs, and with the condensing pressure. This state point represents the exit of the isobaric condensing process. State point 6 is set with the evaporating pressure and with the same specific enthalpy at state point 5, due to the isenthalpic expansion process. State point 7 is set with the intermediate pressure, and with the same specific enthalpy of state point 4. State point 8 is set with the intermediate pressure, and with the specific enthalpy at state point 5. State point 9 is set with the intermediate pressure, and with the injection temperature. Finally, state point 10 is set with the evaporation temperature, and with the specific enthalpy at state point 4.

The desired cooling capacity provided reference to calculate the subsequent mass and volume flow rates through each component, the heat rejection required by the condensers, and power input necessary to operate the compressor. In conjunction with the pressures and temperatures calculated from the state point calculations this provided useful design information when selecting components and accessory equipment to operate the load stand.

2.2 Model Results

The maximum and minimum design conditions of the load stand are 80 tons (281 kW) and 10 tons (35 kW) cooling capacity, respectively, at the following conditions: 55°C condensing temperature, 5°C evaporating temperature, and 10°C superheat and subcooling with the working fluid R134a. The design objective being to have the ability to cover a capacity range suitable for light-commercial compressors of varying sizes and types, specifically small screw compressors and large scroll compressors. Along with this wide light-commercial capacity spectrum, the hot-gas bypass system includes a dedicated economizer circuit allowing for liquid or vapor refrigerant injection, as well as, independent control over oil circulation and injection. With these design conditions, the model was able to set the upper and lower performance bounds of the load stand.

2.2.1 Compressor Size Limitations

The thermodynamic model was additionally used to better understand the compressor size limitations of the load stand by exploring the limitations of the compressor displaced volume at 3550 rpm (representing 60 Hz excitation on a typical asynchronous 2-pole motor). Most compressor manufacturers only give a capacity rating for a certain condition with a particular refrigerant. However, the load stand will see multiple conditions and multiple refrigerants used for a single compressor,

therefore, knowledge of the max/min compressor volume displacement for a particular refrigerant is useful in discerning if a compressor is able to be tested on the load stand. The first step was finding the max/min compressor volume displacement for the design conditions.

To reflect the design conditions previously described (10-80 tons (35-281 kW) on R134a with 55°C condensing), a parametric study conducted using a normal airside condensing temperature range of 25-60°C was performed to explore the various output parameters from the model, including the maximum compressor displacement possible to test at 3550 rpm. It was found that the min-max compressor volume displacement corresponding with the aforementioned 10-80 ton objective was 300 and 2200 cm^3/rev, respectively, as shown in Figure 2.2. The x-axis represents a range of compressor volume displacements, while the y-axis represents the normal airside condensing temperature range. The color spectrum represents the simulated cooling capacity at the corresponding condensing temperature and displacement. Holding parameters such as superheat, subcooling, evaporating temperature, and compressor speed constant, the simulated cooling capacity was found for varying condensing temperatures and volume displacements. Ultimately, the entire load stand operating envelope is found following the capacity color bands through the range of condensing temperatures.

An understanding of the limits of the load stand is essential in selecting the appropriate compressor to be tested. Future testing will require the use of multiple different refrigerants, and the knowledge of an appropriate compressor size and capacity is crucial to the safety and longevity of the load stand. Using the thermodynamic model and the constraint of operation at the design condition, the operating capacity and maximum compressor displacement can be estimated. For working fluids with a lower density then R134a, the maximum displaced volume is limited by the discharge volume flow rate due to pressure drop in the load stand. Therefore, the maximum

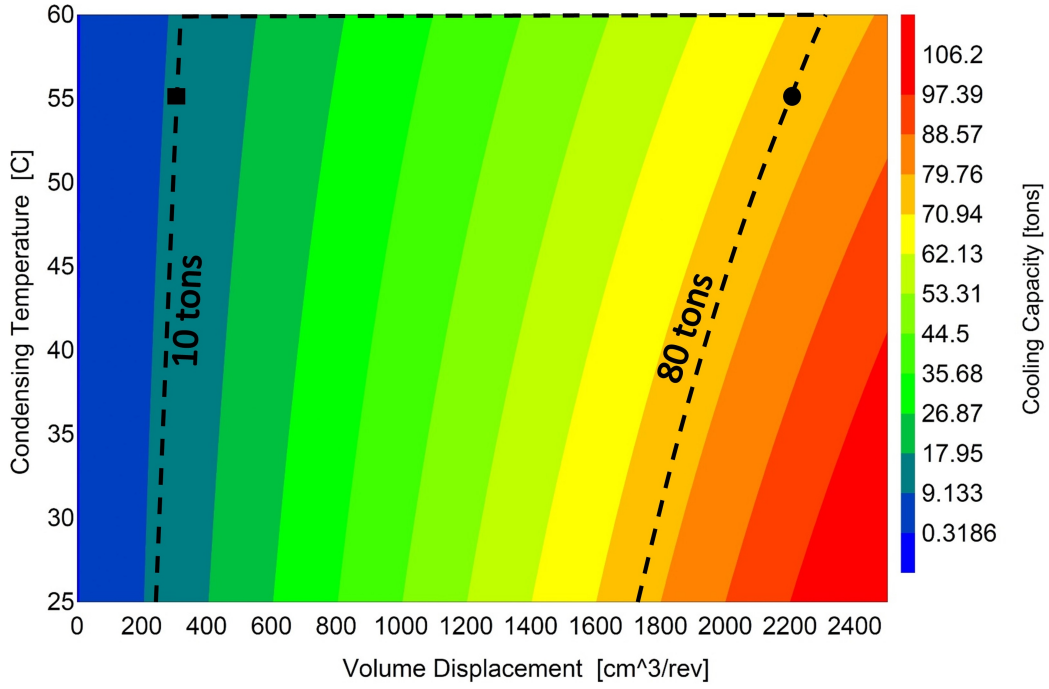

Figure 2.2: Cooling capacity corresponding to various condensing temperatures and volume displacements. Operating envelope found between the 10 ton (square) and 80 ton (circle) limits.

volume flow rate for R134a was used as an input when calculating the maximum capacity and volume displacement values for these lower density fluids. On the other hand, higher density working fluids are limited by the maximum compressor power set with the R134a baseline. By using the power as an input, the maximum capacity and volume displacement values for these higher density fluids are found. Table 2.1 shows some limits of possible refrigerants that will be tested.

Table 2.1: Predicted maximum capacity and accompanying compressor displacements that the load stand will support for 3,550 rpm at 55°C condensing

Working Fluid	Max Capacity in Tons (kW)	Max Volume Displacement (cm^3)
R134a	80 (281)	2200
R1234yf	77 (271)	2265
R410A	72 (253)	893
R32	74 (260)	827
R1234ze(E)	61 (215)	2247

2.2.2 Load Stand Limitations

The other crucial result provided by the model was the maximum and minimum system parameters used for component selection and sizing. To find these max and min values, the normal airside condensing temperature range of 25-60°C was used again. The max/min parameter values were found at the model conditions of 80/10 tons capacity at a compressor speed of 3550rpm. Table 2.2 summarizes the parameter limitation results.

Table 2.2: Maximum and minimum values defining the load stand limitations

Parameter	Minimum Value	Maximum Value
Suction Volume Flow Rate	58 (m^3/h)	422 (m^3/h)
Discharge Volume Flow Rate	13 (m^3/h)	235 (m^3/h)
Mass Flow Rate	937 (kg/h)	6872 (kg/h)
Compressor Power	5 (kW)	94 (kW)
Cooling Capacity	10 (tons)	80 (tons)
Pressure	250[1](psi)	650 (psi)

[1] Value indicates minimum design pressure from ASME-B31.5 (2013). Load stand is capable of pressures from vacuum to the maximum value.

The condensing temperature range directly influenced the discharge volume flow rate and compressor power values. The discharge density increases with higher condensing temperatures, resulting in the minimum and maximum discharge volume flow rates to be found at 60°C and 25°C condensing temperature, respectively. The higher density also increases the amount of work the compressor has to do, resulting in the maximum compressor power to be found at 60°C condensing. The minimum and maximum values for the pressure correspond to the low side and high side limits of the load stand, respectively. To handle high density refrigerants, such as R410A, the low side and high side tubing pressure rating had to meet the minimum design gage pressure specifications for air cooled systems found in ASME-B31.5 (2013). The satu-

ration pressure for R410a with an air cooled system limit was used to get the highest design pressures. These critical system parameters provided a good estimation for the upper and lower bounds of load stand operation. Flow rates in certain sections of the load stand, such as in the economizer and main loop circuits, might drop below the minimum value shown in Table 2.2 due to the refrigerant flow splitting into different directions. These circuits will be discussed in greater detail in the next section of this thesis.

CHAPTER III

LOAD STAND DESIGN

The schematic in Figure 3.1 shows the system layout consisting of all major components and instrumentation. Highlighted in Figure 3.1, the load stand consists of three distinct loops, one for each feature including the main, economizer, and oil loops.

The main loop controls the simulated system operating conditions exposed to the compressor. The operation of this loop starts at the desired suction test condition (1) where the refrigerant enters the compressor at a controlled intake temperature and pressure, and is then discharged at a controlled, sub-critical, pressure. The refrigerant flow then enters a coalescent oil separator before passing through a Coriolis mass flow meter. Exiting the mass flow meter, the refrigerant separates into two distinct paths (2). A majority of the flow is bypassed through a set of electronic gas expansion valves back to suction pressure (3). The remaining flow condenses through two parallel water cooled brazed plate heat exchangers, fed into a liquid receiver, subcooled with another brazed plate heat exchanger (4), and then finally expanded back to suction pressure with a set of liquid electronic expansion valves (5). The bypassed hot gas mixes with the expanded liquid, passes through another Coriolis mass flow meter, and creates the desired suction test condition (1). The two main parameters (temperature and pressure) setting the suction condition are achieved through manipulation of the liquid and bypassed gas expansion valves. The amount of liquid allowed to expand sets the suction superheat, while the amount of discharged gas allowed to bypass sets the suction pressure. The control of cooling water through the condensers and

sub-cooler allows independent control over the compressor discharge pressure.

The dedicated economizer loop follows a similar working principle as the main loop of the load stand. A portion of the subcooled liquid flow (4) is separated from the main loop and passes through another Coriolis mass flow meter before expanding to an intermediate pressure. A portion of the discharge gas (2) is also separated from the main loop, passed through a Coriolis mass flow meter, and expanded to an intermediate pressure. The separated flows mix (6) to create the desired injection condition. Again, manipulation of the expansion valves will allow for injection state control, permitting either liquid or vapor injection.

The oil loop consists of two circuits that return oil separated from the discharge line back to the compressor. One circuit feeds the oil back into the suction line near the compressor, while the second circuit injects the oil into the compressor at any pressure between suction to above discharge. Either circuit is designed to operate independently, but may operate together with the second circuit, or not at all depending on the configuration of the isolation ball valves. Two Coriolis mass flow meters, one on each circuit, ensures that the mass flow rates are measured with any configuration running. Metering valves installed on each circuit throttle the oil to the intermediate pressure, as well as, regulate the mass flow ratio between circuits. In the case of a high-pressure shell compressor, an oil pump is used to create the oil flow, with a Variable Frequency Drive (VFD) hooked up to the oil pump motor to regulate oil flow.

3.1 Main Loop Circuit Design

Due to the large operating range of the stand, careful consideration went into the design of the tubing, most importantly, the sizing. Correct sizing ensures that recommended refrigerant velocities, oil entrainment up system risers, and appropriate mixing are achieved. Tube size was determined using capacity tables specific to R134a

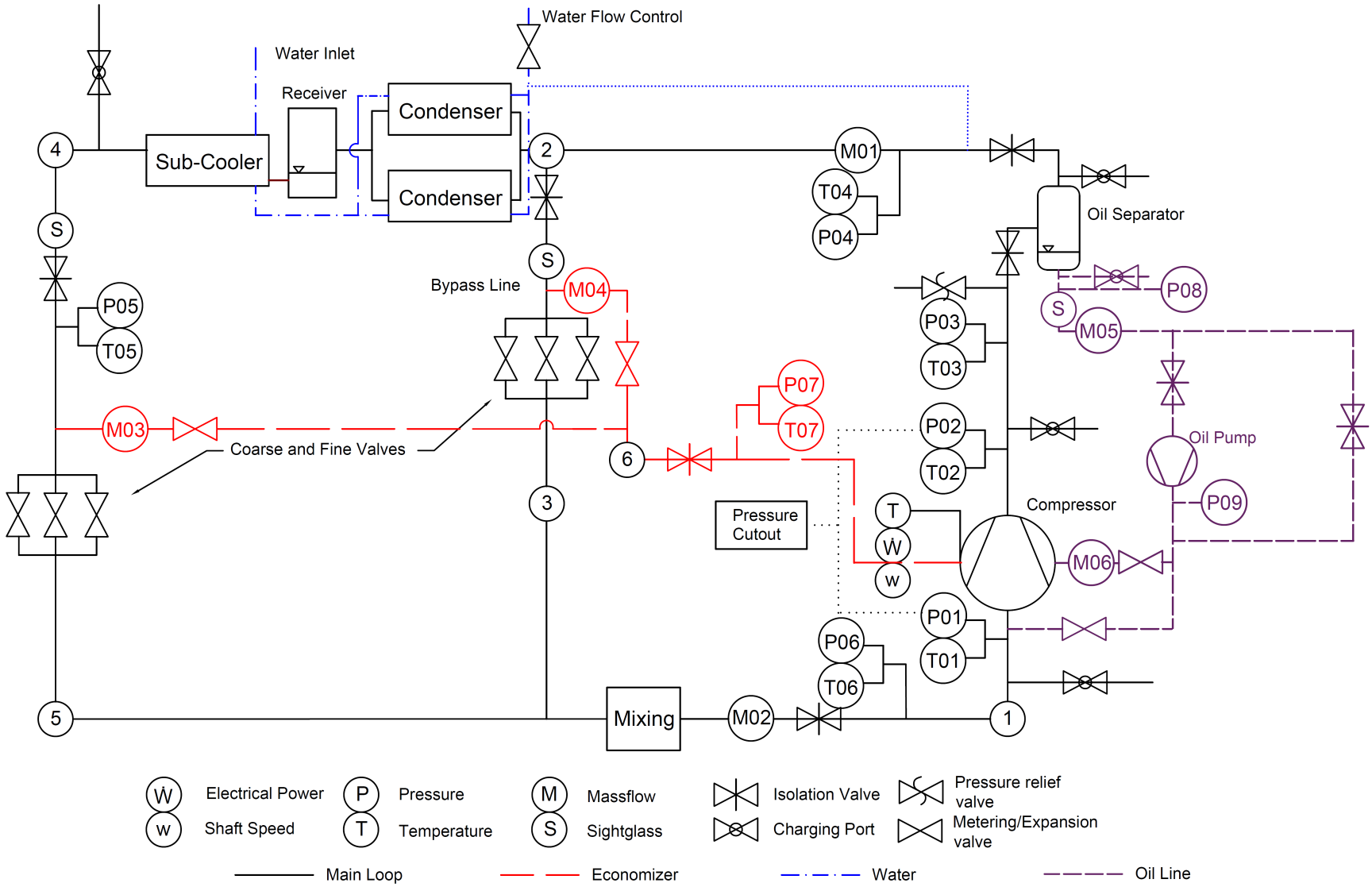

Figure 3.1: Load stand schematic

found in the *2010 ASHRAE Handbook: Refrigeration* (2010). More detail about the tube sizing can be found in the next chapter about component sizing. Three separate circuits of varying sizes, each composed of a bypass, liquid, and suction line, provided the load stand with the versatility to use any configuration of these circuits. Where the bypass lines are defined as the hot-gas bypass plumbing downstream of the separation from the liquid line flow, but upstream of the mixing process. The liquid line is the same definition for the liquid line flow only, and the suction lines are the circuit sizes downstream of the mixing process.

The purpose of this analysis is to obtain acceptable refrigerant velocities when testing across the entire capacity range of compressors so that proper mixing and oil entrainment occurs where the separated mass flows converge in the main loop. This exercise was broken into three separate tasks to evaluate the tube sizing for the hot-gas bypass lines, the suction lines (post-mixing), and the liquid lines of each of the three circuits. A series of decision matrices, seen in Tables 3.1-3.3, were developed using the model results to obtain the optimal combination of sizes for each circuit. The final selected case is shaded for each circuit.

The decision matrix contains proposed line sizes evaluated with one table for each circuit (bypass, suction, and liquid lines). Each table contains multiple cases consisting of a combination of three different tube sizes. Conducting a parametric study in EES, the optimal combination of tube sizes for each line could be determined by evaluating the refrigerant velocity in each proposed line at a range of operating conditions and capacities that represent the extremes the load stand expects to run. This study calculated refrigerant velocities over a range of compressor volume displacements (capacities) and condensing temperatures while holding other parameters such as evaporating temperature, subcooling, and superheat constant. The case that had the most velocities in the recommended range provided on page 1.1 in the *2010 ASHRAE Handbook: Refrigeration* (2010) was selected for the final design. The main

loop circuits in the form (bypass line size, liquid line size, suction line size) selected are (1-1/8, 1/2, 1-3/8), (1-3/8, 7/8, 2-1/8), and (2-1/8, 1-1/8, 3-5/8).

The bypass line table analyzed 12 different cases consisting of the proposed combinations of tube sizes. Each case examined the two extreme condensing temperatures of 25°C and 60°C for a total of 280 velocities calculated, 140 velocities for each temperature. These velocities were then compared to the recommended range of 2000 to 3500 fpm, with the number of acceptable velocities presented in Table 3.1. To help further differentiate a best case, another 20 different velocity sets for each temperature, corresponding to a certain compressor volume displacement were evaluated with acceptable cases also presented in Table 3.1. This set total provided a more reliable metric for a circuit size decision because it expressed if any out of the seven circuit combinations worked for a certain volume displacement. From this analysis, the proposed combination with the most acceptable cases was the combination of 1-1/8, 1-3/8, 2-1/8 tube for the three hot-gas bypass circuits.

Table 3.1: Decision matrix for bypass line circuit combinations considered

Case	1	2	3	4	5	6	7	8	9	**10**	11	12
Bypass Circuit Size(in)	5/8, 1-3/8, 2-5/8	5/8, 1-3/8, 3-1/8	5/8, 1-5/8, 2-5/8	5/8, 1-5/8, 3-1/8	7/8, 1-3/8, 2-1/8	7/8, 1-3/8, 2-5/8	7/8, 1-3/8, 3-1/8	7/8, 1-5/8, 2-5/8	7/8, 1-5/8, 3-1/8	**1-1/8, 1-3/8, 2-1/8**	1-1/8, 1-3/8, 2-5/8	1-1/8, 1-5/8, 2-1/8
Total/280	54	37	55	39	56	59	46	56	39	**57**	56	57
Set-Total/40	24	19	25	20	33	31	31	29	24	**36**	33	33

Table 3.2 presents the options considered for the suction line sizes. The suction line velocities are calculated for only one condensing temperature of 55°C, and then compared to the recommended range of 900 to 4000 fpm, from the *2010 ASHRAE Handbook: Refrigeration* (2010). This analysis resulted in a final suction line combination of 1-3/8, 2-1/8, 3-5/8.

Table 3.3 presents the decision matrix for the two combinations considered for the liquid line. The liquid line table considered both 25°C and 60°C condensing temperatures, and compared the velocities to the recommended 300 fpm for liquid

Table 3.2: Decision matrix for suction line circuit combinations considered

Case	1	2	3	4	5	6	**7**	8
Suction Circuit Size(in)	1-1/8, 1-5/8, 3-5/8	1-1/8, 1-5/8, 4-1/8	1-1/8, 2-1/8, 3-5/8	1-1/8, 2-1/8, 4-1/8	1-3/8, 1-5/8, 3-5/8	1-3/8, 1-5/8, 4-1/8	**1-3/8**, **2-1/8**, **3-5/8**	1-3/8, 2-1/8, 4-1/8
Total/140	72	66	77	71	74	68	**79**	72

lines from the *2010 ASHRAE Handbook: Refrigeration* (2010). This results in a final liquid line combination of 1/2, 7/8, 1-1/8.

Table 3.3: Decision matrix for liquid line circuit combinations considered

Case	**1**	2
Suction Circuit Size(in)	**1/2**, **7/8**, **1-1/8**	3/8, 3/4, 7/8
Total/280	**265**	244

3.2 Instrumentation

The instrumentation consists of gage pressure transducers and T-type thermocouples to determine each of the state points discussed above with the exception of the measurements near the compressor that are used to calculate compressor performance metrics. These critical measurements will use higher accuracy pressure transducers and platinum RTDs for reduced measurement uncertainty. Mass flow measurements are obtained with six Coriolis mass flow meters located on the suction and discharge lines, economizer gas and liquid lines, and on the oil main and injection lines. The discharge line meter (M01) is the primary meter to be used in compressor performance metric calculations. Surface mount thermocouples will measure compressor shell temperature, while an accelerometer will measure the compressor shaft speed. Compressor speed modulation is handled through a 150 horsepower (112 kW) VFD, with a watt transducer measuring the power supplied to the compressor from the VFD. Instrumentation accuracies can be seen in Table 3.4 below. For compliance with ASHRAE-23.1 (2010), the mass flow measurements are redundant (suction and

discharge). Additionally, critical pressure and temperature measurements are redundant to ensure rapid diagnosis of sensor failure or calibration problems.

3.3 Safety Circuits

The load stand is equipped with a low voltage safety circuit that will ensure complete shutdown of all rotary components in the case of an event that could cause danger to the user/equipment and/or an emergency. This circuit consists of a series of safety components powered by the compressor VFD 24 VDC source, described hereafter, and an emergency stop button (4) for a manual shutdown option. The safety components include a high-pressure cutout (5) connected to the discharge line to protect the system tubing and components, and a low-pressure cutout (6) connected to the suction line to protect the compressor. Isolating ball valves located on the discharge (1,2) and suction (3) lines have proximity sensors monitoring the stem location guaranteeing that the valves are open when the stand is operating. Each sensor is powered separately, and is wired to a Single Pole Double Throw (SPDT) relay (model #: 781-1C-24D) that, when sensing that the ball valve is closed, will break power going to the relay, thus breaking the safety circuit. A thermal protection module (7) will monitor the compressor motor temperature to avoid overloading and overheating. Finally, an oil regulator (8) will monitor the amount of oil in the compressor sump, activating when the oil level drops below the required minimum level. These normally closed safety features will break the circuit shutting down the compressor and oil pump motor VFDs. Figure 3.2 shows the main safety circuit wiring diagram with the components numbered to match the numbers above. An independent secondary safety circuit will consist of a water flow switch that will shut down the load stand when there is no supply of cooling water. This circuit is separate because the cooling water needs to remain running in the event of an emergency. As a final line of defense, a pressure relief valve is installed on the discharge-side of the

Table 3.4: Instrumentation specifications

Sensor Type	Quantity	Mfg & Model Number	Measure Range	Accuracy
Pressure Transducer	7	Setra 2061-10CP-G-2M-11-H1-8-GN	0-1,000 psi	± 0.13% FS[1]
Thermocouple T-type	5	Pyromation T28U-XXX[1]-12B-6MC	0-370 °C	± 1 °C or 0.75%
Pressure Transducer P01, P02	2	Setra ASM1-750P-G-2M-11-B3-A-00	0-750 psi	± 0.05% FS[1]
Surface Thermocouple	3	Omega SA1XL-T-72-SRTC	-60 - 175 °C	± 1 °C or 0.75%
Platinum RTD T01, T02	2	Pyromation RAF185L384Z-017-8B15-15-T3006-4,MC,(Z521)	-30 - 300 °C	± (0.1 + 0.0017 · t[1]) °C
Accelerometer	1	Omega ACC101	3 Hz - 5 kHz	± 0.022%[2]
Watt Transducer	1	Ohio Semitronics WV7-23-200-E	0 - 160,000 W	± 0.25% FS[1]
Discharge Mass Flow Meter M01	1	Micromotion CMF200M419N2BAEZZZ	0-10,000 kg/h	± 0.25%
Suction Mass Flow Meter M02	1	Micromotion F200SA37C2BAEZZZ	0-18,137 kg/h	± 0.5%
Economizer Liquid Meter M03	1	Micromotion CMFS015M314N2BAECZZTG	0-330 kg/h	± 0.05% for mass flow ± 0.2 kg/m^3 for density
Economizer Bypass Meter M04	1	Micromotion CMFS075M329N2BAEKZZTG	0-14,000 kg/h	± 0.25%
Oil Mass Flow Meters M05, M06	2	Micromotion CMF025M319NRAAEZZZ	0-2,180 kg/h	± 0.05% for mass flow ± 0.2 kg/m^3 for density

[1] FS-Full Scale; t-Temperature; XXX-Specified length

[2] Estimated by calculating the uncertainty of frequency measurement using NI CompactRio wiht NI 9230 accelerometer card

compressor and is sized to prevent mechanical damage to the load stand.

3.4 Standard Compliance

The load stand complies with industry standards to ensure correct measurement and testing methods, as well as, complies with the proper safety requirements. As mentioned above, the load stand is equipped with two independent mass flow meters for compliance with ASHRAE-23.1 (2010), as well as instrumentation with errors within the allowed tolerance. A pressure relief valve, sized in accordance with ASHRAE-15 (2016), is located on the discharge line between the compressor and the stop valve to allow for the evacuation of refrigerant at the minimum flow of the compressor. The maximum working pressures on the stand for all copper tubing and steel flanges are below the maximum pressures stated in ASME-B16.22 (2013). Finally, as mentioned in section 2.2.2, ASME-B31.5 (2013) design pressure specifications for air cooled systems were followed.

3.5 Uncertainty of Compressor Performance Metric Measurements

One of the primary objectives of the load stand is to measure compressor volumetric and overall isentropic efficiency at a range of simulated operating conditions. The overall isentropic efficiency is the ratio of work done in an isentropic process to the work done by the compressor in the actual process, as shown by,

$$\eta_{o,is} = \frac{\dot{m}(h_{2,s} - h_1)}{\dot{W}} \tag{3.1}$$

The volumetric efficiency is the ratio of refrigerant mass flow to the theoretical maximum mass flow rate; it is given by,

$$\eta_{vol} = \frac{\dot{m}}{\rho v_d \omega} \tag{3.2}$$

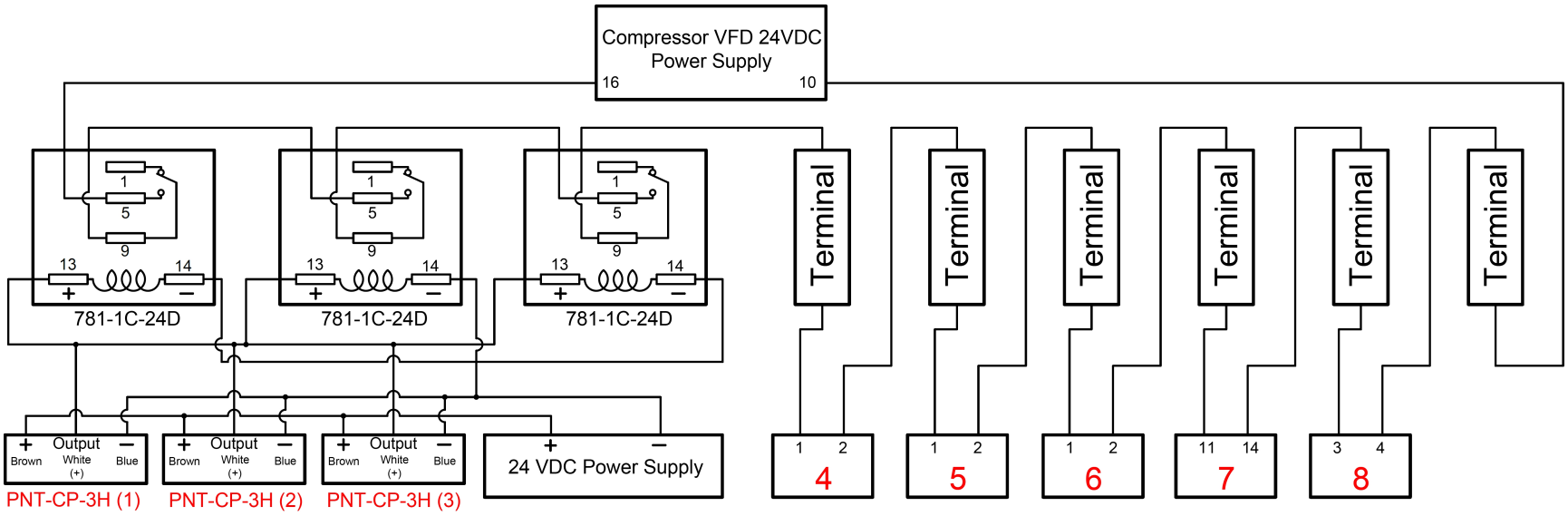

Figure 3.2: Main safety circuit powered by compressor VFD 24 VDC source.

The isentropic efficiency depends on the discharge mass flow meter for mass flow readings, and the watt transducer for the compressor power measurement. The volumetric efficiency calculation will also use the discharge mass flow meter for the mass flow readings, and the accelerometer for the compressor speed. The compressor volume displacement will be given by the compressor manufacturer. The specific enthalpies in the isentropic equation and the suction density in the volumetric equation are a function of the temperature and pressure of the refrigerant entering and exiting the compressor and will use the platinum RTD and Setra ASM for temperature and pressure measurements, respectively.

Using the absolute accuracies of the sensors in Table 3.4, an uncertainty calculation was performed for an R134a cycle at the design conditions. The approach that was used to calculate the uncertainties of each primary efficiency calculation is a propagation of error approach. The following equations, found in the ASME-PTC-19.1 (2005) standard, reports the relative systematic standard uncertainty of a single test result.

$$\Theta_{i'} = \frac{\bar{X}_i}{R}\left(\frac{\delta R}{\delta \bar{X}_i}\right) \tag{3.3}$$

$$\frac{b_R}{R} = \left[\sum_{i=1}^{I}\left(\Theta_{i'}\frac{b_{\bar{x}_i}}{\bar{X}_i}\right)^2\right]^{\frac{1}{2}} \tag{3.4}$$

This approach uses the relative systematic uncertainties of each sensor to determine how they propagate the error and affect the overall uncertainty. Using this approach, the overall isentropic efficiency and the volumetric efficiency were found to have relative uncertainties of $\pm 0.53\%$ and $\pm 0.34\%$, respectively. Each squared term in the summation in equation (3.4) corresponds to the contribution of that parameter to the overall uncertainty. The larger the contribution, the more that parameter affects the uncertainty, this is broken down for each parameter in Table 3.5.

Table 3.5: Parameter contributions to overall uncertainty

Parameter	Isentropic Contribution	Volumetric Contribution
$\dot{m}$	22.10%	54.90%
P_1	8.82%	41.45%
P_2	3.33%	NA[1]
T_1	1.64%	3.23%
$\dot{W}$	64.11%	NA[1]
v_d	NA[1]	0.00%
ω	NA[1]	0.43%

[1] NA-Not Applicable

The results show that the compressor power measurement contributes around 64% to the final isentropic uncertainty value. While the uncertainty for both metrics is acceptable, a replacement sensor and/or a custom calibration of the compressor watt-meter will be considered as a potential mechanism to reduce the uncertainty of the overall isentropic efficiency. This analysis did not account for random error associated with measurement collection as these influences will be addressed through measurement collection strategies that include time-averaged sampling of data to mitigate the influence of random sampling error.

3.6 Physical Layout

A 3-D CAD model of the load stand aided in the design process, offering visualization of critical design aspects such as component placement and tube design. Figure 3.3 shows an isometric view of the load stand design, with the highlighted major components listed in Table 3.6. Figure 3.4 shows the section view of the load stand. The heat exchangers and liquid receiver are vertically arranged so that liquid refrigerant will naturally collect in the receiver and subcooler. This requires that the condensers be above the liquid receiver, which is above the subcooler. Refer to Figure 5.5 in chapter 5 for a close up view of this arrangement. A similar component height arrangement is required for the oil separator and oil pump. The oil pump sits below the oil separator to minimize vapor entering the pump. Label 4 highlights the three

main loop circuits discussed in greater detail later. Double risers designed using the *2010 ASHRAE Handbook: Refrigeration* (2010) are installed on the discharge and economizer lines to ensure proper oil migration in lieu of separate circuits.

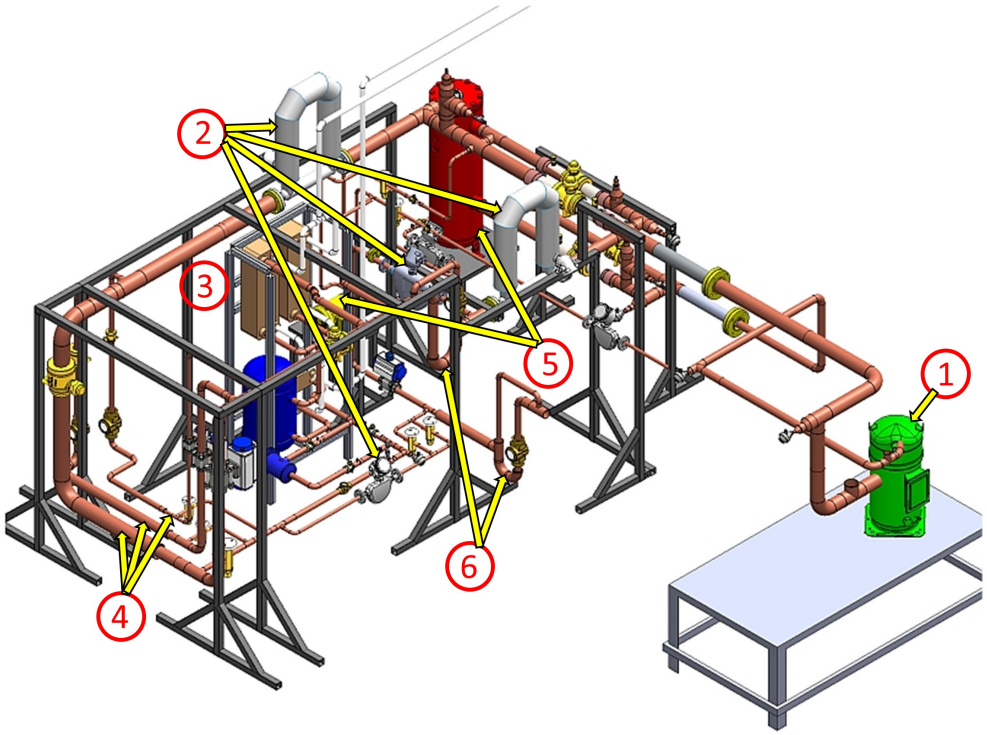

Figure 3.3: Isometric view of load stand design with major components labeled.

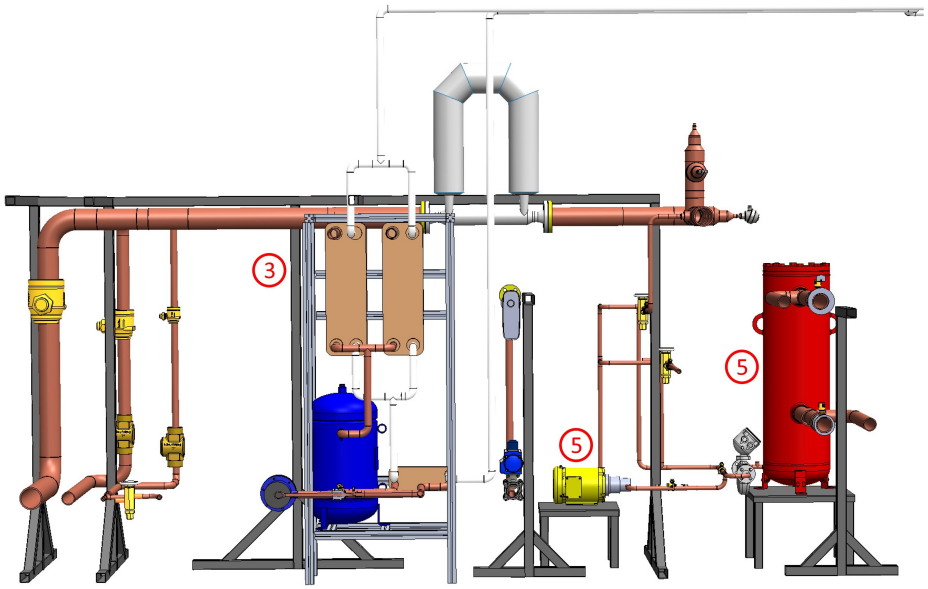

Figure 3.4: Section view of load stand design to highlight the vertical arrangement of the labeled components.

Table 3.6: Component list

Label	**Major Component**
1	Compressor
2	Mass Flow Meters
3	Heat Exchangers and Liquid Receiver
4	Main Loop Circuits
5	Oil Separator and Oil Pump
6	Double Risers

CHAPTER IV

MAJOR COMPONENT SIZING

With the results from the model, the components needed for load stand operation could be sized and selected. This portion of the thesis will detail these sizing efforts, and how the final selection was obtained. All load stand components needed to have a max working pressure of at least 650 psi, and have a max temperature rating of at least 250°F. Due to the discharge vibration absorber, detailed later in this chapter, the current max working pressure is 500 psi.

4.1 Refrigerant Tubing

The load stand will circulate refrigerant throughout the system using copper tubing. The size of the tubing is dependent on its purpose and its location in the system. Using the key parameters found in the thermodynamic model, and utilizing the line sizing tables specific to each refrigerant found in the *2010 ASHRAE Handbook: Refrigeration* (2010), the size of the refrigerant tubing could be determined. A portion of the table used is found in the figure 4.1 below.

At the previously mentioned design conditions corresponding to 80 tons cooling capacity, the model provided the capacity for each of the three line types in the main loop: suction, discharge, and liquid. The proper line size could then be determined for the given capacity, saturated suction temperature, and condensing temperature. Not shown in Figure 4.1 is a table of capacity correction factors relating to the condensing temperature. The results being a suction line/tube size of 4-1/8", a discharge line size of 3-1/8", and a liquid line size of 1-1/8". Due to the high side and low side pressure

Table 5 Suction, Discharge, and Liquid Line Capacities in Tons for Refrigerant 134a (Single- or High-Stage Applications)

Line Size	Suction Lines (Δt = 2°F) Saturated Suction Temperature, °F					Discharge Lines (Δt = 1°F, Δp = 2.2 psi/100 ft)			Line Size	Liquid Lines See notes a and b	
Type L Copper, OD	0	10	20	30	40	Saturated Suction Temperature, °F			Type L Copper, OD	Velocity = 100 fpm	Δt = 1°F Δp = 2.2
	Corresponding Δp, psi/100 ft										
	1.00	1.19	1.41	1.66	1.93	0	20	40			
1/2	0.14	0.18	0.23	0.29	0.35	0.54	0.57	0.59	1/2	2.13	2.79
5/8	0.27	0.34	0.43	0.54	0.66	1.01	1.07	1.12	5/8	3.42	5.27
7/8	0.71	0.91	1.14	1.42	1.75	2.67	2.81	2.94	7/8	7.09	14.00
1 1/8	1.45	1.84	2.32	2.88	3.54	5.40	5.68	5.95	1 1/8	12.10	28.40
1 3/8	2.53	3.22	4.04	5.02	6.17	9.42	9.91	10.40	1 3/8	18.40	50.00
1 5/8	4.02	5.10	6.39	7.94	9.77	14.90	15.70	16.40	1 5/8	26.10	78.60
2 1/8	8.34	10.60	13.30	16.50	20.20	30.80	32.40	34.00	2 1/8	45.30	163.00
2 5/8	14.80	18.80	23.50	29.10	35.80	54.40	57.20	59.90	2 5/8	69.90	290.00
3 1/8	23.70	30.00	37.50	46.40	57.10	86.70	91.20	95.50	3 1/8	100.00	462.00
3 5/8	35.10	44.60	55.80	69.10	84.80	129.00	135.00	142.00	3 5/8	135.00	688.00
4 1/8	49.60	62.90	78.70	97.40	119.43	181.00	191.00	200.00	4 1/8	175.00	971.00
5 1/8	88.90	113.00	141.00	174.00	213.00	323.00	340.00	356.00	—	—	—
6 1/8	143.00	181.00	226.00	280.00	342.00	518.00	545.00	571.00	—	—	—

Figure 4.1: Line sizing table for R134a. From ©ASHRAE, www.ashrae.org. (2010) ASHRAE Handbook-(Refrigeration).

requirements, type K refrigeration tubing was used for the suction and discharge lines. Additionally, the discharge line used parallel tubes of size 2-5/8" and 2-1/8", whose total cross-sectional area is closest to cross-sectional area of the 3-1/8" tube, to accommodate for the 3-1/8s tube low design pressure. The capacity tables were also used for the economizer circuit, resulting in an economizer liquid line size of 1/2", a bypass line of 1-3/8", and a suction line of 2-1/8".

Risers are incorporated into a refrigeration system to achieve greater vertical height. When using risers, it is important to ensure that oil is carried up with the refrigerant to be returned to the compressor. Incorporated into the main discharge line, and into the economizer suction line, are double risers. This is due to the vertical arrangement of the heat exchangers and liquid receiver. Even with the oil separator, small amounts of oil will have to be properly managed throughout the load stand. The purpose of the double riser is to entrain oil up the riser at all load conditions, while keeping pressure drop at a minimum. Figure 4.2 below shows two examples of how one might use double risers in the suction line.

Regardless of method type, riser A is sized to return oil at the minimum load, while riser B is sized so that the combined cross sectional area of A and B is slightly greater than the cross sectional area of a single riser sized for maximum load. An oil

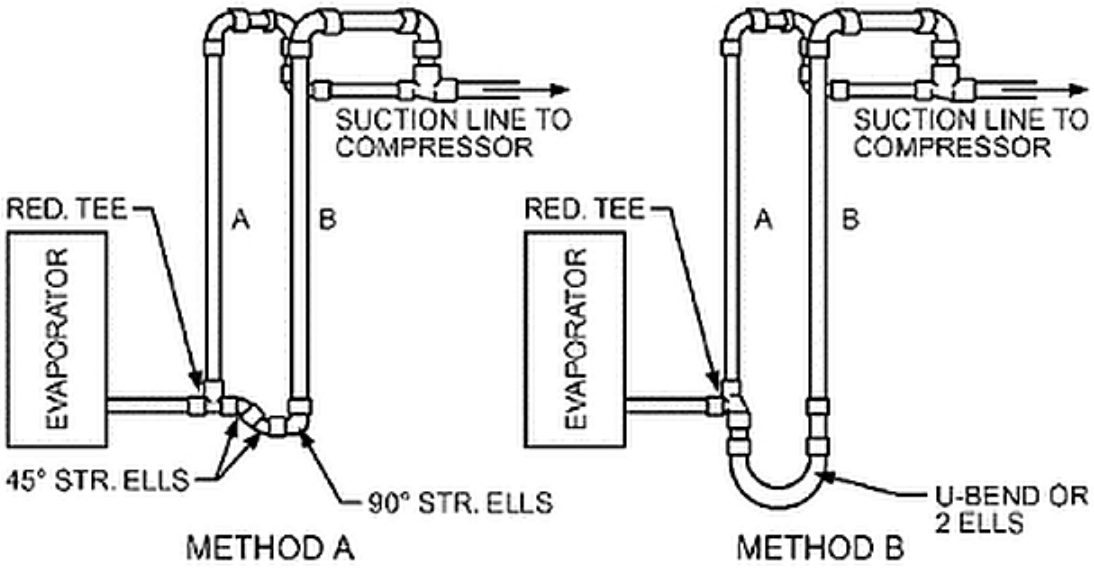

Figure 4.2: Double riser configurations. From ©ASHRAE, www.ashrae.org. (2010) ASHRAE Handbook-(Refrigeration).

trap is created between the two tubes, that when operating at part load, the trap will fill with oil forcing the refrigerant flow up the smaller riser A. Using the riser sizing tables in the *2010 ASHRAE Handbook: Refrigeration* (2010), the two double risers could be sized. The results of which are: Discharge riser A 2-1/8, B 2-5/8, Economizer riser A 1-3/8, B 1-5/8.

4.2 Water Piping

The load stand water loop circulates water through the subcooler and condensers to provide the required amount of cooling necessary to reject the work done by the compressor. The water is cooled in two intermediate brazed plate heat exchangers by the chilled water supplied by OSU. It is then pumped to the load stand where it absorbs the heat from the refrigerant, and then returns to transfer that heat back to the campus chilled water. Figure 4.3 shows the water line schematic. Water PVC piping had already been run to the location of the load stand from previous projects, so depending on the pipe size requirements, this piping could be re-used. A maximum

water mass flow rate of 1 kg/s had been determined from the heat exchanger sizing calculator, and needed to flow through the 1" PVC pipe that was to be reused. The pressure drop the pump needed to overcome at 1 kg/s could be determined using the energy equation (4.1) for a single path pipe system.

$$\left(\frac{p_1}{\rho} + \alpha_1 \frac{\bar{V}_1^2}{2} + gz_1\right) - \left(\frac{p_2}{\rho} + \alpha_2 \frac{\bar{V}_2^2}{2} + gz_2\right) = \sum h_l + \sum h_{l_m} \tag{4.1}$$

$$h_l = f\frac{L}{D}\frac{\bar{V}^2}{2} \tag{4.2}$$

$$h_{l_m} = K\frac{\bar{V}^2}{2} \tag{4.3}$$

The pipe length was estimated to be 92 feet. Minor losses (K) coming from 28 90°elbows, four tees, and two ball valves, added up to a value of 27.7. Using these values with the known mass flow rate and diameter, the pressure drop of the water line piping and components was found to be around 30 psi. This required pressure drop and flowrate is easily achieved with the current water pump and VFD talked about later in this chapter.

4.3 Oil Separator

Downstream of the compressor, but upstream of the discharge mass flow meter, is an oil separator. Its purpose is to remove most of the oil from the discharge refrigerant gas, and send it back to the compressor through the oil circuit described earlier. A coalescent type oil separator was chosen due to its superior filtering ability compared to conventional oil separators. Figure 4.4 below illustrates the working mechanism behind these type of separators.

The discharge refrigerant flow enters the oil separator and passes through the filter where the oil droplets collide to form larger droplets, and eventually fall to

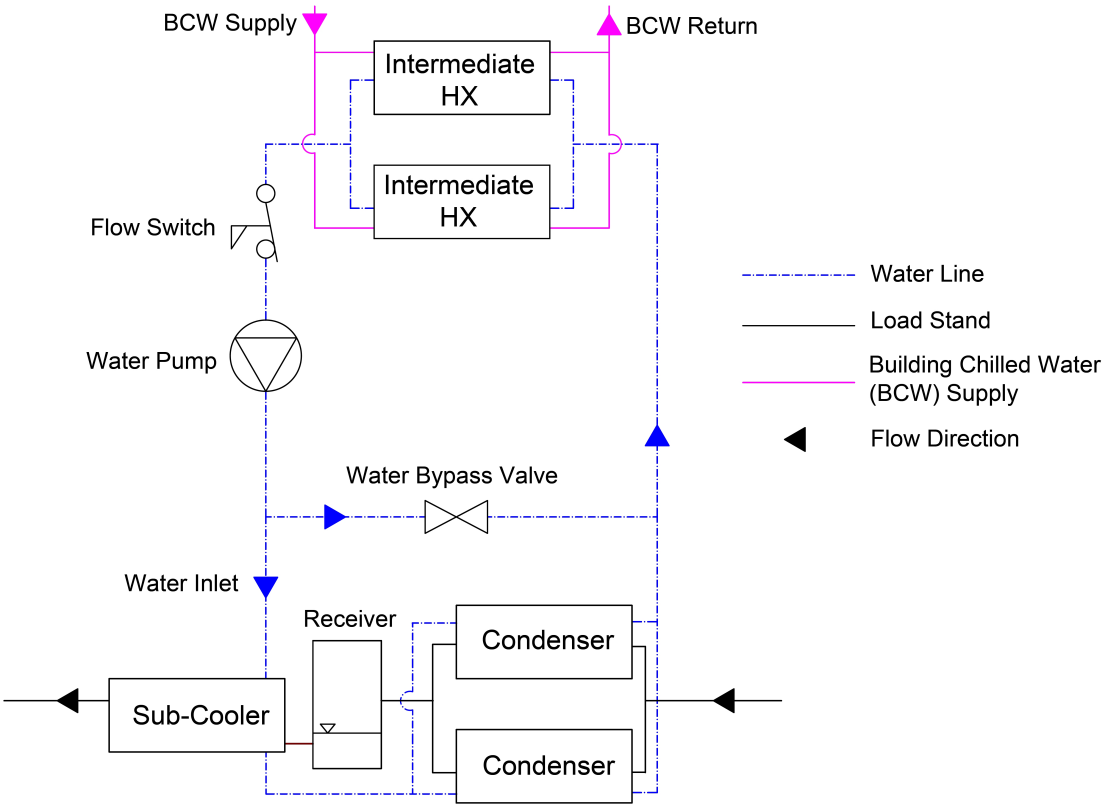

Figure 4.3: Schematic of the load stand water loop.

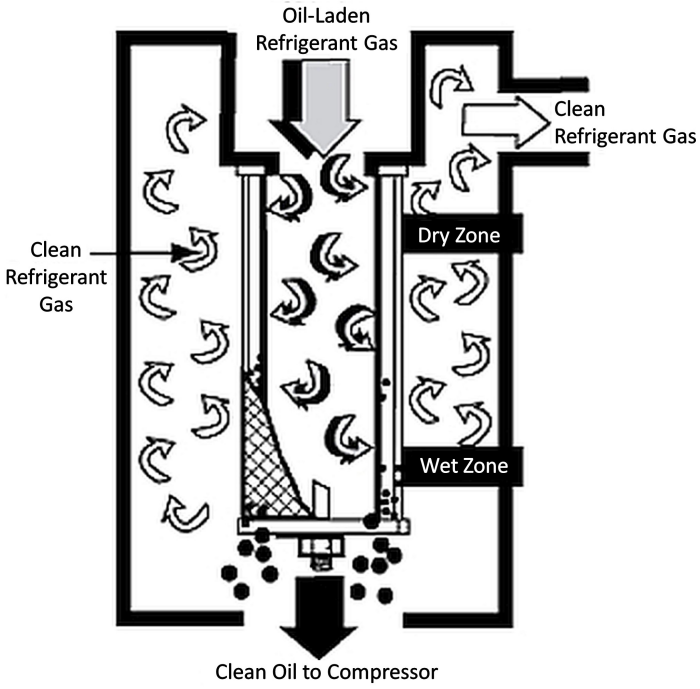

Figure 4.4: Coalescent oil separator cross section. Source: Temprite (2018)

	Model	922 922R	923 923R	924 924R	925 925R	926 926R	927 927R	928 928R	930 930R
	Connection Size	5/8"	7/8"	1-1/8"	1-3/8"	1-5/8"	2-1/8"	2-5/8"	3-1/8"
Refrigerant	Temp °F	Tons @ 100°F Condensing 10°F Superheat 0°F Subcooling							
R-1234yf	+40	5.4	7.5	13.5	20.5	35.1	47.9	80.0	136.0
	+30	4.4	6.1	10.9	16.6	28.4	38.7	64.7	110.1
	+20	3.5	4.9	8.8	13.3	22.8	31.1	52.0	88.3
	+10	2.8	3.9	7.0	10.6	18.1	24.7	41.3	70.3
	0	2.2	3.1	5.5	8.4	14.3	19.5	32.6	55.3
	-10	1.8	2.5	4.5	6.8	11.7	15.9	26.6	45.1
	-20	1.3	1.8	3.3	5.0	8.6	11.7	19.5	33.2
	-30	1.0	1.4	2.5	3.8	6.5	8.9	14.9	25.2
	-40	0.8	1.0	1.9	2.9	4.9	6.7	11.1	18.9
R-1234ze	+40	4.3	5.9	10.7	16.2	27.7	37.8	63.1	107.3
	+30	3.4	4.7	8.5	13.0	22.2	30.3	50.6	86.1
	+20	2.7	3.8	6.8	10.3	17.7	24.1	40.3	68.4
	+10	2.1	3.0	5.3	8.1	13.9	19.0	31.7	53.8
	0	1.7	2.3	4.2	6.3	10.8	14.7	24.6	41.9
	-10	1.3	1.8	3.2	4.9	8.3	11.3	18.9	32.2
	-20	1.0	1.3	2.4	3.7	6.3	8.6	14.4	24.5
	-30	0.7	1.0	1.8	2.8	4.7	6.4	10.8	18.3
	-40	0.5	0.7	1.3	2.0	3.5	4.7	7.9	13.5
R-134a	+45	6.31	8.78	15.80	24.02	41.12	56.05	93.82	159.21
	+40	5.7	7.9	14.2	21.6	37.0	50.5	84.4	143.4
	+30	4.6	6.4	11.5	17.5	30.0	40.8	68.2	116.0
	+20	3.7	5.1	9.2	14.0	24.0	32.7	54.6	92.8
	+10	2.9	4.1	7.3	11.1	19.0	25.9	43.3	73.6
	0	2.3	3.2	5.7	8.7	14.9	20.4	34.0	57.9

Figure 4.5: Oil separator sizing tables. Source: Temprite (2018) - values in table are subject to change without notice.

the bottom of the separator where it collects in the built in reservoir. The clean refrigerant gas is then passed through the separator exit to move on to the rest of the system. According to Temprite, the coalescent style is able to remove around 98.5% of the oil in the refrigerant.

To determine the appropriate separator model, the sizing charts found on the Temprite (2018) website were used. Entering the appropriate conditions shown in Figure 4.5 into the model, the 928R most closely matched the capacity results. The final selection, however, was the 930R model. Temprite specifies to select an oil separator with a connection size no less than the discharge line size, thus requiring the next model size up with a 3-1/8" connection size. A bigger separator will also help with minimizing pressure drop, as well as, ensuring enough oil is returned.

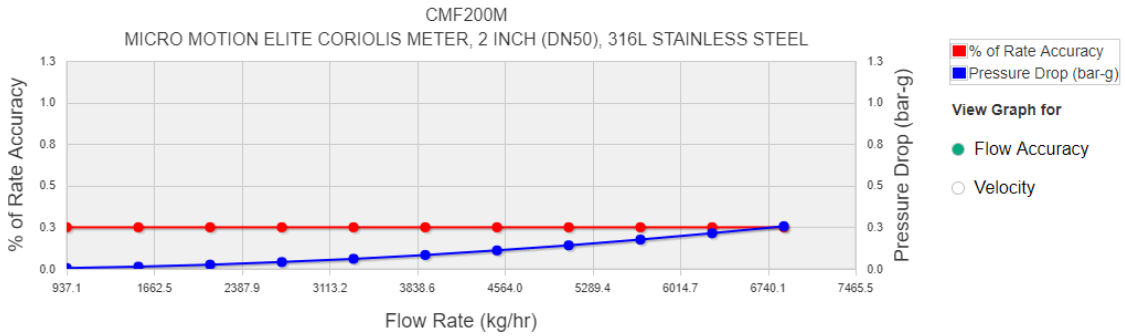

Figure 4.6: Mass flow rate vs. accuracy and pressure drop for the discharge flow meter selection. Source: Emerson (2018*b*)

4.4 Mass Flow Meters

Due to the hot-gas bypass style of the load stand, several mass flow meters are required, and are strategically placed throughout the load stand to measure the refrigerant mass flow rate. The position of these flowmeters can be found in Figure 3.1. Coriolis mass flow meters are used due to their high accuracy when compared to the many other types of mass flow meters, such as an orifice plate flow meter. Refer back to Table 3.4 to find the accuracies of the load stand meters. These type of meters use the Coriolis effect to create two sine waves from the voltage generated from oscillating tubes as mass is passed through them. The time delay between the sine waves is proportional to the mass flow rate.

Sizing the flow meters required the use of the sizing calculator found on the Emerson (2018*b*) website. Inputting the required parameters found from the model into the calculator results in a list of suitable meter candidates. The best candidate would have the least amount of pressure drop without sacrificing accuracy. Figure 4.6 shows the graph of accuracy and pressure drop vs flow rate over the entire load stand capacity range, refer back to Table 2.2, given by the calculator for the discharge mass flow meter. It illustrates relatively low pressure drop while maintaining constant accuracy. The list of chosen flow meters is found in Table 3.4.

4.5 Heat Exchangers

Two parallel water cooled brazed plate heat exchangers are used as condensers, and another water cooled brazed plate heat exchanger downstream of the liquid receiver is used as a subcooler. The purpose of the condensers are to reject the heat or work from the compressor, while the subcooler ensures that the liquid refrigerant does not flash before reaching the liquid expansion valves. Danfoss provides a heat exchanger sizing calculator, Hexact (2018), so that the appropriate selection could be made. Providing the calculator with inputs such as required load, refrigerant mass flow rates, and water inlet and outlet temperatures to just name a few, the right model could be chosen. The required load is 88 kW and 8 kW for the parallel condensers and subcooler, respectively. The design refrigerant mass flow rate is 0.5 kg/s, with a water inlet and outlet temperature of 11°C and 34°C. Ultimately, the required parameters were sent to Danfoss representatives for heat exchanger selection. The results are as follows: Condenser B3-095-50-4.5-L ; Subcooler B3-027-8-4.5-L. Appendix D shows the calculator inputs with the results.

4.6 Liquid Receiver

The liquid receiver is located between the condensers and the subcooler. The purpose of the liquid receiver is to ensure liquid refrigerant is supplied to the subcooler, and additionally acts as a reservoir for refrigerant charge storage and control. The selection procedure from Henry Technologies suggests to base storage capacity needs on the operating charge of all system components, including liquid and gas tubing. To calculate the required charge for the maximum load stand conditions, the total volume of all tubes and components needed to be determined. Based on whether gas or liquid would occupy the tube or component, the volume would then be divided by its liquid/gas specific volume to find the refrigerant mass. The mass was found for the discharge, suction, liquid, and economizer tubing, the heat exchangers, compressor,

and a percentage of the liquid receiver.

Using a condensing temperature of 158°F with the corresponding saturation pressure of 230 psi, the specific volume of R134a at a saturated vapor state and a saturated liquid state is found to be 0.134 ft^3 lbm^{-1} and 0.0162 ft^3 lbm^{-1}, respectively. The volumes of the gas and liquid tubing and components divided by its respective specific volume yields the refrigerant mass in each component. The total mass of the refrigerant gas is found to be 27.62 lbm, while the mass of the liquid is 64.37 lbm.

Another significant source of refrigerant mass that needs to be taken into account is the mass dissolved in the oil. Equation 4.4 is used to find this dissolved refrigerant mass.

$$m_{ref,oil} = m_{oil}(1 - x_{oil}) \tag{4.4}$$

Using the Daniel plots for a 32 POE oil from Lubrizol, the oil mass fraction at the conditions stated above is found to be 0.697. The mass of the oil is calculated from the full capacity value of the oil separator (5.7 gallons) and the oil density. The resulting mass of refrigerant dissolved in oil is 14.13 lbm.

The resulting refrigerant charge needed for maximum load stand operation is 106lb of R134a. This value is very generous as it assumes all the heat exchanger volumes are filled with liquid, as well as, 40% of the liquid receiver is filled with liquid. The final selection found to be sufficient is the model S-8550-HP, which has a pump down capacity of around 97lbs of R134a.

4.7 Filter Drier

The filter drier is located in the main liquid line downstream of the subcooler. Its purpose is to remove moisture and acid while also providing filtration of any small particulates. The drier can be isolated from the system and bypassed by isolation ball valves at its inlet and exit. This is useful for servicing the component, or for

situations in which it will not be used. Danfoss assisted with the selection, with the result being the DCR0489s with the 48-DC filter. This type of filter was chosen so that both moisture and acid are addressed and removed.

4.8 Oil Pump and Motor

The independent oil management circuit is equipped with an oil motor and oil pump. The pump is used when the head pressure or compressor shell pressure is high enough to cause limited to no oil flow. When the pressure difference between the oil line and the suction line or compressor shell is high, then the pump and motor are bypassed altogether. Assuming the maximum needed oil flow rate is 3% of the maximum compressor mass flow rate, the appropriate pump and motor is selected. The Micropump GC-M25.PVS.E is selected with the Baldor CEM3545 motor.

4.9 Control Valves

4.9.1 Main Line Bypass Expansion Valves

The main line bypass valves serve the purpose of expanding the hot discharge gas to suction pressure before it is mixed with the expanded liquid refrigerant. The sizes of each were determined from sizing tables on the Emerson (2018*a*) website, with those tables found in Appendix C. Using the thermodynamic model, the nominal capacities in tons for each bypass line were found based on the evaporating temperature, condensing temperature, and amount of subcooling. With verification with the Emerson representatives, the valves selected for the large, medium, and small bypass lines were the EX8, EX7, and EX7, respectively.

4.9.2 Main Line Liquid Expansion Valves

The main line liquid valves serve the purpose of expanding the liquid refrigerant to suction pressure before it is mixed with the expanded discharge gas. Using the

Coolselector2 (2018) sizing program from Danfoss, the appropriate valves were selected. Coolselector2 takes inputs such as the capacity or mass flow rate through the valve, the evaporating and condensing temperatures, and the amount of superheat and subcooling. Again, using the model to enter the maximum and minimum conditions for each liquid line tube size, the ETS 25, ETS 12.5, and ETS 6-18 were selected for the large, medium, and small liquid lines, respectively.

4.9.3 Economizer Circuit Bypass and Liquid Expansion Valves

With identical purposes as listed above, the economizer bypass and liquid valves help create the desired injection condition. The two liquid valves sized by Coolselector2 were found to be the ETS 6-18 and ETS 6-10. The two bypass valves were sized with help from Sporlan, with the selected models being the SDR 5 and SDR 3.

4.9.4 Oil Metering Valve

There is one oil metering valve on each circuit of the independent oil management system. These valves will control the ratio of flow split between the suction return line and the injection line if both circuits are used simultaneously. If only one circuit is being used, the valve will control the amount of oil returning to the compressor. The Cv factor needed to be calculated before a valve size could be chosen. Equation (4.5) was used to find the Cv value at the design conditions with a maximum oil flowrate of 1 gpm. The design Cv value is 0.07, with a pressure difference of 193.3 psi and a specific gravity of 0.98.

$$Cv = \frac{GPM}{\sqrt{\frac{\Delta p}{S.G.}}} \tag{4.5}$$

With the required Cv value, the appropriate selection could be made with the Cv vs Number of Valve Handle Turns graph found on the HOKE website. The 2315F4Y of the 2300 Series metering valves for liquids and gas was chosen with the 0121A2E

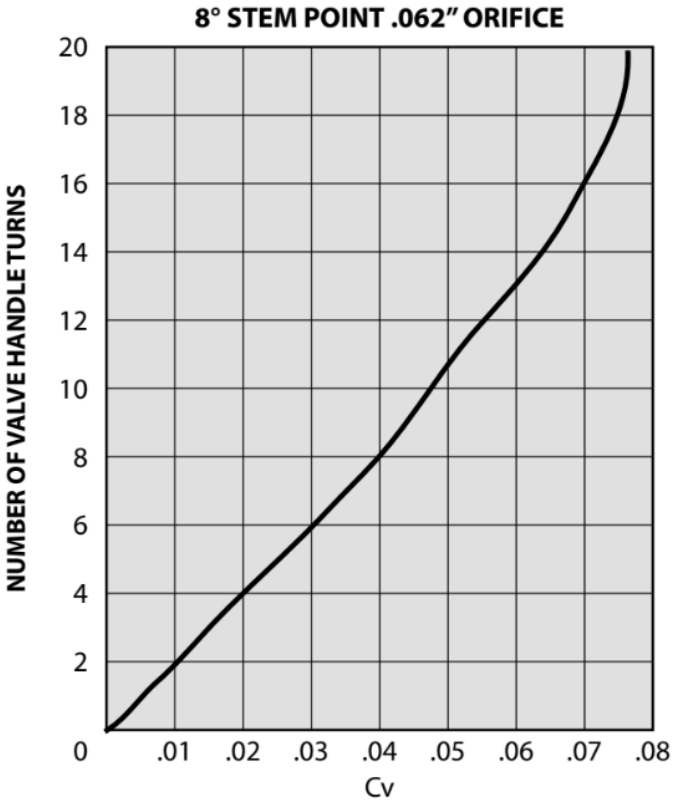

Figure 4.7: Cv vs. number of valve handle turns for the selected 2300 series metering valve. Source: Hoke (2018)

electric actuator, and the accompanying graph shown in Figure 4.7.

4.9.5 Water Bypass Valve

A water bypass valve is located above the heat exchangers between the supply and return cooling water lines. It will be used for course control over the water flowrate heading toward the subcooler and condensers. The valve needed to be able to handle the estimated maximum water flow rate of 1 kg/s (16 gpm), which was determined from the heat exchanger sizing data. The Danfoss 1-1/4 ABQM pressure independent control valve was selected, having a maximum flow rating of 17.5 gpm. Along with the valve, the AME120NLX-1 electric actuator was chosen for valve control.

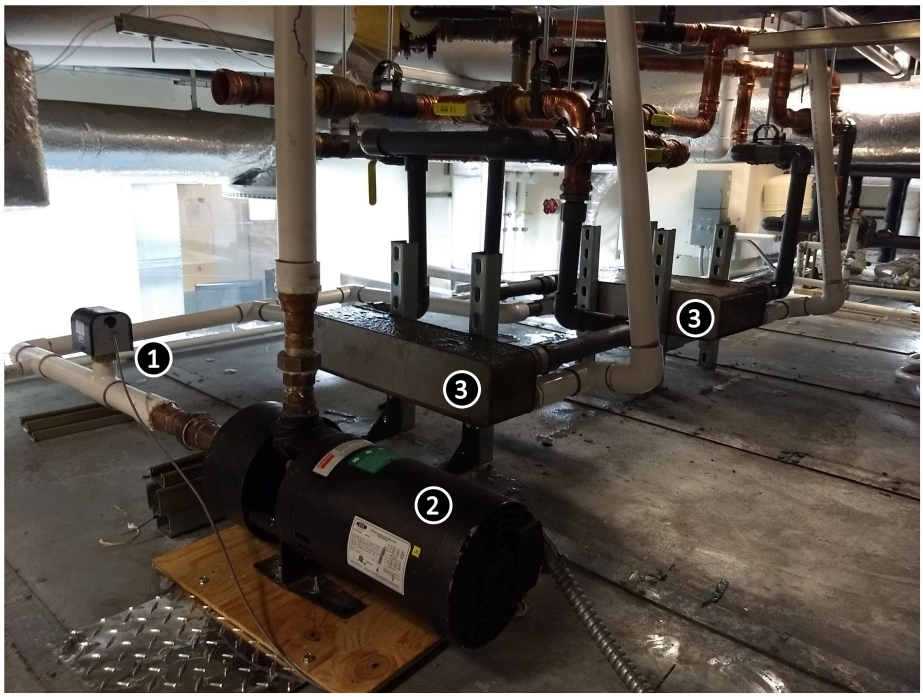

Figure 4.8: New campus chilled water piping with new arrangement of flow switch (1), water pump (2), and heat exchangers (3). Picture taken on top of psychrometric rooms.

4.10 Water Pump and Flow Switch

The pump and water flow switch being used for the water loop were re-used from past experiments. The pump is a Dayton 2 horsepower booster pump (5UXJ1) that is capable of about twice the required pressure drop for the maximum water flow rate of 16 gpm. The flow switch is a model FS-251 from McDonnell & Miller. The water pump is powered with a 5hp VFD, and will serve as the fine control over the water flowrate. To ensure no refrigerant leakage into the campus chilled water line, two brazed plate heat exchangers serve as intermediate heat exchangers between the campus chilled water and the load stand water loop. All of these components sit on top of the psychrometric chambers that are located adjacent to the load stand in the ATRC high bay area. A complete overhaul of the campus water piping was completed for ease of maintenance while working on top of the rooms, as well as, for future projects. A picture of the new waterline setup is shown in the Figure 4.8.

4.11 Variable Speed Drives

The load stand is equipped with three variable frequency drives: one for the compressor, one for the oil pump, and one for the water pump. The compressor VFD is sized for 110kW (150hp), which is based of the estimated maximum compressor power (94kW) from the model plus 10%. The oil pump VFD is sized for 1.5hp, corresponding to the the previously mentioned 1 hp oil motor. The water pump VFD is sized for 5 hp, thus giving some wiggle room if a bigger sized water pump is ever needed. The compressor VFD is an ABB ACH550-BCR-180A-4+F267, the oil pump VFD is an ABB ACH550-UH-03A3-4, and the water pump VFD is a DURApulse GS3-45P0.

4.12 Vibration Eliminators

Due to the high vibration levels some of the bigger compressors will generate, vibration eliminators are installed on the suction,discharge, and economizer lines. Their purpose is to protect the load stand from these vibrations that can cause mechanical damage and failure over time. For selection, the vibration eliminators needed to be able to withstand the maximum pressure of 650 psi on the discharge line, 250 psi on the suction line, and 260 psi on the economizer line. The highest pressure rating available for a 2-5/8 vibration eliminator for the discharge line is 500psi. When testing compressors with high density refrigerants, the vibration eliminator will have to be replaced with regular copper tubing. The resulting selection from Henry Technologies was the VS-2-5/8, VS-4-1/8, and V-2-5/8 for the discharge, suction, and economizer lines, respectively.

4.13 Pressure Relief Valve

As the last line of defense, a pressure relief valve is installed on the discharge line between the compressor and the discharge isolation ball valves to protect from over pressurization. This valve needed to be able to evacuate the high pressure refrigerant at the minimum regulated mass flow of the compressor. Assuming a compressor turn down rate of 60%, the example in ASHRAE-15 (2016) is followed. The result is a design SCFM of 556 ft^3/min of air. Using this air-equivalent design flow rate, a pressure relief valve could now be chosen. Currently, a valve has not yet been selected, due to the pressure limit of the vibration absorber on the discharge line being so low.

CHAPTER V

CONSTRUCTION

The load stand was set to be constructed in the high bay area of the ATRC lower basement in room 042. Prior to building, a few maintenance tasks needed to be completed. First, an old dynalene chiller located outside of the indoor psychrometric room, seen in Figure 5.2, was disassembled and removed along with two other items. Secondly, a mezzanine was constructed in room 042 so that the load stand could sit underneath. The purpose of this mezzanine was for storage, as well as, for needed infrastructure supporting the load stand. With these tasks completed, the area was clear and ready for construction.

The load stand takes up approximately 108 sq. ft., and has the overall dimensions 13-6 long, 8 wide, and 5-10 high, with the highest point (top of discharge mass flow meter) being 6-6. It is positioned in the far back corner entirely underneath the 280 sq. ft. mezzanine. The overall dimensions of the mezzanine are 17-8 long, 15-8 wide, and 9 under clearance. Figure 5.1 shows the mezzanine deck plan, with its placement shown in Figure 5.2. Figure 5.3 shows the load stand underneath the mezzanine. Both the mezzanine and load stand had to be at least 3 feet from the wall and/or electrical panel to allow enough space to walk through.

5.1 Frame

The supporting structure of the stand is composed of 1/4 thick steel 2 square tubing. Leg pieces welded by Stillwater Steel are positioned around the main loop, and are connected by straight pieces of steel tubing. The connecting joints are held

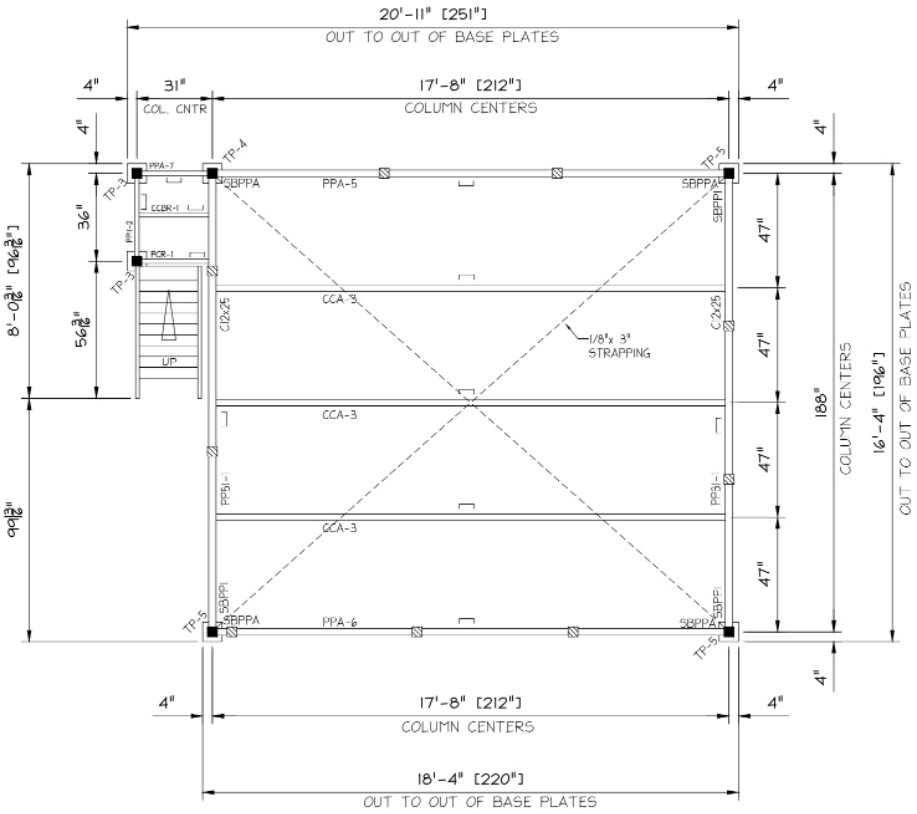

Figure 5.1: Mezzanine framing plan, top view

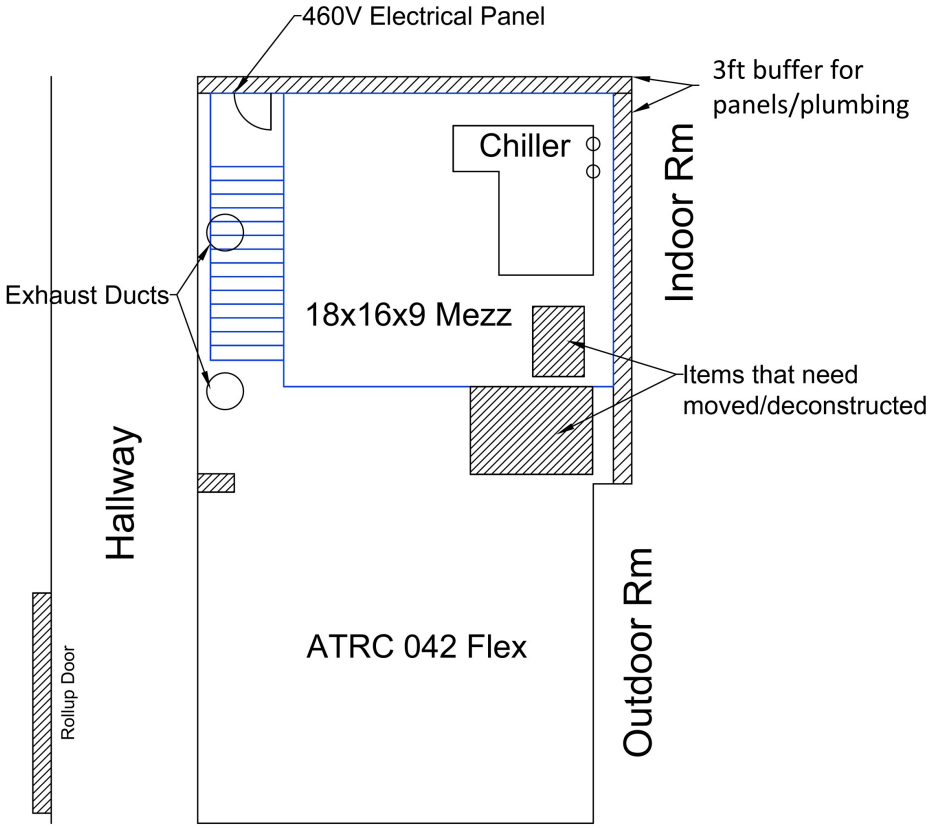

Figure 5.2: Location of mezzanine in ATRC 042

Figure 5.3: Completed load stand (red) underneath the mezzanine (blue)

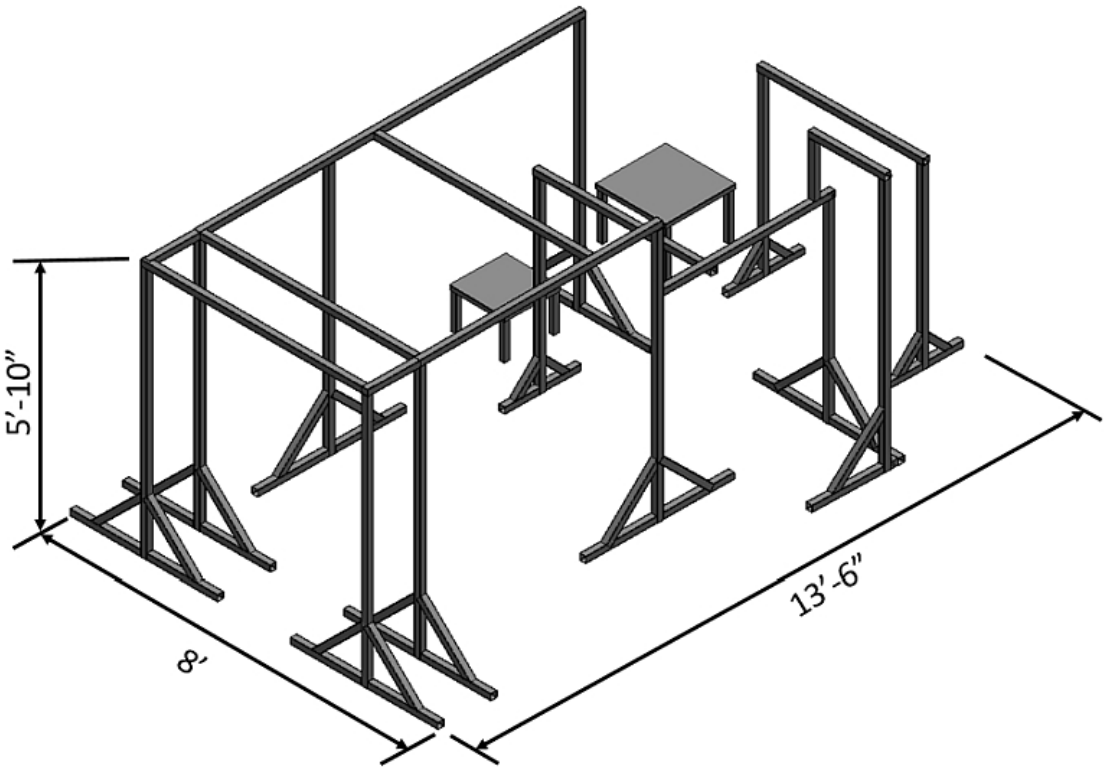

Figure 5.4: 3D CAD model of the load stand frame

together by 3/16 thick steel brackets and 3/8 bolts. Each leg has been bolted to the concrete floor to ensure stability and strength when exposed to the extreme vibrations caused by compressor testing. Two small tables also welded together by Stillwater Steel provide support to the oil separator and oil pump motor. The top piece is a 3/16 steel plate on top of four 1/4 thick steel 1-1/2" square tubing. Both the motor and separator have been bolted to its respective table. All of the framing and both tables have been powder coated in a black matte finish for corrosion protection, as well as, for a professional visual presentation. Figure 5.4 shows the frame design.

The vertical arrangement of the heat exchangers and liquid receiver are supported by 1-1/2" t-slotted aluminum framing. This type of framing allowed for greater flexibility to accommodate slight design changes and orientations of the components. Like the steel framing, this aluminum stand is bolted to the ground. A drain channel, with grating along the top, runs underneath a portion of this stand. Unable to be

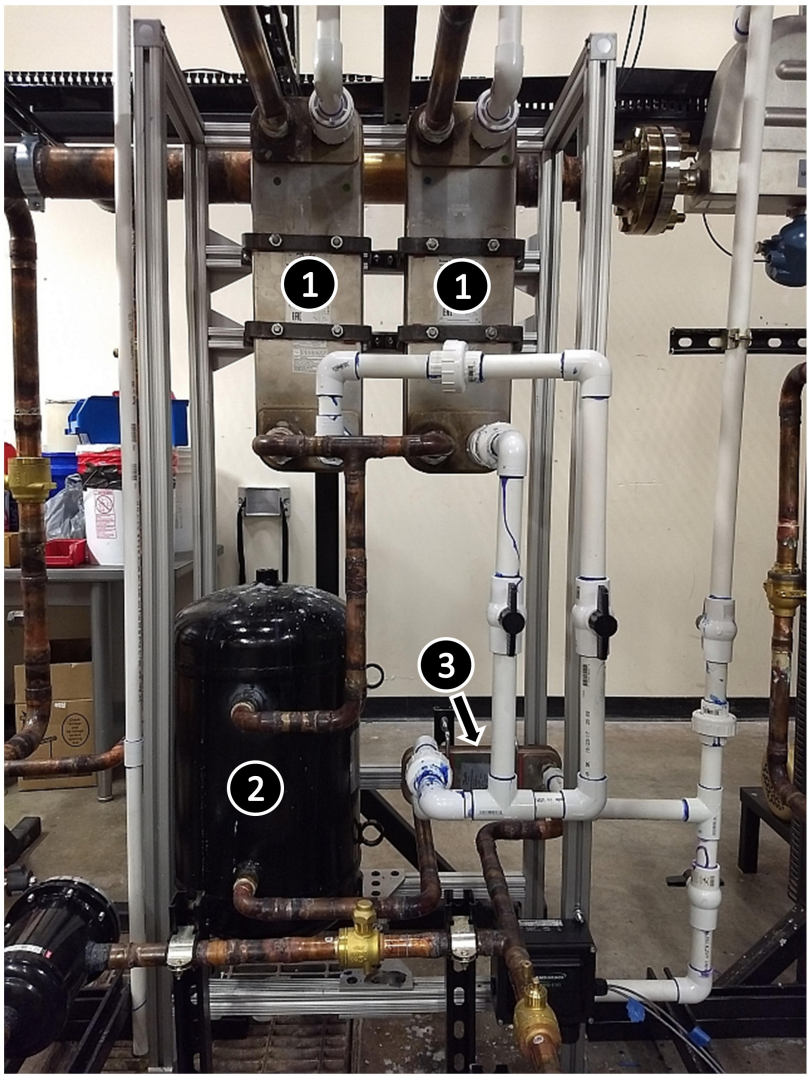

Figure 5.5: Vertical arrangement of condensers (1), liquid receiver (2), and subcooler (3) oriented on the aluminum framing stand and bolted to the concrete and drain grate.

bolted to the concrete, the two legs that sit on the grating are anchored down by u-bolts. Figure 5.5 shows the vertical arrangement.

The original frame design did not account for support of the main liquid line, economizer liquid line, and their various components. To provide this needed support, a structure of unistrut pieces was built underneath the liquid lines. This structure is composed of a base of horizontal unistrut pieces spanning across the length and width of the liquid and economizer tubing. The base is bolted to the concrete, and vertical unistrut pieces anchored to the base rise vertically to a height just above the

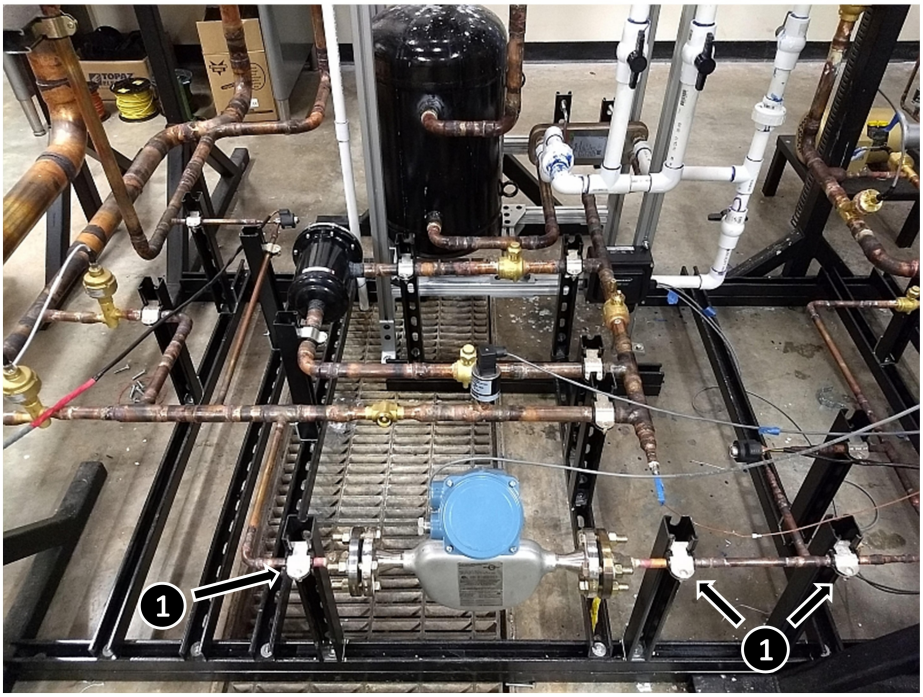

Figure 5.6: Unistrut structure built to support liquid and economizer tubing and components with unistrut tube clamps (1).

tubing to clamp onto the tube. Figure 5.6 shows the unistrut structure.

Unistrut was used for much more than just the structure mentioned above, it also provided support for most components and tubing on the load stand. Wherever a supporting connection was needed, unistrut was bolted to the frame to provide the needed connection. Unistrut was used for its ease to work with, as well as, its large library of readily available mounting components, such as the Hydra Zorb tube clamps seen in Figure 5.6. Another example of unistrut support is seen in Figure 5.7. All mass flow meters have been supported like the ones shown in Figures 5.6 and 5.7. The tube clamps used for tubing support have a vibration damping plastic cushion. These tube clamps are good to use on the discharge tubing as their maximum temperature limit is above 250°F.

The compressor sits on a heavy duty machine table with a capacity of 14,000 lbs. The top is 1/4" thick steel plate that is 6 long and 3 wide, and that sits 2 off of the ground. The table sits on 7/8 thick vibration damping pads for vibration isolation,

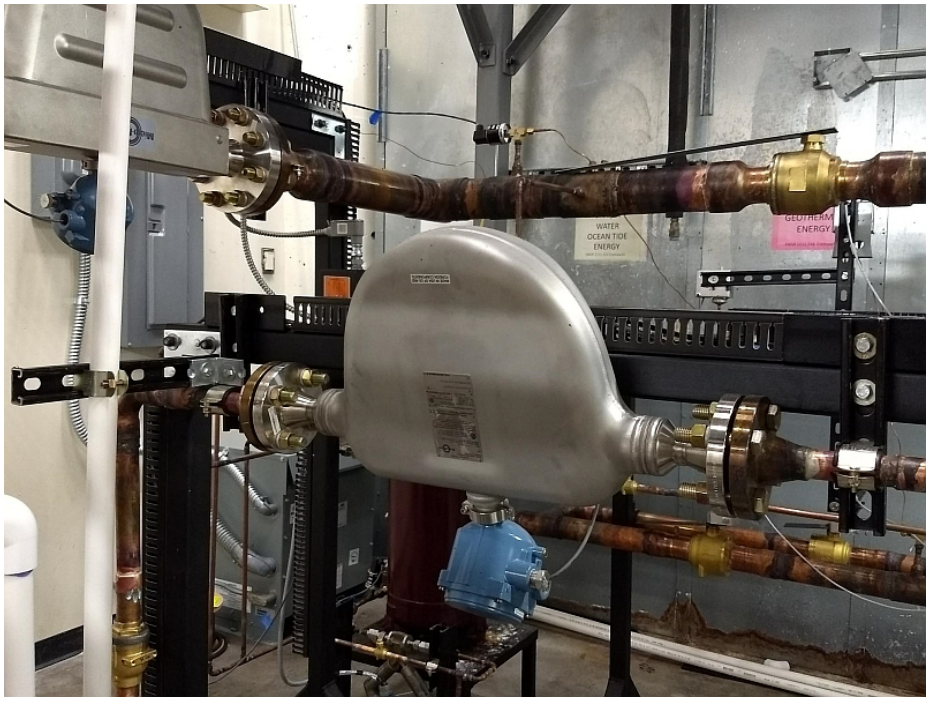

Figure 5.7: Economizer gas mass flow meter supported by unistrut tube clamps, with added unistrut support for the PVC water line piping (left).

with the compressor bolted to the table as shown in Figure 5.8. The table needed to be positioned toward the very front of the mezzanine to allow for access of a fork lift when swapping out different compressors for testing.

5.2 Brazing and Tube Layout

Perhaps the most time consuming aspect of the construction was the brazing and assembly of the copper tubing. With the frame completed and bolted to the ground, tubing could then be assembled and attached to the supporting structure. To begin, a couple of fixed reference points were needed for correct measurement and spacing. The discharge and suction mass flow meters, and the vertical aluminum stand served as these references. Using the solid works model, the suction and discharge mass flow meters were placed and supported on the frame with temporary unistrut mounts. Then the aluminum stand was assembled and positioned with the corresponding components mounted in place. With these components now in the correct

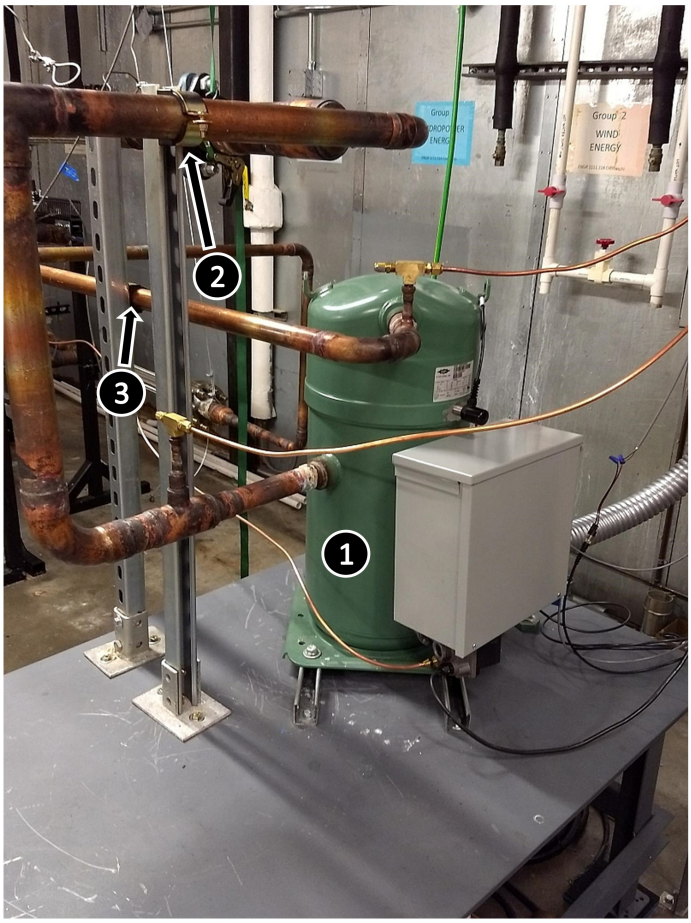

Figure 5.8: 40 ton scroll compressor (1) bolted down to steel machine table with unistrut tube clamps supporting the suction (2) and discharge (3) lines.

position, the rest of the stand could be assembled and built up around them. The solidworks model served as a rough guideline for the layout and orientation of the tubing and components, but exact measurements had to be taken as the assembly progressed to ensure that the tube joints lined up correctly.

Brazing was done with an oxy-acetylene torch setup with a variety of torch tips. 15% silver braze rod was used for the copper to copper joints, while high silver (45-55%) rod was used for copper to steel joints. The smaller tube sizes, up to 1-1/8, just needed the small 0 tip size welding nozzle that came standard with the torch kit. The medium tube sizes, up to 2-5/8, required the use of the MFA 4 rose bud heating nozzle. The large tube sizes, up to 4-1/8, required the use of the MFA 6 rose bud heating nozzle. When possible, brazing was performed away from the stand, and on

Figure 5.9: Beginning of tube assembly process as main loop tube sections are attached to the frame.

the welding tables in the high bay. This gave for more working space, and allowed the tubes to be oriented in the position that made brazing as easy as possible. Brazing the tubes in position on the stand was only done when necessary. Because of this, the majority of the load stand tubing was brazed in sections on the welding table, and then assembled on the load stand, thus limiting the amount of difficult brazing. Figure 5.9 shows the beginning process of assembling the tube sections.

Another benefit of brazing the tube in sections was that by strategically breaking up the load stand, misalignment of the tubes while assembling could be avoided. This was done by leaving at least two degrees of freedom for each section to allow for movement and adjustment when needed. Typically, straight tube runs in the vertical and horizontal direction were left between sections to allow for this freedom. In order to connect these different tube sections together, the use of temporary supports was needed. Many times this support came from rope or ratchet straps that hung from the frame or the mezzanine above. Figures 5.10 and 5.11 show some examples of how

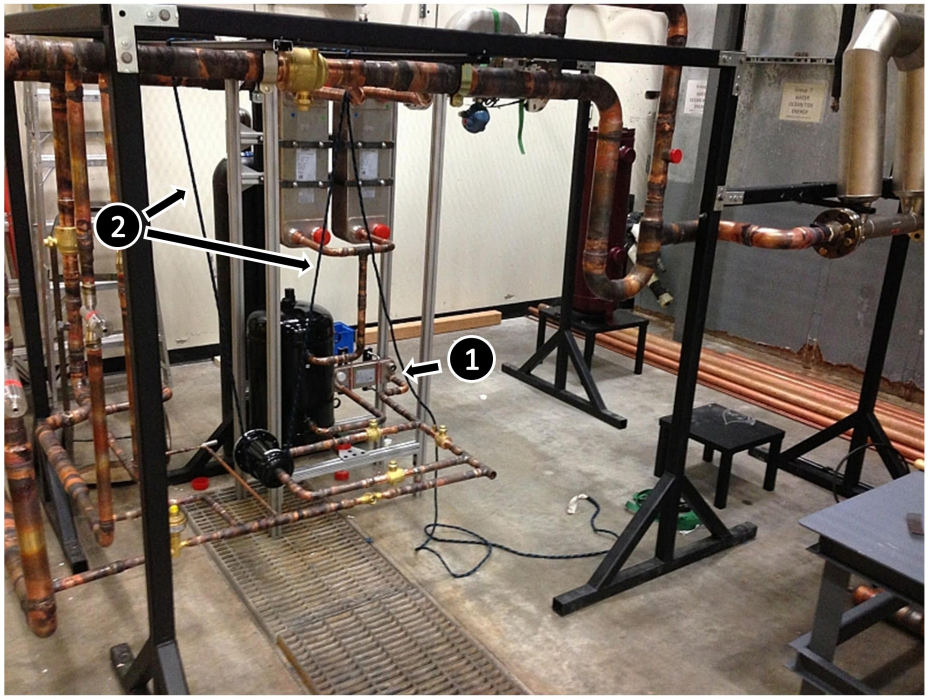

Figure 5.10: Liquid line section put in position and held up by subcooler (1) and temporary rope support (2).

these temporary supports were used.

Soon the majority of the tubing layout was completed up to the compressor manifold. The compressor manifold being defined as all tubing leading to the compressor downstream of the flanged or rotolock connections. All lines leading to the compressor including the suction line, discharge line, and economizer line, have flanged connections, with the oil line having a rotolock adapter. All the flanged connections come directly after the vibration absorbers on the compressor side. Different compressors will require different size tubing and have different port locations for the tubing. The flanged and rotolock connections provide an easy way to disconnect and build a new compressor manifold without having to change anything on the load stand side of the flanges. Figure 5.12 shows most of the tubing completed and assembled on the load stand frame with the exception of the tubing leading to the compressor (compressor manifold). Figure 5.13 shows a completed compressor manifold with the exception of the suction line flange connection after the vibration absorber.

Figure 5.11: Undergraduate research assistant Jake Singleton brazing discharge mass flow meter in place with the help of ratchet straps (1) and the presto lift (2).

Figure 5.12: Most tube assembly completed and showcasing the parallel discharge tubing (right) required due to high pressure requirements.

Figure 5.13: Compressor manifold assembly with the suction line flange connection incomplete.

5.3 Leak Checking and Pressure Testing

When all the tubing is complete, and the system is closed off from the atmosphere, the next step is leak checking. Leaks in the tube system are detrimental when testing, and recharging the system with refrigerant constantly is extremely costly. The only way to know if a brazed joint is leaking is by closing the system and charging it with dry nitrogen through a charging port. Separating the system into smaller sections by using isolating ball valves is recommended to make the leak checking process easier to manage. The process is broken down into four steps.

- **Step 1** The first step is to charge the system to a low pressure with dry nitrogen (in this case to 50 psi), and listen for any audible sounds indicating a leak. This is the easiest step, as it is very clear where the leak is coming from. Mark the joints that need fixing, depressurize the system, and re-braze the joint. Repeat this step until there are no more audible leaks.

- **Step 2** The next step is to charge the system to a higher pressure (in this case 100-150psi), and coat each joint with a leak detection bubble solution. Make sure that the solution completely covers each joint, and after a few minutes check each joint for the formation of any bubbles. Very small leaks might take up to 20 minutes before a bubble colony starts to form, but bigger leaks will create large and visible bubbles. Figure 5.14 shows a small leak bubble colony. Again, mark the joints that need fixing, and re-braze. Once no more bubble colonies are found, pressurize the system, and leave it pressurized overnight. This leads into step 3.

- **Step 3** First record the pressure before it is left overnight, and then check the pressure the next day. Any large decrease in pressure (over 5 psi) indicates that there is still a leak. If steps 2 and 3 are repeated and a leak is still present, then the last step is to use the electronic refrigerant detector.

- **Step 4** Charge the system with a small amount of refrigerant (10 psi), and then charge it with nitrogen to the higher pressures used in previous steps. Move the refrigerant detector around each joint until it alerts that refrigerant is in the air. Mark the joint and re-braze. These four steps should ensure a leak tight system.

Step 3 is a good example of why dry nitrogen is used for leak checking instead of refrigerant. The pressure gauge reads saturation pressure for refrigerants. A leak would not be detected is there is liquid refrigerant in the system because as the refrigerant vapor escapes, the liquid refrigerant would boil off and the saturation pressure would remain the same. Assuming no liquid in the system, a decrease in pressure overnight is possible without any leakage due to the refrigerant being absorbed in the compressor oil. Due to this unreliability, dry nitrogen is used for leak checking.

Once the system is leak free, it then needs to be pressure tested. Both the high

Figure 5.14: Formation of bubble colony due to small leak in brazed joint

side and low side of the system were charged with nitrogen up to the design pressures mentioned earlier (500 psi-high side; 250 psi-low side). The pressures were held for about a minute, and then released safely back to atmospheric through the economizer ball valve.

5.4 Vacuuming and Refrigerant Charging

With the system leak free, pressure tested, and totally closed, the next task was to pull the system under a vacuum using a vacuum pump. This is done before any refrigerant is charged into the system to remove as much moisture as possible. Using a digital vacuum gage for precise vacuum measurement, the system was pulled down to under 500 microns. After waiting 5 minutes to allow for a stable reading, the gage read 750 microns. This indicated that a small amount of moisture was still in the system, but with the use of the filter drier, this remaining moisture could be removed

and the system could be charged with refrigerant. For preliminary testing, around 80 lbs of R134a was put into the system using the charging port on the liquid line.

CHAPTER VI

WIRING AND CONTROLS

6.1 Control and Data Acquisition

The load stand is equipped with a CompactRIO (cRIO) system from National Instruments (NI) that will handle all data acquisition and control requirements. The cRIO is a real-time controller chassis with re-configurable Input/Output (I/O) modules for sensor measurements and valve control, and with a built in FPGA module for more time-critical processes, all of which are programmed with LabVIEW. There are 10 I/O modules, requiring an Ethernet expansion chassis (NI 9144) to overcome the 8 slot limit on the main cRIO chassis (NI 9035). Table 6.1 shows an overview of the different types of cards used for the load stand. All electronic valves, with the exception of the water bypass valve and oil metering valves, utilize controllers that take the 4-20mA current output from the data acquisition system (referred to as the DAQ) and relay the information to the valve. The water bypass valve actuator takes the 4-20mA output directly from the DAQ, while the oil bypass valves require a more complicated method of control. All mass flow meters use remote mount transmitters for control communication.

The oil valve actuators are not operated using a 4-20mA control signal. Because of this, control of these valves became quite challenging. To open and close the valve, 115 VAC is supplied to different terminals, turning the valve stem either clockwise or counterclockwise. With no feedback built into the actuator, there was no way of knowing the stem position at any given time. The solution is to measure the current being supplied to the valves, and to use LabVIEW to record the time it takes to move

Table 6.1: Input/Output module overview

Card #	Type	# of Channels
NI 9266	Current Output	8
NI 9266	Current Output	8
NI 9208	Current Input	16
NI 9208	Current Input	16
NI 9216	RTD's	8
NI 9214	Thermocouple's	16
NI 9205	Voltage Input	16
NI 9472	Digital 24VDC Output	8
NI 9230	Accelerometer	3
NI 9227	Current Measurement	4

from fully open to fully closed. By measuring the current with an Ohio Semitronics current transducer (model# 10418), one is able to determine if the valve is moving or if the valve has reached its upper/lower limit. By knowing the total stem travel time, one can move the valve to any set percentage of open/close.

Most of the I/O modules use the cRIO scan mode due to its ease of development when compared with FPGA programming. Scan mode utilizes the NI scan engine, which automatically detects the I/O modules, and allows for instantaneous read and write ability. The I/O variables can easily be dragged and dropped into the LabVIEW project. Scan mode does not require any FPGA programming, but can only read signals at rates up to 1 kHz. This is fine for most of the load stand measurement and controls, which are using scan mode at a rate of 10 Hz. However, reading the accelerometer and current feeding the oil valves require FPGA programming, at a rate of 12 kHz. The higher rates are required to prevent aliasing, and to provide accurate readings.

All instrumentation and controls, including the LabVIEW cRIO chassis, are powered by either 24 VDC or 24 VAC, excluding the oil valves. The 24 VDC power supply can provide 25 amps, while the 24 VAC supply provides 7 amps. To correctly size the DC supply, the required current draw for all DC powered components needed to be estimated. Table 6.2 below shows the maximum power draw of the DC powered

Table 6.2: Amp draw from 24 VDC powered components

Component	Power Consumption (VA)	Supply Voltage (V)	Quantity	Amp Draw (A)
Danfoss Valve Controller	5	24	4	.83
Danfoss Valve Step Motor	1.3	24	4	.22
Emerson Valve Controller	10	24	3	1.25
2700 Transmitter	11	24	2	.92
2500 Transmitter	6.3	24	4	1.05
Sporlan Valve Controller	40	24	2	3.33
Danfoss Water Valve	4.5	24	1	0.19
cRIO 9035	100	24	1	4.17
NI 9144	48	24	1	2
Proximity Sensors	2.5	24	2	.21
Total Amp Draw Needed	-	-	-	14.16

components given from the manufacturer. Only two or three components needed 24 VAC power, so the amp draw analysis was not completed, and an old 24 VAC power supply was re-used.

6.2 Data Acquisition Enclosure

Housing the chassis, controllers, transmitters, and power supplys is a freestanding 72x60x18 padlocking enclosure. Figure 6.1 shows the inside of this enclosure, with Table 3.6 listing the various labeled components. To provide extra support, the enclosure was mounted to the mezzanine by two unistrut pieces. To ensure that the panel inside the enclosure had enough space for all the components, a simple model in solidworks was created and is shown in Figure 6.2. Beside the enclosure is the host computer which is connected to the main chassis via Ethernet. Figure 6.3 shows the host computer next to the enclosure.

6.3 Wiring

Control wiring was done with 24 gage, twisted pair cable with foil shielding. Cable management is an important aspect to consider when running wires from the components and sensors back to the DAQ enclosure. Open slot wire ducting is strategically bolted along the frame to lead the wires to the corner of the load stand closest to the

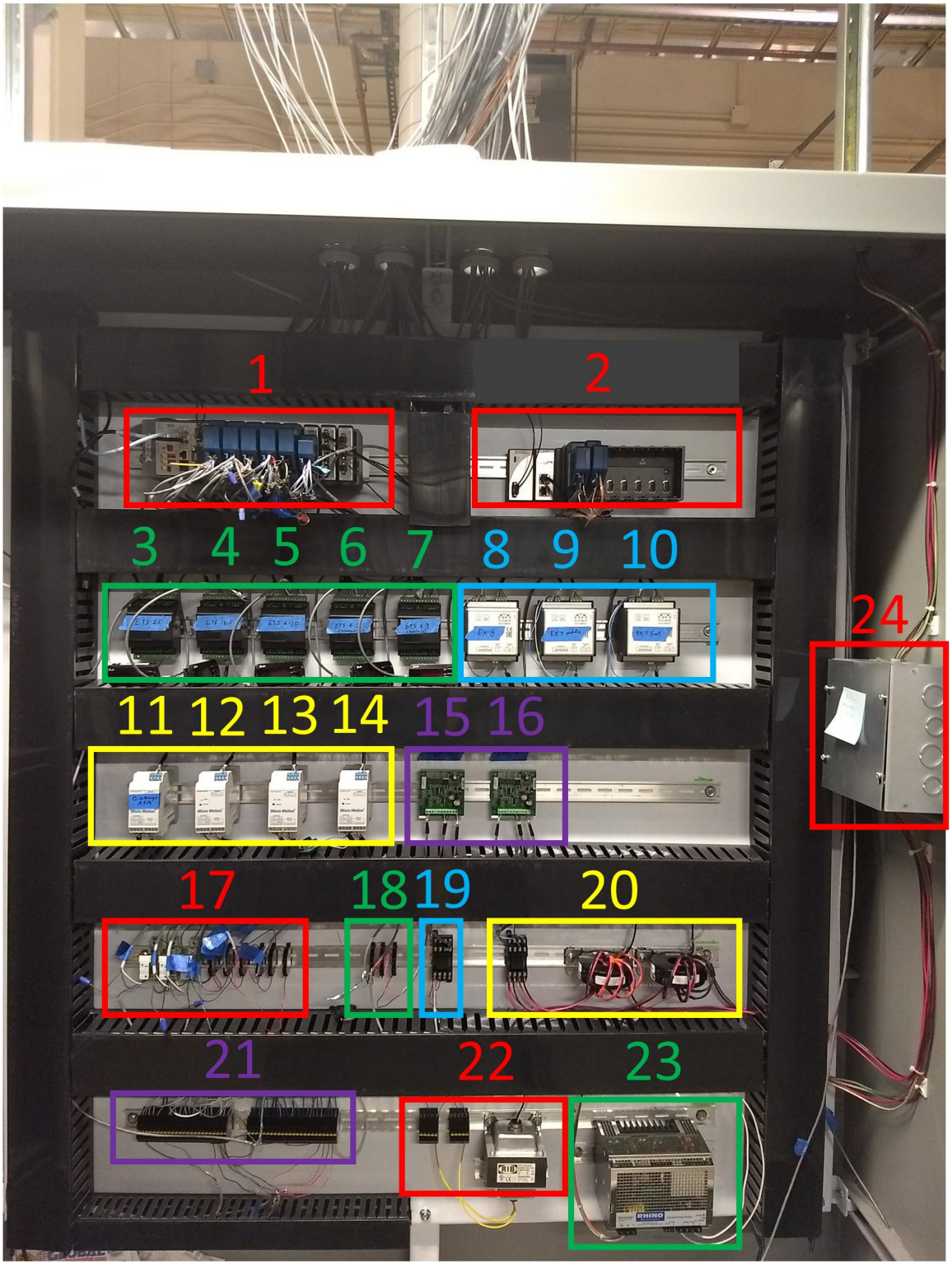

Figure 6.1: Inside of DAQ enclosure

Table 6.3: DAQ panel component descriptions

#	**Component**
1	Main cRIO chassis - NI 9035
2	Expansion chassis - NI 9144
3-7	Danfoss ETS valve controller
8-10	Emerson EX# valve controller
11-14	Micromotion 2500 flowmeter transmitter
15-16	Sporlan SDR valve controller
17	Main safety circuit
18	Secondary safety circuit
19	Relay for VFD start\stop control
20	Current transducers for oil valves
21	24 VDC power supply bus
22	24 VAC power supply bus and power supply
23	24 VDC power supply
24	240/115 VAC power supply for 24 VDC/VAC power supply's

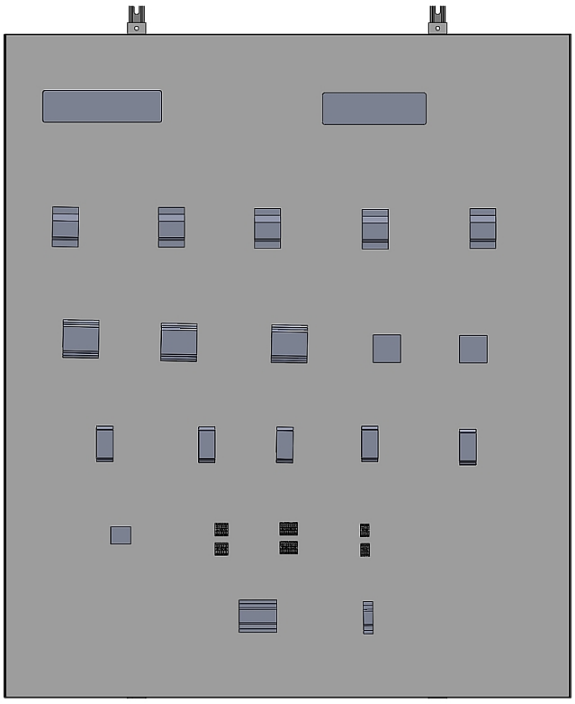

Figure 6.2: 3D CAD model of DAQ panel for correct sizing

Figure 6.3: Host computer setup next to the DAQ enclosure

enclosure. From that corner, the wire is placed in a cable tray suspended from the mezzanine. This cable tray holds all wires going from the load stand and VFDs to the enclosure. A smaller cable tray is routed from the enclosure to the compressor for all components near that area. Figure 6.4 shows the cable management.

Figure 6.4: Wiring from the load stand following the suspended cable tray to the DAQ enclosure

CHAPTER VII

PRELIMINARY RESULTS

Preliminary tests were conducted on the load stand with a scroll compressor rated at 40 tons of capacity with R410A. Because the current working fluid in the stand is R134a, a better estimate for the compressor capacity is around half, or 20 tons. These tests were conducted to ensure that the load stand was in proper working order, and could be controlled manually through LabVIEW to reach a desired condition. The correct operation of electronic valves, the proper sensor and instrumentation readings, the correct feedback signals from the VFD's, the proper working order of the safety features, and the correct load stand response to changes in the electronic valve positions all constituted to the criteria of a properly operating load stand. Since every compressor load stand is unique, another desired result of the preliminary testing was to familiarize the load stand's behavior when operating.

The preliminary test condition was a condensing temperature of 43.3 °C (110°F), an evaporating temperature of 6.7°C (45°F), a suction pressure of 3.8 bar (55 psi), a discharge pressure of 11.1 bar (161 psi), and a superheat of 20°C. A semi-steady condition close to the condition above was achieved after two hours of control manipulation. Manual load stand control, and the smaller compressor size relative to the maximum 80 ton limit, are the cause of the long time required to reach this condition. Data was collected after these two hours over a 25 minute time span, resulting in the collection of 1000 data points, one point every 1.5 seconds. The plots of the critical parameters over this 25 minute collection period are shown below.

The mass flow rates in Figure 7.1, the temperatures in Figure 7.4, and the super-

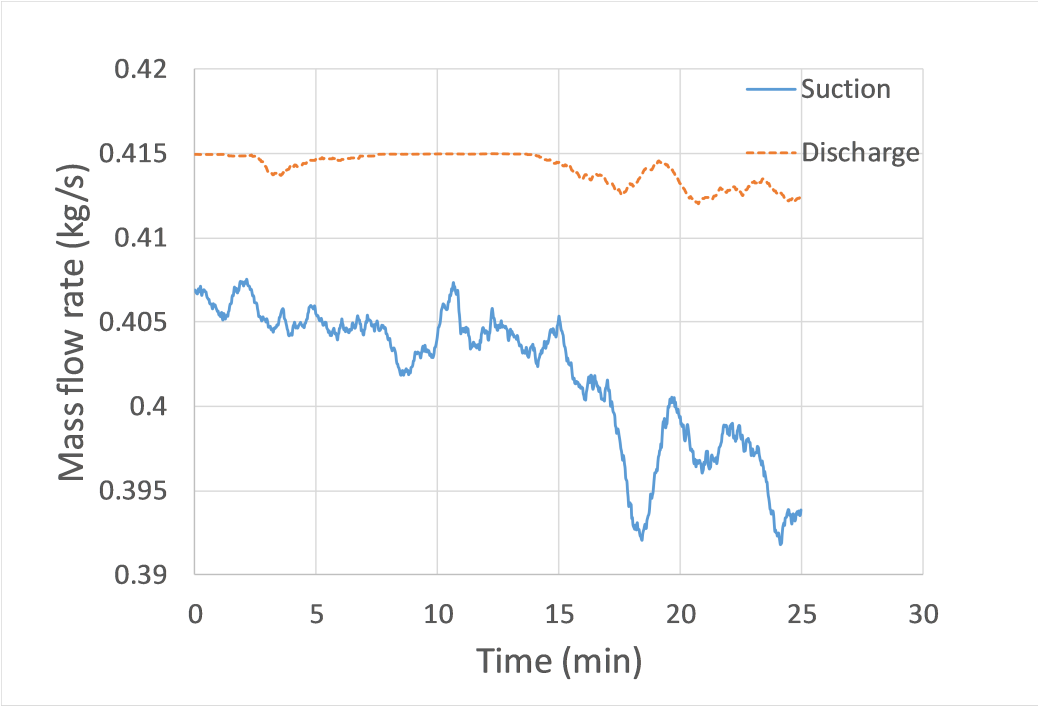

Figure 7.1: Mass flow rate values for the discharge and suction lines over a 25 minute time period

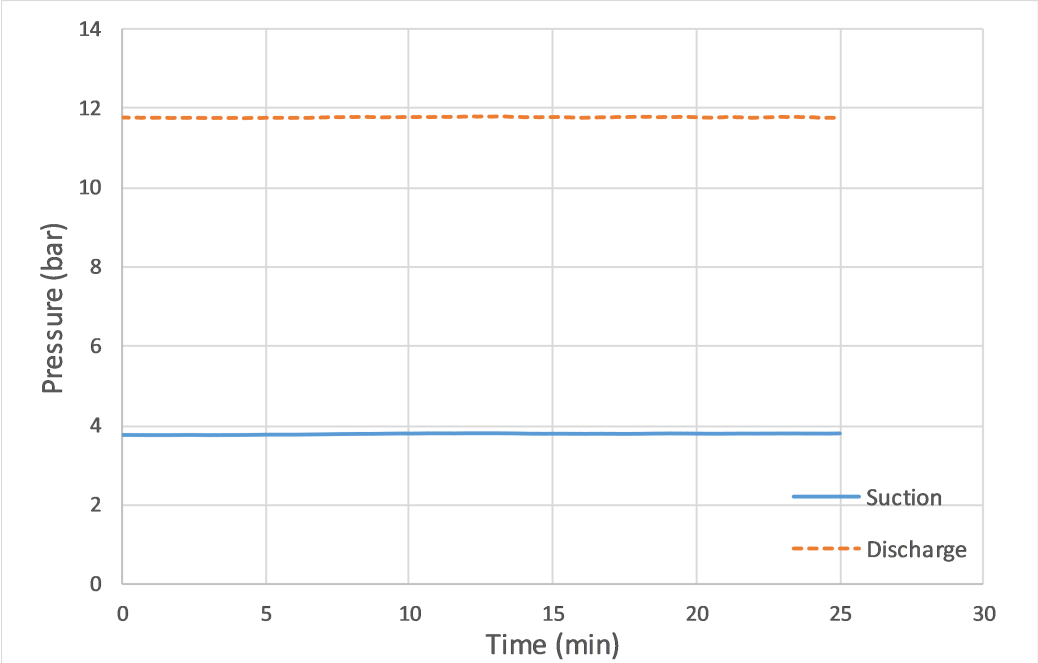

Figure 7.2: Pressure values for the discharge and suction lines near the compressor over a 25 minute time period

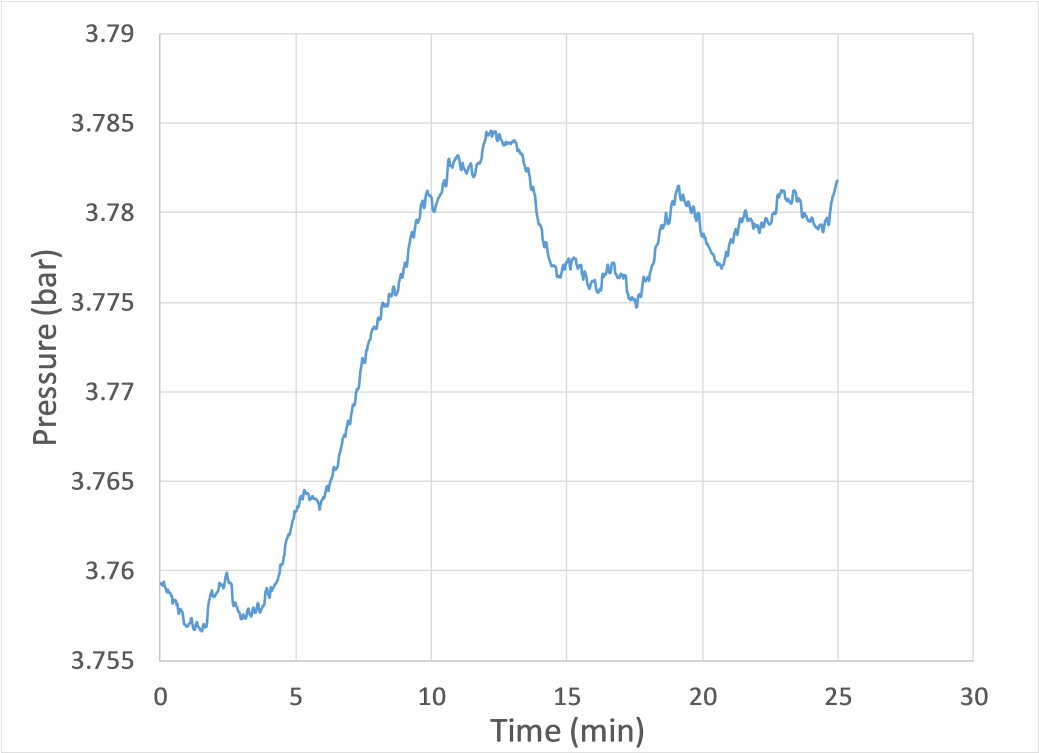

(a) Suction Pressure

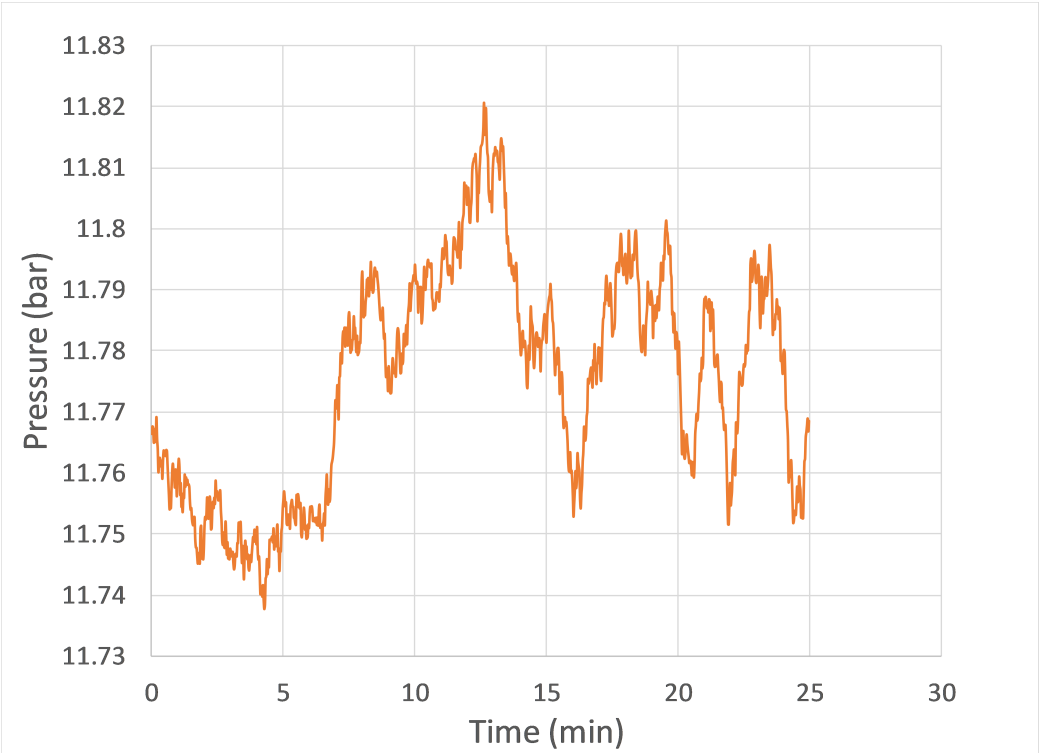

(b) Discharge Pressure

Figure 7.3: Pressure values for the discharge and suction lines near the compressor over a 25 minute time period

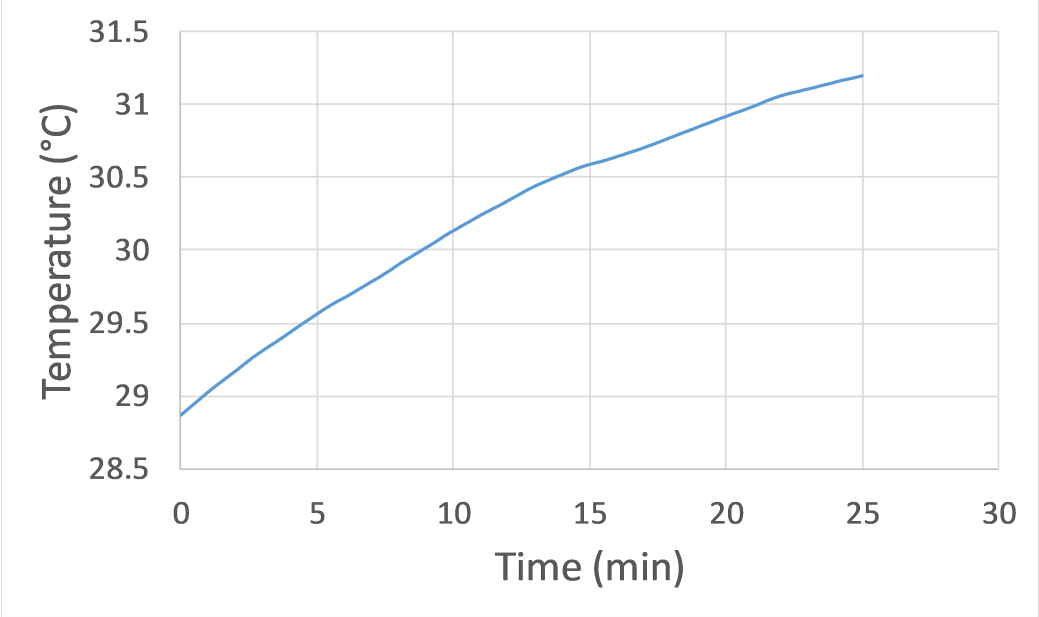

(a) Suction Temperature

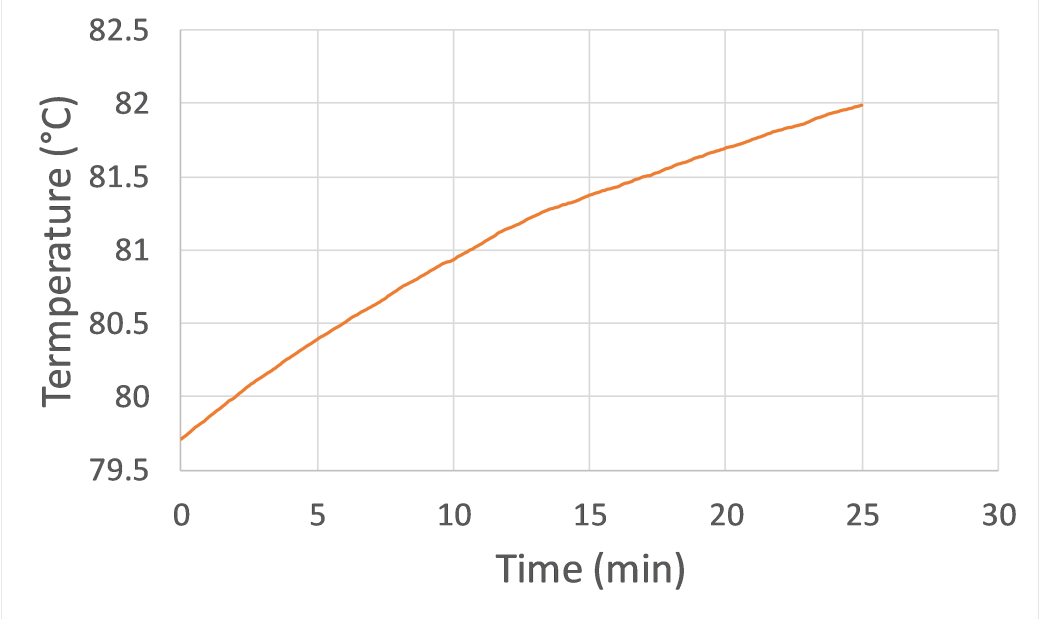

(b) Discharge Temperature

Figure 7.4: Temperature values for the discharge and suction lines near the compressor over a 25 minute time period

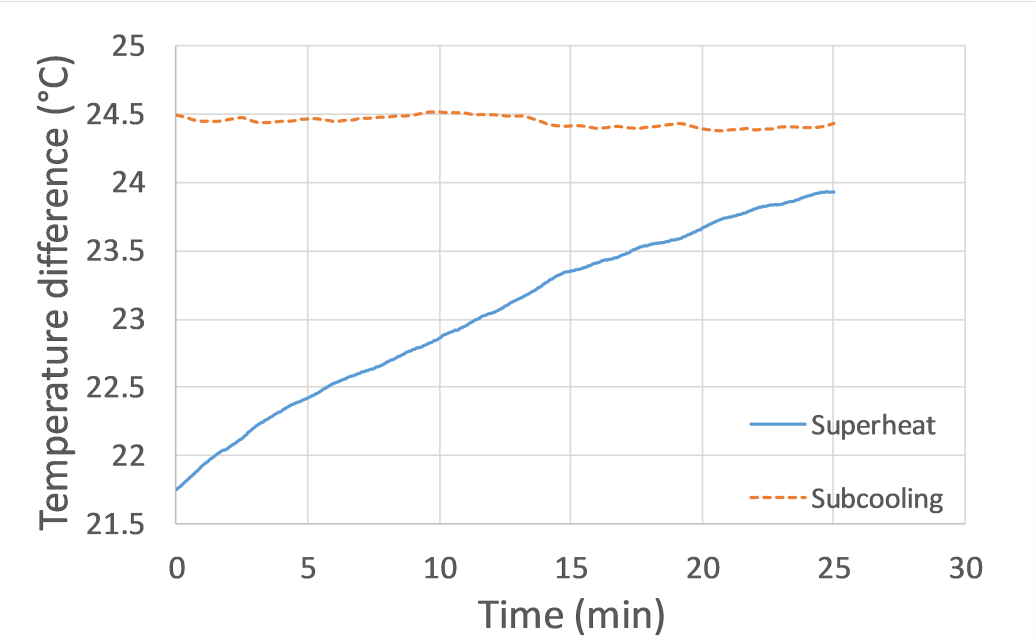

Figure 7.5: Superheat and subcooling amount over a 25 minute time period

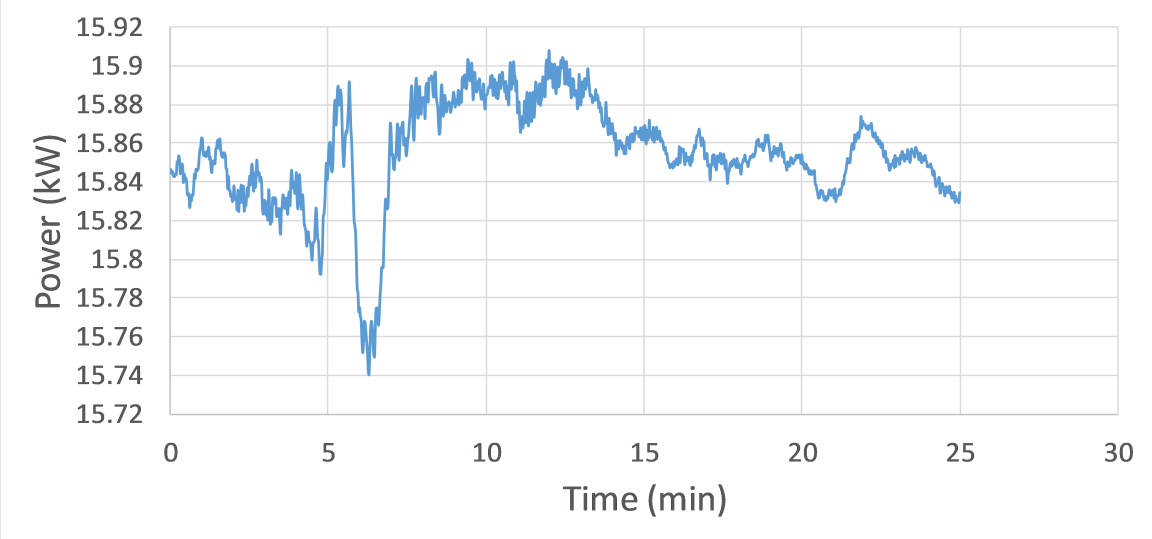

Figure 7.6: Compressor power over a 25 minute time period

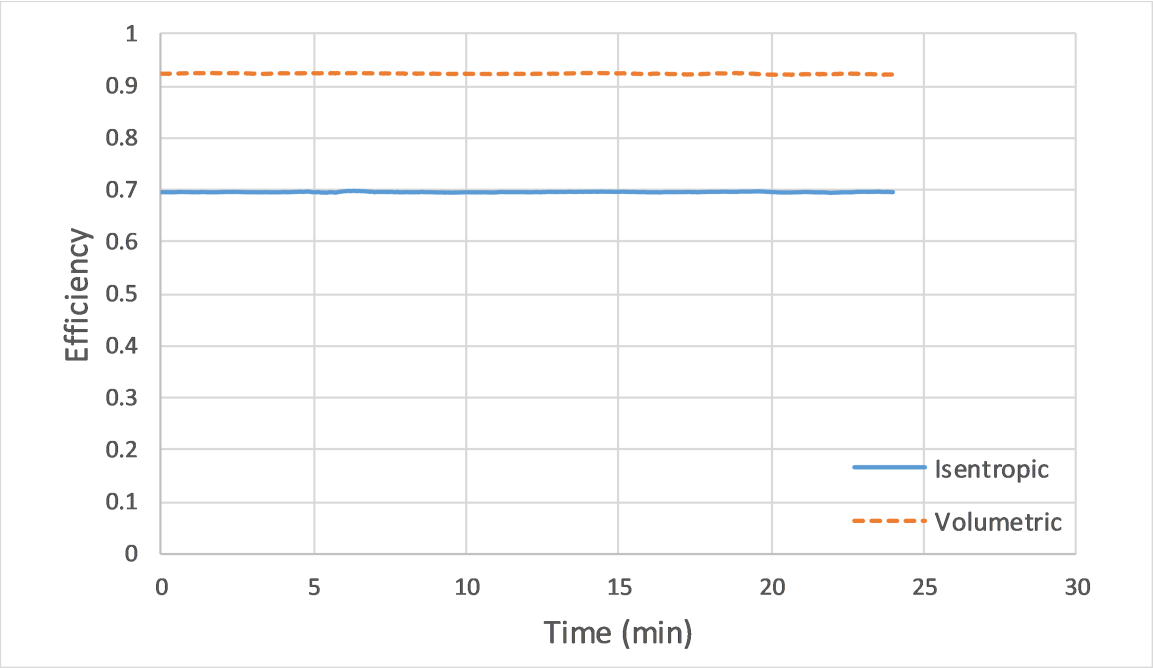

Figure 7.7: Volumetric and Isentropic efficiencies over a 25 minute time period

heat values in Figure 7.5 show why this was referred to as a semi-steady condition. Even after the two hours required to reach this condition, the suction temperature never fully reached steady state, climbing over 2°C during the time period. Due to this, the superheat and discharge temperature did not reach steady state as well. A longer ramp up time is required for these parameters to stabilize. A solution for quicker stabilization times is automatic control, which is a main priority for future works. However, the suction and discharge pressures shown in Figures 7.2 and 7.3 were quick to stabilize, and hold constant over the 25 minutes. The compressor power in Figure 7.6 showed held constant, and provided reliable isentropic and volumetric efficiencies shown in Figure 7.7. An average isentropic efficiency of 0.69, and average volumetric efficiency of 0.92 are reasonable values that are not seen as questionable with this compressor and refrigerant. Ultimately, the preliminary test results give confidence that the load stand is capable of reaching a design condition through manual control, and that faster stabilization times could be achieved with an automatic control scheme. At the very least, the data proves the compressor load stand runs

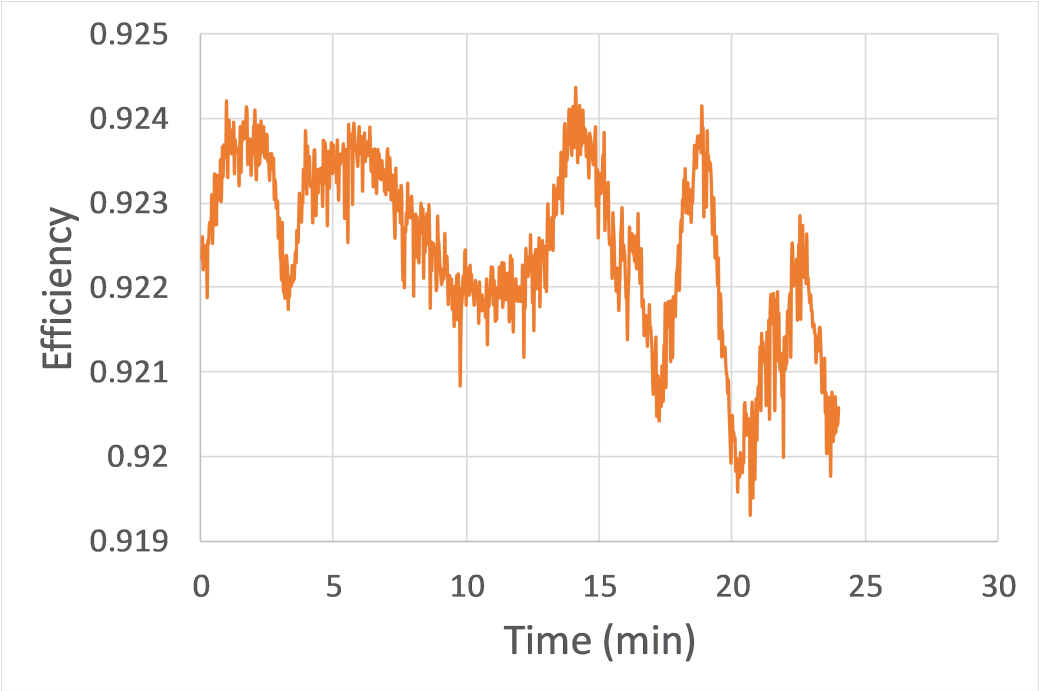

(a) Volumetric Efficiency

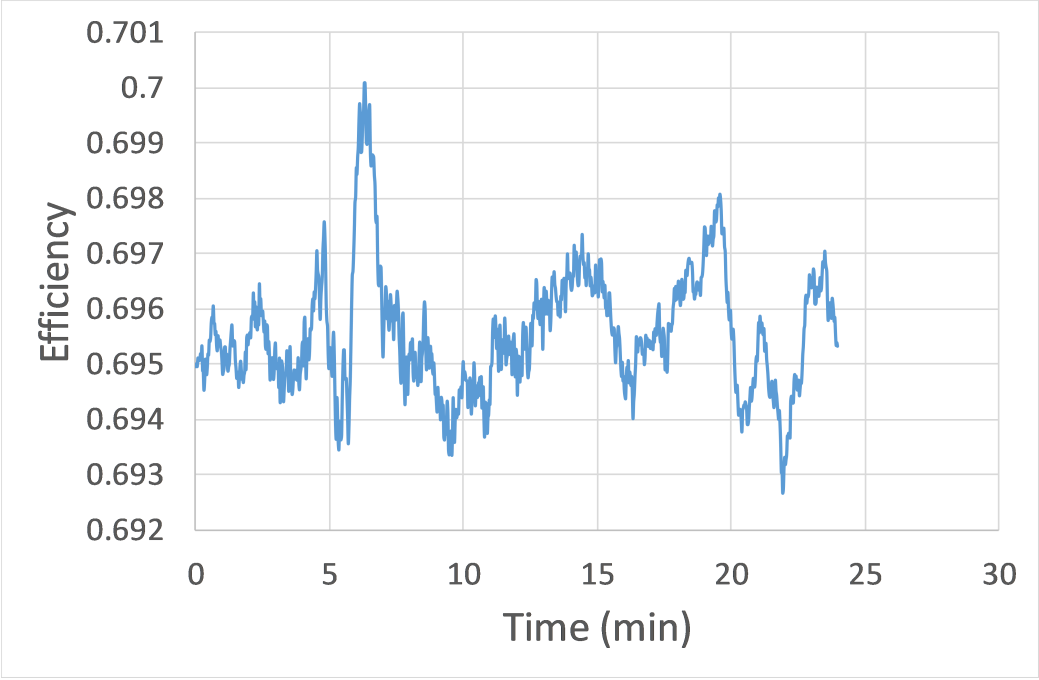

(b) Isentropic Efficiency

Figure 7.8: Compressor efficiencies over a 25 minute time period

and operates as desired.

CHAPTER VIII

CONCLUSIONS AND FUTURE WORK

8.1 Conclusion

A hot-gas bypass compressor load stand was designed and constructed in the ATRC lower basement at Oklahoma State University. The purpose of the load stand is to test the performance of light-commercial compressors, specifically large scroll and small screw compressors, with low-GWP refrigerants. Common cycle modifications, such as an economizer circuit for liquid/vapor injection, and an oil management system for oil injection, have been built into the load stand to allow for the largest variety of compressor tests possible. A thermodynamic model was developed to represent the physical behavior of the load stand. The design condition is a maximum and minimum cooling capacity of 80 tons and 10 tons, respectively, at 55°C condensing, 5°C evaporating, 10°C superheat, and 10°C subcooling with the working fluid R134a. With the design constraints, the model outputs the critical system parameters such as mass flow rates and maximum pressures and temperatures. A parametric study was conducted to find the maximum compressor volume displacement the load stand could support, as well as, the maximum volume displacements for other working fluids the stand might see. A 3D solidworks model was created to aid in the design of the physical layout of the load stand. Due to the large capacity range of 10-80 tons, carefully designed circuits were incorporated into the main line tubing layout to support proper mixing and oil entertainment. Using the critical system parameters from the model, the appropriate selections for the components and instrumentation were made. A mezzanine was built in the high bay area to serve as supporting infras-

tructure for the load stand. The load stand frame was then constructed underneath the mezzanine, onto which the brazed tubing sections were mounted. The system was leak checked and pressure tested, before being put under a vacuum and charged with R134a. A LabVIEW cRIO system has been installed and wired to the load stand instrumentation and components. This real time controller chassis is equipped with re-configurable input/output modules that allow for sensor measurement and valve control. Preliminary testing on a 40 ton scroll compressor confirms that the load stand has the capability to control and hold a steady state point.

8.2 Future Work

The next steps for the load stand include continuing work on the control scheme in LabVIEW, and the commissioning of the load stand with a 75-ton screw compressor on R134a. The current state of the LabVIEW programming is a control scheme that relies completely on manual tuning and manipulation of the load stand electronic valves to reach a desired condition. PID feedback loops need to be incorporated into the LabVIEW code, ultimately leading to the load stand being able to reach a desired test condition with only a one-time user input of the condition parameters.

With a proper control scheme in place, the load stand will need to be commissioned. The 40 ton scroll compressor will be swapped out with the 75-ton screw. Multiple steady state test conditions will need to be reached, and then compared to the manufacturer data to see how well the load stand performs.

REFERENCES

2010 ASHRAE Handbook: Refrigeration (2010), American Society of Heating, Refrigerating and Air-Conditioning Engineers, Inc.

ASHRAE-15 (2016), *ASHRAE Standard: Safety Standard for Refrigeration Systems*, American Society of Heating, Refrigerating and Air-Conditioning Engineers, Inc.

ASHRAE-23.1 (2010), *ASHRAE Standard: Methods of Testing for Rating the Performance of Positive Displacement Refrigerant Compressors and Condensing Units that Operate at Subcritical Temperatures of the Refrigerant*, American Society of Heating, Refrigerating and Air-Conditioning Engineers, Inc.

ASME-B16.22 (2013), *Wrought Copper and Copper Alloy Solder Joint Pressure Fittings*, ASME.

ASME-B31.5 (2013), *Refrigeration Piping and Heat Transfer Components*, ASME.

ASME-PTC-19.1 (2005), *Test Uncertainty*, ASME.

Bell, I. H. (2011), Theoretical and experimental analysis of liquid flooded compression in scroll compressors, PhD thesis, Purdue University.

Bradshaw, C. R. (2014), 'Compressor performance measurements using hot-gas bypass load stands'. Lecture presented at Short Course on Experimental Techniques to Measure Compressor Performance and Reliability in Purdue University, West Lafayette, IN.

Bradshaw, C. R. and Groll, E. A. (2013), 'A comprehensive model of a novel rotating spool compressor', *International Journal of Refrigeration* **36**(7), 1974–1981.

Bradshaw, C. R., Groll, E. A. and Garimella, S. V. (2011), 'A comprehensive model of a miniature-scale linear compressor for electronics cooling', *International Journal of Refrigeration* **34**(1), 63–73.

Cogswell, F. and Verma, P. (2018), High efficiency low global warming potential compressor, Technical report, United Technolgies Research Center, East Hartford, CT (United States).

Coolselector2 (2018). Danfoss. Version 2.2.5.

Cuevas, C., Lebrun, J., Lemort, V. and Winandy, E. (2010), 'Characterization of a scroll compressor under extended operating conditions', *Applied thermal engineering* **30**(6-7), 605–615.

Doniger, D. (2016), 'Countries adopt kigali amendment to phase down HFCs', https://www.nrdc.org/experts/david-doniger/countries-adopt-kigali-amendment-phase-down-hfcs. Retrieved May 15, 2018.

Duggan, M. G., Hundy, C. F. and Lawson, S. (1988), 'Refrigeration compressor performance using calorimeter and flowrater techniques', *International Compressor Engineering Conference* .

EIA (2018), 'Monthly energy review', https://www.eia.gov/totalenergy/data/monthly/archive/00351804.pdf. Retrieved May 29, 2018 from US Enery Information Administration.

Emerson (2018*a*), 'Ex valves and controls'. Retrieved November 6, 2018.
URL: *https://climate.emerson.com/documents/ex4-ex8-electrical-control-valve-catalog-en-us-2884012.pdf*

Emerson (2018*b*), 'Selection and sizing'. Retrieved November 6, 2018.
URL: *https://businessapps.emerson.com/OA_HTML/xxibeFlowSizingTool.jsp*

Gu, R. and Mathison, M. M. (2014), 'Design of a compressor load stand capable of supplying two-phase refrigerant at two intermediate pressures', *International Compressor Engineering Conference* .

Hexact (2018). Danfoss. Version 5.1.20.

Hoke (2018), 'Metering valves'. Retrieved November 6, 2018.
URL: *http://www.hoke.com/pdf/metering_valves_catalog_79013_10.12.pdf*

In, S., Cho, K., Lim, B., Kim, H. and Youn, B. (2014), 'Performance test of residential heat pump after partial optimization using low GWP refrigerants', *Applied Thermal Engineering* **72**(2), 315–322.

Kelso, J. D. (2012), 'Buildings energy data book', *Department of Energy* .

Klein, S. A. and Alvarado, F. (1992), *EES: Engineering equation solver for the Microsoft Windows operating system*, F-Chart software.

Marriott, L. W. (1973), Control of a Refrigeration Compressor Calorimeter for Minimum Testing Time, PhD thesis.

Orosz, J., Bradshaw, C. R., Kemp, G. and Groll, E. A. (2014), 'An update on the performance and operating characteristics of a novel rotating spool compressor', *International Compressor Engineering Conference* .

Orosz, J., Bradshaw, C. R., Kemp, G. and Groll, E. A. (2016), 'Updated performance and operating characteristics of a novel rotating spool compressor', *International Compressor Engineering Conference* .

Roth, K. W., Westphalen, D., Dieckmann, J., Hamilton, S. D. and Goetzler, W. (2002), 'Energy consumption characteristics of commercial building HVAC systems volume III: Energy savings potential', *US Department of Energy* .

Sathe, A., Groll, E. A. and Garimella, S. (2008), 'Experimental evaluation of a miniature rotary compressor for application in electronics cooling', *International Compressor Engineering Conference* .

Shrestha, S. S., Mahderekal, I., Sharma, V. and Abdelaziz, O. (2013), Compressor calorimeter test of R-410A alternatives R-32, DR-5, and L-41a, Technical report, Oak Ridge National Lab.(ORNL), Oak Ridge, TN (United States); Building Technologies Research and Integration Center (BTRIC).

Tan, K. M., Choo, W. C., Chee, M., Law, K., Iswan, I. and Ooi, K. T. (2014), 'Performance measurement of revolving vane compressor', *International Compressor Engineering Conference* .

Temprite (2018), 'Oil separator cross section'. Retrieved November 6, 2018.
URL: *https://temprite.com*

Tillner-Roth, R. and Baehr, H. D. (1994), 'An international standard formulation for the thermodynamic properties of 1, 1, 1, 2tetrafluoroethane (HFC134a) for temperatures from 170 K to 455 K and pressures up to 70 MPa', *Journal of Physical and Chemical Reference Data* **23**(5), 657–729.

Wujekand, S. S., Bowers, C. D., Okarma, P., Urrego, R. A., Hessell, E. T. and Benanti, T. L. (2014), 'Effect of lubricant-refrigerant mixture properties on compressor efficiencies', *International Compressor Engineering Conference* .

APPENDICES

APPENDIX A

Other Refrigeration Line Sizing Tables

4. Values based on 105°F condensing temperature. Multiply table capacities by the following factors for other condensing temperatures.

Condensing Temperature, °F	Suction Line	Discharge Line
80	1.11	0.79
90	1.07	0.88
100	1.03	0.95
110	0.97	1.04
120	0.90	1.10
130	0.86	1.18
140	0.80	1.26

Figure A.1: Capacity correction factors based on condensing temperature used with Figure 4.1. From ©ASHRAE, www.ashrae.org. (2010) ASHRAE Handbook-(Refrigeration).

Table 19 Minimum Refrigeration Capacity in Tons for Oil Entrainment up Hot-Gas Risers (Type L Copper Tubing)

Refrigerant	Saturated Temp., °F	Discharge Gas Temp., °F	Pipe OD, in. 1/2	5/8	3/4	7/8	1 1/8	1 3/8	1 5/8	2 1/8	2 5/8	3 1/8	3 5/8	4 1/8
			Area, in^2 0.146	0.233	0.348	0.484	0.825	1.256	1.780	3.094	4.770	6.812	9.213	11.970
22	80.0	110.0	0.235	0.421	0.695	1.05	2.03	3.46	5.35	10.7	18.3	28.6	41.8	57.9
		140.0	0.223	0.399	0.659	0.996	1.94	3.28	5.07	10.1	17.4	27.1	39.6	54.9
		170.0	0.215	0.385	0.635	0.960	1.87	3.16	4.89	9.76	16.8	26.2	38.2	52.9
	90.0	120.0	0.242	0.433	0.716	1.06	2.11	3.56	5.50	11.0	18.9	29.5	43.0	59.6
		150.0	0.226	0.406	0.671	1.01	1.97	3.34	5.16	10.3	17.7	27.6	40.3	55.9
		180.0	0.216	0.387	0.540	0.956	1.88	3.18	4.92	9.82	16.9	26.3	38.4	53.3
	100.0	130.0	0.247	0.442	0.730	1.10	2.15	3.83	5.62	11.2	19.3	30.1	43.9	60.8
		160.0	0.231	0.414	0.884	1.03	2.01	3.40	5.26	10.5	18.0	28.2	41.1	57.0
		190.0	0.220	0.394	0.650	0.982	1.91	3.24	3.00	9.96	17.2	26.8	39.1	54.2
	110.0	140.0	0.251	0.451	0.744	1.12	2.19	3.70	5.73	11.4	19.6	30.6	44.7	62.0
		170.0	0.235	0.421	0.693	1.05	2.05	3.46	3.35	10.7	18.3	28.6	41.8	57.9
		200.0	0.222	0.399	0.658	0.994	1.94	3.28	5.06	10.1	17.4	27.1	39.5	54.8
	120.0	150.0	0.257	0.460	0.760	1.15	2.24	3.78	5.85	11.7	20.0	31.3	45.7	63.3
		180.0	0.239	0.428	0.707	1.07	2.08	3.51	5.44	10.8	18.6	29.1	42.4	58.9
		210.0	0.225	0.404	0.666	1.01	1.96	3.31	5.12	10.2	17.6	27.4	40.0	55.5
134a	80.0	110.0	0.199	0.360	0.581	0.897	1.75	2.96	4.56	9.12	15.7	24.4	35.7	49.5
		140.0	0.183	0.331	0.535	0.825	1.61	2.72	4.20	8.39	14.4	22.5	32.8	45.6
		170.0	0.176	0.318	0.512	0.791	1.54	2.61	4.02	8.04	13.8	21.6	31.4	43.6
	90.0	120.0	0.201	0.364	0.587	0.906	1.76	2.99	4.61	9.21	15.8	24.7	36.0	50.0
		150.0	0.184	0.333	0.538	0.830	1.62	2.74	4.22	8.44	14.5	22.6	33.0	45.8
		180.0	0.177	0.320	0.516	0.796	1.55	2.62	4.05	8.09	13.9	21.7	31.6	43.9
	100.0	130.0	0.206	0.372	0.600	0.926	1.80	3.05	4.71	9.42	16.2	25.2	36.8	51.1
		160.0	0.188	0.340	0.549	0.848	1.65	2.79	4.31	8.62	14.8	23.1	33.7	46.8
		190.0	0.180	0.326	0.526	0.811	1.58	2.67	4.13	8.25	14.2	22.1	32.2	44.8
	110.0	140.0	0.209	0.378	0.610	0.942	1.83	3.10	4.79	9.57	16.5	25.7	37.4	52.0
		170.0	0.191	0.346	0.558	0.861	1.68	2.84	4.38	8.76	15.0	23.5	34.2	47.5
		200.0	0.183	0.331	0.534	0.824	1.61	2.72	4.19	8.38	14.4	22.5	32.8	45.5
	120.0	150.0	0.212	0.383	0.618	0.953	1.86	3.14	4.85	9.69	16.7	26.0	37.9	52.6
		180.0	0.194	0.351	0.566	0.873	1.70	2.88	4.44	8.88	15.3	23.8	34.7	48.2
		210.0	0.184	0.334	0.538	0.830	1.62	2.74	4.23	8.44	14.5	22.6	33.0	45.8

Notes:
1. Refrigeration capacity in tons based on saturated suction temperature of 20°F with 15°F superheat at indicated saturated condensing temperature with 15°F subcooling. For other saturated suction temperatures with 15°F superheat, use correction factors in the table at right.
2. Table computed using ISO 32 mineral oil for R-22, and ISO 32 ester-based oil for R-134a.

Refrigerant	Saturated Suction Temperature, °F −40	−20	0	+40
22	0.92	0.95	0.97	1.02
134a	—	—	0.96	1.04

Figure A.2: Table used to size hot-gas risers. From ©ASHRAE, www.ashrae.org. (2010) ASHRAE Handbook-(Refrigeration).

Table 20 Minimum Refrigeration Capacity in Tons for Oil Entrainment up Suction Risers (Type L Copper Tubing)

Refrigerant	Saturated Suction Temp., °F	Suction Gas Temp., °F	Pipe OD, in. 1/2	5/8	3/4	7/8	1 1/8	1 3/8	1 5/8	2 1/8	2 5/8	3 1/8	3 5/8	4 1/8
			Area, in^2 0.146	0.233	0.348	0.484	0.825	1.256	1.780	3.094	4.770	6.812	9.213	11.970
22	–40.0	–30.0	0.067	0.119	0.197	0.298	0.580	0.981	1.52	3.03	5.20	8.12	11.8	16.4
		–10.0	0.065	0.117	0.194	0.292	0.570	0.963	1.49	2.97	5.11	7.97	11.6	16.1
		10.0	0.066	0.118	0.195	0.295	0.575	0.972	1.50	3.00	5.15	8.04	11.7	16.3
	–20.0	–10.0	0.087	0.156	0.258	0.389	0.758	1.28	1.98	3.96	6.80	10.6	15.5	21.5
		10.0	0.085	0.153	0.253	0.362	0.744	1.26	1.95	3.88	6.67	10.4	15.2	21.1
		30.0	0.086	0.154	0.254	0.383	0.747	1.26	1.95	3.90	6.69	10.4	15.2	21.1
	0.0	10.0	0.111	0.199	0.328	0.496	0.986	1.63	2.53	5.04	8.66	13.5	19.7	27.4
		30.0	0.108	0.194	0.320	0.484	0.942	1.59	2.46	4.92	8.45	13.2	19.2	26.7
		50.0	0.109	0.195	0.322	0.486	0.946	1.60	2.47	4.94	8.48	13.2	19.3	26.8
	20.0	30.0	0.136	0.244	0.403	0.608	1.18	2.00	3.10	6.18	10.6	16.6	24.2	33.5
		50.0	0.135	0.242	0.399	0.603	1.17	1.99	3.07	6.13	10.5	16.4	24.0	33.3
		70.0	0.135	0.242	0.400	0.605	1.18	1.99	3.08	6.15	10.6	16.5	24.0	33.3
	40.0	50.0	0.167	0.300	0.495	0.748	1.46	2.46	3.81	7.60	13.1	20.4	29.7	41.3
		70.0	0.165	0.296	0.488	0.737	1.44	2.43	3.75	7.49	12.9	20.1	29.3	40.7
		90.0	0.165	0.296	0.488	0.738	1.44	2.43	3.76	7.50	12.9	20.1	29.3	40.7
134a	0.0	10.0	0.089	0.161	0.259	0.400	0.78	1.32	2.03	4.06	7.0	10.9	15.9	22.1
		30.0	0.075	0.135	0.218	0.336	0.66	1.11	1.71	3.42	5.9	9.2	13.4	18.5
		50.0	0.072	0.130	0.209	0.323	0.63	1.07	1.64	3.28	5.6	8.8	12.8	17.8
	10.0	20.0	0.101	0.182	0.294	0.453	0.88	1.49	2.31	4.61	7.9	12.4	18.0	25.0
		40.0	0.084	0.152	0.246	0.379	0.74	1.25	1.93	3.86	6.6	10.3	15.1	20.9
		60.0	0.081	0.147	0.237	0.366	0.71	1.21	1.87	3.73	6.4	10.0	14.6	20.2
	20.0	30.0	0.113	0.205	0.331	0.510	0.99	1.68	2.60	5.19	8.9	13.9	20.3	28.2
		50.0	0.095	0.172	0.277	0.427	0.83	1.41	2.17	4.34	7.5	11.6	17.0	23.6
		70.0	0.092	0.166	0.268	0.413	0.81	1.36	2.10	4.20	7.2	11.3	16.4	22.8
	30.0	40.0	0.115	0.207	0.335	0.517	1.01	1.70	2.63	5.25	9.0	14.1	20.5	28.5
		60.0	0.107	0.193	0.311	0.480	0.94	1.58	2.44	4.88	8.4	13.1	19.1	26.5
		80.0	0.103	0.187	0.301	0.465	0.91	1.53	2.37	4.72	8.1	12.7	18.5	25.6
	40.0	50.0	0.128	0.232	0.374	0.577	1.12	1.90	2.94	5.87	10.1	15.7	22.9	31.8
		70.0	0.117	0.212	0.342	0.528	1.03	1.74	2.69	5.37	9.2	14.4	21.0	29.1
		90.0	0.114	0.206	0.332	0.512	1.00	1.69	2.61	5.21	8.9	14.0	20.4	28.3

Notes:
1. Refrigeration capacity in tons is based on 90°F liquid temperature and superheat as indicated by listed temperature. For other liquid line temperatures, use correction factors in table at right.
2. Values computed using ISO 32 mineral oil for R-22. R-134a computed using ISO 32 ester-based oil.

Refrigerant	Liquid Temperature, °F 50	60	70	80	100	110	120	130	140
22	1.17	1.14	1.10	1.06	0.98	0.94	0.89	0.85	0.80
134a	1.26	1.20	1.13	1.07	0.94	0.87	0.80	0.74	0.67

Figure A.3: Table used to size suction risers. From ©ASHRAE, www.ashrae.org. (2010) ASHRAE Handbook-(Refrigeration).

APPENDIX B

Mass Flow Meter Calculation Summaries

Micro Motion Calculation Summary

Date:	05/04/17
Company:	Drew Schmidt
Project Name:	Oklahoma State University
Service:	R134A
Sensor Model #:	CMF200M419N2BMEZZZ
Sensor Tag(s):	
Transmitter Model #:	
Transmitter Tag(s):	
Wetted Material:	316L stainless steel
Fluid:	R134A
Fluid State:	Gas
Mass Flow Accuracy at Operating. Flow (+/- % of Rate):	0.35000
Density Accuracy at all Rates (+/-):	
Pressure Drop at Operating Flow:	0.22317 bar
Sensor Minimum Pressure at operating conditions:	bar-g
Velocity at Operating Flow:	33.96259 m/sec

	Min	Operating*	Max	Design	Units
Flow Rate:	937.100	4061.000	6872.000		kg/hr
Pressure:	6.660	6.660	6.660		bar-g
Process Fluid Temperature:	43.260	43.260	43.260		C
Ambient Temperature:	70.000	70.000	70.000		F
Density:	29.280	29.280	29.280		kg/m3
Viscosity:		0.013			cP

Gas only	**Base Reference Temperature:**	F	60.0	Density:	
	Base Reference Pressure:	psia	14.696		
	Base Reference Density:	kg/m3	4.23745		

Process Connection:	2-inch CL300 ASME B16.5 F316/F316L Weld neck flange Raised face
Process Connection Pressure Rating:	48.962 bar-g
@ Temperature:	43.260 C

Flow Rate kg/hr	Mass Flow Accuracy +/- % of Rate	Pressure Drop* bar	Velocity* m/sec	Re
6872.000	0.350	0.631	57.471	3574792.804
6278.510	0.350	0.527	52.508	3266061.171
5685.020	0.350	0.433	47.544	2957329.538
5091.530	0.350	0.349	42.581	2648597.905
4498.040	0.350	0.273	37.618	2339866.272
4061.000	0.350	0.223	33.963	2112519.438
3311.060	0.350	0.149	27.691	1722403.007
2717.570	0.350	0.101	22.727	1413671.374
2124.080	0.350	0.063	17.764	1104939.741
1530.590	0.350	0.033	12.800	796208.108
937.100	0.350	0.013	7.837	487476.475

*All pressure drop and velocity results are based on the process conditions (except flow rate) that are entered in the Operating column.

Notes:

Prepared by:		**Project ID:**	001-20170504-000009
Instrument Toolkit	Version: 3.0 (Build201C)	**Application:**	Discharge 25C

Figure B.1: Discharge line at 25°C condensing

Micro Motion Calculation Summary

Date:		05/04/17				
Company:		Drew Schmidt				
Project Name:		Oklahoma State University				
Service:		R134A				
Sensor Model #:		CMF200M419N2BMEZZZ				
Sensor Tag(s):						
Transmitter Model #:						
Transmitter Tag(s):						
Wetted Material:		316L stainless steel				
Fluid:		R134A				
Fluid State:		Gas				
Mass Flow Accuracy at Operating. Flow (+/- % of Rate):		0.35000				
Density Accuracy at all Rates (+/-):						
Pressure Drop at Operating Flow:		0.09207	bar			
Sensor Minimum Pressure at operating conditions:			bar-g			
Velocity at Operating Flow:		13.94509	m/sec			
		Min	**Operating***	**Max**	**Design**	**Units**
Flow Rate:		937.100	4061.000	6872.000		kg/hr
Pressure:		16.830	16.830	16.830		bar-g
Process Fluid Temperature:		86.890	86.890	86.890		C
Ambient Temperature:		70.000	70.000	70.000		F
Density:		71.310	71.310	71.310		kg/m3
Viscosity:			0.015			cP
Gas only	**Base Reference Temperature:** F	60.0			Density:	
	Base Reference Pressure: psia	14.696				
	Base Reference Density: lb/ft3	0.31526				
Process Connection:		2-inch CL300 ASME B16.5 F316/F316L Weld neck flange Raised face				
Process Connection Pressure Rating:		43.547	bar-g			
@ Temperature:		86.890	C			

Flow Rate kg/hr	**Mass Flow Accuracy +/- % of Rate**	**Pressure Drop* bar**	**Velocity* m/sec**	**Re**
6872.000	0.350	0.260	23.598	3072087.566
6278.510	0.350	0.217	21.560	2806771.319
5685.020	0.350	0.179	19.522	2541455.072
5091.530	0.350	0.144	17.484	2276138.825
4498.040	0.350	0.113	15.446	2010822.578
4061.000	0.350	0.092	13.945	1815446.392
3311.060	0.350	0.062	11.370	1480190.084
2717.570	0.350	0.042	9.332	1214873.837
2124.080	0.350	0.026	7.294	949557.590
1530.590	0.350	0.014	5.256	684241.343
937.100	0.350	0.005	3.218	418925.096

*All pressure drop and velocity results are based on the process conditions (except flow rate) that are entered in the Operating column.

Notes:

Prepared by:		**Project ID:**	001-20170504-000009
Instrument Toolkit	Version: 3.0 (Build201C)	**Application:**	Discharge 60C

Figure B.2: Discharge line at 60°C condensing

Micro Motion Calculation Summary

Date:		05/04/17				
Company:		Drew Schmidt				
Project Name:		Oklahoma State University				
Service:		R134A				
Sensor Model #:		CMFS075M329N2BMEKZZ				
Sensor Tag(s):						
Transmitter Model #:						
Transmitter Tag(s):						
Wetted Material:		316L stainless steel				
Fluid:		R134A				
Fluid State:		Gas				
Mass Flow Accuracy at Operating. Flow (+/- % of Rate):		0.25000				
Density Accuracy at all Rates (+/-):						
Pressure Drop at Operating Flow:		0.35985	bar			
Sensor Minimum Pressure at operating conditions:			bar-g			
Velocity at Operating Flow:		33.35561	m/sec			
		Min	**Operating***	**Max**	**Design**	**Units**
Flow Rate:		161.100	698.100	1181.000		kg/hr
Pressure:		6.700	6.700	6.700		bar-g
Process Fluid Temperature:		44.300	44.300	44.300		C
Ambient Temperature:		70.000	70.000	70.000		F
Density:		29.100	29.100	29.100		kg/m3
Viscosity:		0.013	0.013	0.013		cP
Gas only	**Base Reference Temperature:** F	60.0			Density:	
	Base Reference Pressure: psia	14.696				
	Base Reference Density: lb/ft3	0.26241				
Process Connection:		1-inch CL300 ASME B16.5 F316/F316L Weld neck flange Raised face				
Process Connection Pressure Rating:		48.833	bar-g			
@ Temperature:		44.300	C			

Flow Rate kg/hr	**Mass Flow Accuracy +/- % of Rate**	**Pressure Drop* bar**	**Velocity* m/sec**	**Re**
1181.000	0.250	1.016	56.429	1459315.528
1079.010	0.250	0.850	51.556	1333290.472
977.020	0.250	0.698	46.683	1207265.417
875.030	0.250	0.562	41.809	1081240.361
773.040	0.250	0.440	36.936	955215.305
698.100	0.250	0.360	33.356	862614.877
569.060	0.250	0.241	27.190	703165.194
467.070	0.250	0.163	22.317	577140.139
365.080	0.250	0.101	17.444	451115.083
263.090	0.250	0.053	12.571	325090.027
161.100	0.250	0.021	7.697	199064.972

*All pressure drop and velocity results are based on the process conditions (except flow rate) that are entered in the Operating column.

Notes:

Prepared by:		**Project ID:**	001-20170504-000009
Instrument Toolkit	Version: 3.0 (Build201C)	**Application:**	Economizer Gas 25C

Figure B.3: Economizer gas line at 25°C condensing

Micro Motion Calculation Summary

Date:		05/04/17				
Company:		Drew Schmidt				
Project Name:		Oklahoma State University				
Service:		R134A				
Sensor Model #:		CMFS075M329N2BMEKZZ				
Sensor Tag(s):						
Transmitter Model #:						
Transmitter Tag(s):						
Wetted Material:		316L stainless steel				
Fluid:		R134A				
Fluid State:		Gas				
Mass Flow Accuracy at Operating. Flow (+/- % of Rate):		0.25000				
Density Accuracy at all Rates (+/-):						
Pressure Drop at Operating Flow:		0.09835 bar				
Sensor Minimum Pressure at operating conditions:		bar-g				
Velocity at Operating Flow:		11.02662 m/sec				
		Min	**Operating***	**Max**	**Design**	**Units**
Flow Rate:		131.600	570.200	965.000		kg/hr
Pressure:		16.800	16.800	16.800		bar-g
Process Fluid Temperature:		85.600	85.600	85.600		C
Ambient Temperature:		70.000	70.000	70.000		F
Density:		71.900	71.900	71.900		kg/m3
Viscosity:		0.015	0.015	0.015		cP
Gas only	**Base Reference Temperature:** F	60.0			Density:	
	Base Reference Pressure: psia	14.696				
	Base Reference Density: lb/ft3	0.31726				
Process Connection:		1-inch CL300 ASME B16.5 F316/F316L Weld neck flange Raised face				
Process Connection Pressure Rating:		43.707 bar-g				
@ Temperature:		85.600 C				

Flow Rate kg/hr	**Mass Flow Accuracy +/- % of Rate**	**Pressure Drop* bar**	**Velocity* m/sec**	**Re**
965.000	0.250	0.277	18.661	1030770.987
881.660	0.250	0.232	17.050	941750.827
798.320	0.250	0.191	15.438	852730.667
714.980	0.250	0.153	13.826	763710.508
631.640	0.250	0.120	12.215	674690.348
570.200	0.250	0.098	11.027	609062.815
464.960	0.250	0.066	8.991	496650.029
381.620	0.250	0.045	7.380	407629.869
298.280	0.250	0.028	5.768	318609.710
214.940	0.250	0.015	4.157	229589.550
131.600	0.250	0.006	2.545	140569.391

*All pressure drop and velocity results are based on the process conditions (except flow rate) that are entered in the Operating column.

Notes:

Prepared by:		**Project ID:**	001-20170504-000009
Instrument Toolkit	Version: 3.0 (Build201C)	**Application:**	Economizer Gas 60C

Figure B.4: Economizer gas line at 60°C condensing

Micro Motion Calculation Summary

Date:		05/04/17				
Company:		Drew Schmidt				
Project Name:		Oklahoma State University				
Service:		R134A				
Sensor Model #:		CMFS015M314N2BMECZZ				
Sensor Tag(s):						
Transmitter Model #:						
Transmitter Tag(s):						
Wetted Material:		316L stainless steel				
Fluid:		R134A				
Fluid State:		Liquid				
Mass Flow Accuracy at Operating. Flow (+/- % of Rate):		0.10000				
Density Accuracy at all Rates (+/-):		2.00000	kg/m3			
Pressure Drop at Operating Flow:		0.04729	bar			
Sensor Minimum Pressure at operating conditions:			bar-g			
Velocity at Operating Flow:		1.27157	m/sec			
		Min	**Operating***	**Max**	**Design**	**Units**
Flow Rate:		17.300	75.000	126.900		kg/hr
Pressure:		6.700	6.700	6.700		bar-g
Process Fluid Temperature:		15.000	15.000	15.000		C
Ambient Temperature:		70.000	70.000	70.000		F
Density:		1244.000	1244.000	1244.000		kg/m3
Viscosity:		0.220	0.220	0.220		cP
Gas only	**Base Reference Temperature:** F				Density:	
	Base Reference Pressure: psia					
	Base Reference Density: lb/ft3					
Process Connection:		1/2-inch CL300 ASME B16.5 F316/F316L Weld neck flange Raised face				
Process Connection Pressure Rating:		49.642	bar-g			
@ Temperature:		15.000	C			

Flow Rate kg/hr	**Mass Flow Accuracy +/- % of Rate**	**Pressure Drop* bar**	**Velocity* m/sec**	**Re**
126.900	0.100	0.126	2.152	35227.190
115.940	0.100	0.106	1.966	32184.716
104.980	0.100	0.088	1.780	29142.241
94.020	0.100	0.072	1.594	26099.767
83.060	0.100	0.057	1.408	23057.293
75.000	0.100	0.047	1.272	20819.852
61.140	0.100	0.032	1.037	16972.344
50.180	0.100	0.023	0.851	13929.869
39.220	0.100	0.014	0.665	10887.395
28.260	0.100	0.008	0.479	7844.920
17.300	0.100	0.003	0.293	4802.446

*All pressure drop and velocity results are based on the process conditions (except flow rate) that are entered in the Operating column.

Notes:

Prepared by:		**Project ID:**	001-20170504-000009
Instrument Toolkit	Version: 3.0 (Build201C)	**Application:**	Economizer Liquid 25C

Figure B.5: Economizer liquid line at 25°C condensing

Micro Motion Calculation Summary

Date:		05/04/17				
Company:		Drew Schmidt				
Project Name:		Oklahoma State University				
Service:		R134A				
Sensor Model #:		CMFS015M314N2BMECZZ				
Sensor Tag(s):						
Transmitter Model #:						
Transmitter Tag(s):						
Wetted Material:		316L stainless steel				
Fluid:		R134A				
Fluid State:		Liquid				
Mass Flow Accuracy at Operating. Flow (+/- % of Rate):		0.10000				
Density Accuracy at all Rates (+/-):		2.00000	kg/m3			
Pressure Drop at Operating Flow:		0.17563	bar			
Sensor Minimum Pressure at operating conditions:			bar-g			
Velocity at Operating Flow:		2.79181	m/sec			
		Min	**Operating***	**Max**	**Design**	**Units**
Flow Rate:		33.800	146.400	247.800		kg/hr
Pressure:		16.800	16.800	16.800		bar-g
Process Fluid Temperature:		50.000	50.000	50.000		C
Ambient Temperature:		70.000	70.000	70.000		F
Density:		1106.000	1106.000	1106.000		kg/m3
Viscosity:		0.143	0.143	0.143		cP
Gas only	**Base Reference Temperature:** F				Density:	
	Base Reference Pressure: psia					
	Base Reference Density: lb/ft3					
Process Connection:		1/2-inch CL300 ASME B16.5 F316/F316L Weld neck flange Raised face				
Process Connection Pressure Rating:		48.125	bar-g			
@ Temperature:		50.000	C			

Flow Rate kg/hr	**Mass Flow Accuracy +/- % of Rate**	**Pressure Drop* bar**	**Velocity* m/sec**	**Re**
247.800	0.100	0.479	4.725	105681.106
226.400	0.100	0.403	4.317	96554.489
205.000	0.100	0.333	3.909	87427.872
183.600	0.100	0.270	3.501	78301.255
162.200	0.100	0.213	3.093	69174.638
146.400	0.100	0.176	2.792	62436.295
119.400	0.100	0.119	2.277	50921.404
98.000	0.100	0.082	1.869	41794.788
76.600	0.100	0.052	1.461	32668.171
55.200	0.100	0.028	1.053	23541.554
33.800	0.100	0.011	0.645	14414.937

*All pressure drop and velocity results are based on the process conditions (except flow rate) that are entered in the Operating column.

Notes:

Prepared by:		**Project ID:**	001-20170504-000009
Instrument Toolkit	Version: 3.0 (Build201C)	**Application:**	Economizer Liquid 60C

Figure B.6: Economizer liquid line at 60°C condensing

Micro Motion Calculation Summary

Date:		05/04/17				
Company:		Drew Schmidt				
Project Name:		Oklahoma State University				
Service:		R134A				
Sensor Model #:		F200S418C2BMEZZZZ				
Sensor Tag(s):						
Transmitter Model #:						
Transmitter Tag(s):						
Wetted Material:		316L stainless steel				
Fluid:		R134A				
Fluid State:		Gas				
Mass Flow Accuracy at Operating. Flow (+/- % of Rate):		0.50000				
Density Accuracy at all Rates (+/-):						
Pressure Drop at Operating Flow:		0.30595	bar			
Sensor Minimum Pressure at operating conditions:			bar-g			
Velocity at Operating Flow:		61.00855	m/sec			
		Min	**Operating***	**Max**	**Design**	**Units**
Flow Rate:		937.100	4061.000	6872.000		kg/hr
Pressure:		3.500	3.500	3.500		bar-g
Process Fluid Temperature:		15.000	15.000	15.000		C
Ambient Temperature:		70.000	70.000	70.000		F
Density:		16.300	16.300	16.300		kg/m3
Viscosity:		0.012	0.012	0.012		cP
Gas only	**Base Reference Temperature:** F	60.0			Density:	
	Base Reference Pressure: psia	14.696				
	Base Reference Density: lb/ft3	0.22801				
Process Connection:		2-inch CL150 ASME B16.5 F316/F316L Weld neck flange Raised face				
Process Connection Pressure Rating:		18.961	bar-g			
@ Temperature:		15.000	C			

Flow Rate kg/hr	**Mass Flow Accuracy +/- % of Rate**	**Pressure Drop*** bar	**Velocity*** m/sec	**Re**
6872.000	0.500	0.869	103.238	3932301.243
6278.510	0.500	0.726	94.322	3592693.928
5685.020	0.500	0.596	85.406	3253086.614
5091.530	0.500	0.479	76.490	2913479.300
4498.040	0.500	0.375	67.574	2573871.985
4061.000	0.500	0.306	61.009	2323788.613
3311.060	0.500	0.204	49.742	1894657.356
2717.570	0.500	0.138	40.826	1555050.042
2124.080	0.500	0.086	31.910	1215442.728
1530.590	0.500	0.046	22.994	875835.413
937.100	0.500	0.018	14.078	536228.099

*All pressure drop and velocity results are based on the process conditions (except flow rate) that are entered in the Operating column.

Notes:

Prepared by:		**Project ID:**	001-20170504-000009
Instrument Toolkit	Version: 3.0 (Build201C)	**Application:**	Sunction Side

Figure B.7: Suction line

APPENDIX C

Emerson Valve Sizing Charts

Nominal Capacities in Tons (10% - 100%)

Valve Type	R-407C	R-22	R-134a	R-404A	R-410A	R-23	R-124	R-744
EX4	.6 – 5	.6 – 4.7	.3 – 3.6	.3 – 3.3	.6 – 5.5	.6 – 5.1	.3 – 2.6	.9 – 9.5
EX5	1.4 – 15.1	1.4 – 14.2	1.1 – 11.1	1.1 – 10	1.7 – 16.5	1.4 – 15.4	.9 – 8	2.8 – 29
EX6	4.3 – 35.8	4.3 – 34.1	2.8 – 26.4	2.8 – 23.9	4.3 – 39.8	3.7 – 37	2 – 19.1	6.8 – 69.4
EX7	10 – 98.7	10 – 93.8	7.1 – 72.5	7.1 – 65.4	11.4 – 109.5	–	–	19.9 – 190.5
EX8	28.4 – 263	25.6 – 250.2	19.9 – 193.4	17.1 – 174.3	28.4 – 292	–	–	51.2 – 508.7

Note 1: EX Bi-flow versions are not released for use with R-124 and R-23 refrigerants.
Note 2: EX Bi-flow versions have identical capacity in both flow direction.

Refrigerant	Evaporating Temperature	Condensing Temperature	Subcooling
R-22, R-134a, R-404A, R-410A	+40 °F	+100°F	2°F
R-407C	+40°F dew point	+100°F bubble	2°F
R-124	+68°F	+176°F	2°F
R-23	-76°F	-13°F	2°F
R-744	-40°F	14°F	2°F

The nominal capacity is based on the following conditions:

APPENDIX D

Heat Exchanger Sizing Results

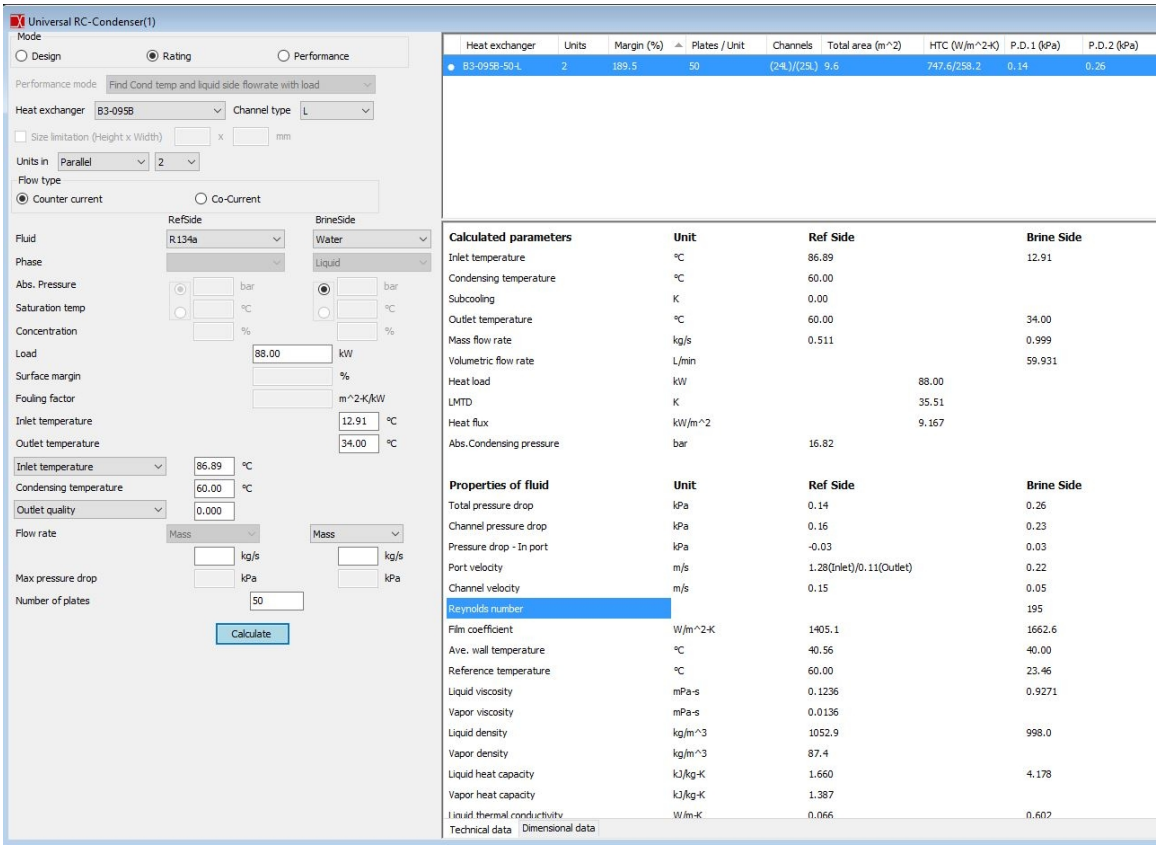

Figure D.1: Inputs and results from the Danfoss Hexact software for determining condenser model and size.

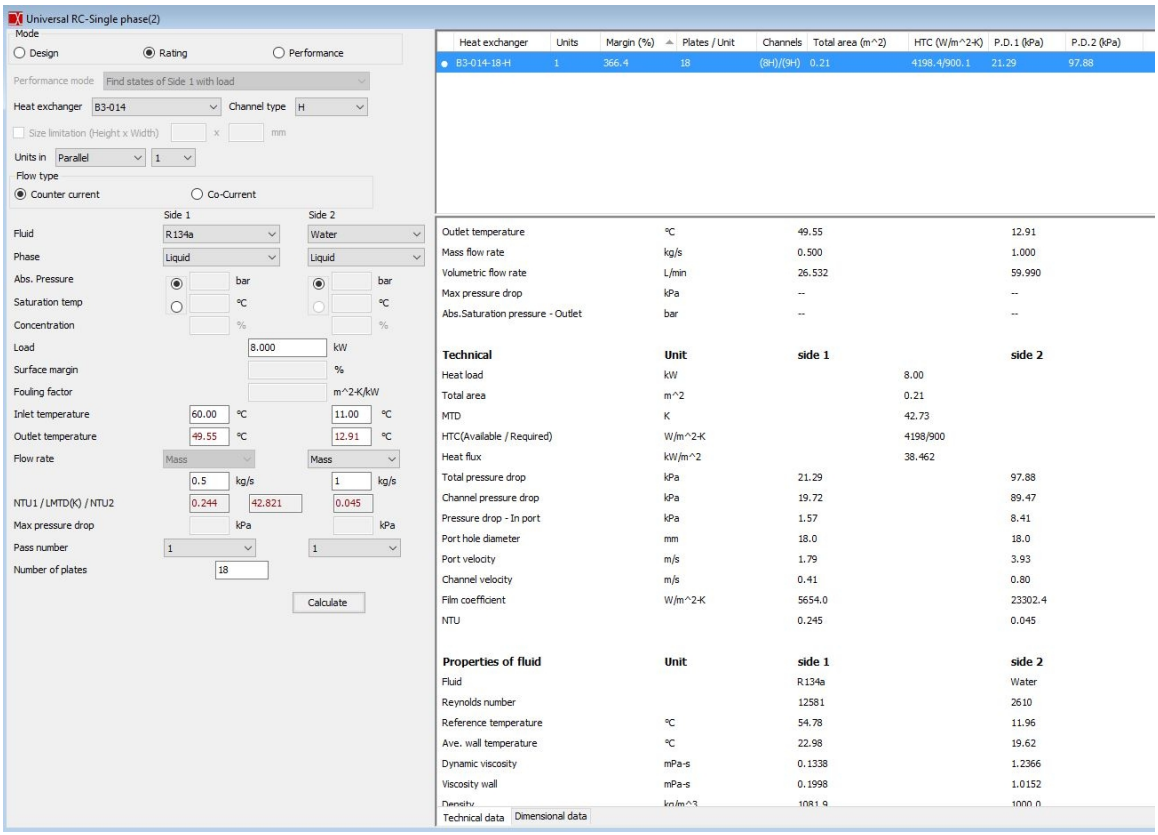

Figure D.2: Inputs and results from the Danfoss Hexact software for determining subcooler model and size.

APPENDIX E

EES economization code

```
Procedure economization(R$,T_evap,T_sup,T_cond,T_sub,P_cond,
    T_inj,ETA_comp,n,V_%Econ,V_%Reg:T[1..10],P[1..10],h
    [1..10],s[1..10],rho[1..10])
"Procedure to model a vapor compression cycle with
    economization"

      "Compressor 1"

         T[1]= T_evap + T_sup
         P[1]=pressure(R$,T=T_evap,x=1)
         h[1]=enthalpy(R$,T=T[1],P=P[1])
         s[1]=entropy(R$,T=T[1],P=P[1])
         rho[1]=density(R$,T=T[1],P=P[1])

         P[2]= sqrt(P[1]*P_cond)
         h_s[2]=enthalpy(R$,P=P[2],s=s[1])
         h[2]=(h_s[2]-(h[1]-ETA_comp*h[1]))/ETA_comp
         T[2]=temperature(R$,P=P[2],h=h[2])
         s[2]=entropy(R$,P=P[2],h=h[2])
         rho[2]=density(R$,P=P[2],h=h[2])

         "Injection Conditions"

         T_EconSat = temperature(R$,P=P[2],x=1)      "
            saturation temperature at the economizing pressure
            "

         "if statement to set the injection point as a vapor"
         If T_inj > T_EconSat Then
         T[9] = T_inj
         P[9]=P[2]
         h[9]=enthalpy(R$,T=T[9],P=P[9])
         s[9]=entropy(R$,T=T[9],P=P[9])
         rho[9]=density(R$,T=T[9],P=P[9])
         Else
         P[9]=P[2]
         h[9]=enthalpy(R$,P=P[2],x=1)
```

```
        T[9]=temperature(R$,P=P[9],h=h[9])
        s[9]=entropy(R$,P=P[9],h=h[9])
        rho[9]=density(R$,P=P[9],h=h[9])
        Endif

        "Compressor 2"

        P[3]=P[2]
        h[3]=V_%Econ*h[9]+V_%Reg*h[2]
        T[3]=temperature(R$,P=P[3],h=h[3])
        s[3]=entropy(R$,P=P[3],h=h[3])
        rho[3]=density(R$,P=P[3],h=h[3])

        P[4]= P_cond
        h_s[4]=enthalpy(R$,P=P[4],s=s[3])
        h[4]=(h_s[4]-(h[3]-ETA_comp*h[3]))/ETA_comp
        T[4]=temperature(R$,P=P[4],h=h[4])
        s[4]=entropy(R$,T=T[4],P=P[4])
        rho[4]=density(R$,T=T[4],P=P[4])

        "Condenser"

        T[5]=T_cond-T_sub
        P[5]=P[4]
        h[5]=enthalpy(R$,T=T[5],P=P[5])
        s[5]=entropy(R$,T=T[5],P=P[5])
        rho[5]=density(R$,T=T[5],P=P[5])

        "Expansion Valve for Economization"

        h[8]=h[5]
        P[8]=P[2]
        T[8]=temperature(R$,P=P[8],h=h[8])
        s[8]=entropy(R$,P=P[8],h=h[8])
        rho[8]=density(R$,P=P[8],h=h[8])

        "Subcooled from Economization"

    P[6]=P[1]
        h[6]= h[5]
        T[6]=temperature(R$,P=P[6],h=h[6])
        s[6]=entropy(R$,P=P[6],h=h[6])
        rho[6]=density(R$,P=P[6],h=h[6])

{       P[6]=P[5]
```

```
        h[6]=  ((V_%Reg*h[5]+V_%Econ*h[8])-V_%Econ*h[9])/V_%
            Reg
        T[6]=temperature(R$,P=P[6],h=h[6])
        s[6]=entropy(R$,P=P[6],h=h[6])
        rho[6]=density(R$,P=P[6],h=h[6])}

        "Expansion Valve"

        h[7]=h[4]
        P[7]=P[2]
        T[7]=temperature(R$,P=P[7],h=h[7])
        s[7]=entropy(R$,P=P[7],h=h[7])
        rho[7]=density(R$,P=P[7],h=h[7])

        "bypass valve"
        P[10] = P[1]
        h[10] = h[4]
    T[10]=temperature(R$,P=P[10],h=h[10])
        s[10]=entropy(R$,P=P[10],h=h[10])
        rho[10]=density(R$,P=P[10],h=h[10])
End

"Inputs"

R$='R134a'
   "type of refrigerant"
T_evap = 5 [C]                                                    "
   evaporation temperature"
T_sup = 10[C]                                                     "
   superheat temperature"
T_cond = 55 [C]                                                  "
   condensing temperature"
P_cond = pressure(R$,T=T_cond,x=0)          "pressure at
   condensing temp"
T_sub = 10[C]                                                     "
   subcooling temperature"
ETA_comp = 0.7                                                   "
   assumed compressor effeciency"
ETA_vol = 0.9                                                     "
   assumed volumetric effeciency"


n=3550 [1/min]                                                   "speed
    of compressor"
```

```
V_%Econ = .15                                    "percent of
    total volume used for economizing"
V_%Reg= 1-V_%Econ                                "percent of total
    volume through regular cycle"

V_tot = 2200 [cm^3]                              "total
    volume of compressor"
V_econ = V_%Econ*V_tot                           "volume used for
    economizing"
V_reg = V_%Reg*V_tot                             "volume used for
    regular cycle"

V_dot_tot = V_tot*n*convert(cm^3/min,m^3/hr)     "total
    volumetric flowrate"
V_dot_reg = V_reg*n*convert(cm^3/min,m^3/hr)     "regular
    volumetric flowrate"

m_dot_tot = (V_dot_tot*rho[1]*ETA_vol)/V_%Reg    "
    massflow through condenser"
m_dot_suc = V_dot_tot*rho[1]*ETA_vol{*V_%Reg}
m_dot_suc*h[1] = m_dot_cond_left*h[6] + m_dot_bypass_left*h
    [10]

{m_dot_bypass_econ + m_dot_cond_econ = V_%Econ * m_dot_tot}
m_dot_bypass_left + m_dot_cond_left = V_%Reg * m_dot_tot
m_dot_tot = m_dot_bypass_econ + m_dot_bypass_left +
    m_dot_cond_econ + m_dot_cond_left

m_dot_9*h[9] = m_dot_cond_econ*h[8] + m_dot_bypass_econ*h[7]
m_dot_tot*h[3] = m_dot_9*h[9] + m_dot_suc*h[2]


"injection conditions"
T_inj = 35 [C]
                                                 "
    injection temperature"

"Cooling Capacity"
Q_dot_cool = m_dot_suc*(h[1]-h[6])*convert(kJ/h,tons)
Q_dot_cool_kW = m_dot_suc*(h[1]-h[6])*convert(kJ/h,kW)
"Compressor Work"
W_dot_comp = (m_dot_suc*(h[2]-h[1]) + m_dot_tot*(h[4]-h[3]))*
    convert(kJ/h,kJ/s)

"Heat Rejection"
```

```
Q_dot_hr=(m_dot_cond_left+m_dot_cond_econ)*(h[4]-h[5])*
    convert(kJ/h,kJ/s)

"miscellaneous"
mu=viscosity(R134a,T=T[4],P=P[4])

reference_density=density(R134a,T=15.55,P=1)

P_sat=p_sat(R134a,T=T[4])

sdasdfasdf = pressure(R134a, T=T[5], x=1)

test_Z=compressibilityfactor(R134a,T=T[4],P=P[4])
test_cp=cp(R134a,T=T[4],P=P[4])
test_cv=cv(R134a,T=T[4],P=P[4])
test_ratio = test_cp/test_cv
test_mu=viscosity(R134a,T=T[4],P=P[4])*convert(kg/m-s,cp)

Call economization (R$,T_evap,T_sup,T_cond,T_sub,P_cond,T_inj
    ,ETA_comp,n,V_%Econ,V_%Reg:T[1..10],P[1..10],h[1..10],s
    [1..10],rho[1..10])
```

APPENDIX F

EES regular cycle code

```
"Compressor"
        T[1]= T_evap + T_sup
        P[1]=pressure(R$,T=T_evap,x=1)
        h[1]=enthalpy(R$,T=T[1],P=P[1])
        s[1]=entropy(R$,T=T[1],P=P[1])
        rho[1]=density(R$,T=T[1],P=P[1])

        P[2]=pressure(R$,T=T_cond,x=0)
        h_s[2]=enthalpy(R$,P=P[2],s=s[1])
        h[2]=(h_s[2]-(h[1]-ETA_comp*h[1]))/ETA_comp
        T[2]=temperature(R$,P=P[2],h=h[2])
        s[2]=entropy(R$,T=T[2],P=P[2])
        rho[2]=density(R$,T=T[2],P=P[2])

        "Extra output to have six outputs"
        P[3]=P[2]
        h[3]=h[2]
        T[3]=T[2]
        s[3]=s[2]
        rho[3]=rho[2]

        "Bypass Valve"
        h[4]=h[2]
        P[4]=P[1]
        T[4]=temperature(R$,P=P[4],h=h[4])
        s[4]=entropy(R$,P=P[4],h=h[4])
        rho[4]=density(R$,P=P[4],h=h[4])

        "Condenser"
        T[5]=T_cond-T_sub
        P[5]=pressure(R$,T=T_cond,x=0)
        h[5]=enthalpy(R$,T=T[5],P=P[5])
        s[5]=entropy(R$,T=T[5],P=P[5])
        rho[5]=density(R$,T=T[5],P=P[5])

        "Liquid expansion valve"
        h[6]=h[5]
```

```
        P[6]=P[1]
        T[6]=temperature(R$,P=P[6],h=h[6])
        s[6]=entropy(R$,P=P[6],h=h[6])
        rho[6]=density(R$,P=P[6],h=h[6])

"System"

$ifnot Parametric then
R$='R134a'                          {refrigerant being used in
   system}
$endif
T_sup= 10[C]                        {superheat}
T_sub= 10[C]                        {subcooling}
ETA_comp=0.7                      {assumed compressor effeciency}
ETA_vol=0.9                         {assumed volumetric effeciency}

 "Variables"
T_evap= 5[C]                         {evaporating temperature}
n=3550 [rev/min]                        {compressor speed}
$ifnot Parametric then
V_displ=2200[cm^3/rev]                {volumetric displacement}
T_cond = 60[C]                         {condensing temperature}
$endif

"Volume flow rate"
V_dot=n*V_displ*convert(cm^3/min,m^3/h)

"mass flow rate"
{m_dot = abs(Q_dot_cc/(h[6]-h[1]))*convert(kg/s,kg/h)}
m_dot_tot=V_dot*rho[1]*ETA_vol

"heat rejection"
Q_dot_hr = abs(m_dot_c*(h[5]-h[3])*convert(kJ/h,kW))

"Compressor Power"
W_dot_cp = m_dot_tot*(h[2]-h[1])*convert(kJ/h,kW)

"Energy Balance"
m_dot_bypass*h[4] + m_dot_c*h[6] = m_dot_tot*h[1]

m_dot_bypass = m_dot_tot-m_dot_c

"Cooling Capacity"
Q_dot_cool = m_dot_tot*(h[1]-h[6])*convert('kJ/hr','tons')
```

```
"mass flow balance"

m_dot_tot = rho[2]*V_dot_discharge

m_dot_bypass = rho[2]*V_dot_bypass

mu=viscosity(R134a,T=T[1],P=P[1])

reference_density=density(Air_ha,T=T[2],P=P[2])
SG= rho[2]/reference_density

test_Z=compressibilityfactor(R134a,T=T[2],P=P[2])
test_cp=cp(R134a,T=T[2],P=P[2])
test_cv=cv(R134a,T=T[2],P=P[2])
test_ratio = test_cp/test_cv
test_mu=viscosity(R134a,T=T[2],P=P[2])*convert(kg/m-s,cp)



"Efficiency"
ETA_is=(h_s[2]-h[1])/(h[2]-h[1])

"Velocities"

{$ifnot parametric}
D_inside_small = 1.025 [in]
D_inside_med = 1.265 [in]
D_inside_large = 2.465 [in]
{$endif}
A_cross_nom = ((pi*2.945^2)/4)*convert(in^2,m^2)
A_cross_small = ((pi*D_inside_small^2)/4)*convert(in^2,m^2)
A_cross_med = ((pi*D_inside_med^2)/4)*convert(in^2,m^2)
A_cross_large = ((pi*D_inside_large^2)/4)*convert(in^2,m^2)

m_dot_medlarge = (A_cross_med/(A_cross_large+A_cross_med))*
    m_dot_bypass "mass flow in medium tube"
m_dot_largemed = m_dot_bypass - m_dot_medlarge "mass flow in
    large tube"

m_dot_smallmed = (A_cross_small/(A_cross_med+A_cross_small))*
    m_dot_bypass "mass flow in small tube"
m_dot_medsmall= m_dot_bypass - m_dot_smallmed "mass flow in
    med tube"

m_dot_smalllarge = (A_cross_small/(A_cross_large+
```

```
    A_cross_small))*m_dot_bypass "mass flow in small tube"
m_dot_largesmall= m_dot_bypass - m_dot_smalllarge "mass flow
    in med tube"

m_dot_three_s = (A_cross_small/(A_cross_large+A_cross_med+
    A_cross_small))*m_dot_bypass
m_dot_three_m = (A_cross_med/(A_cross_large+A_cross_med+
    A_cross_small))*m_dot_bypass
m_dot_three_L = (A_cross_large/(A_cross_large+A_cross_med+
    A_cross_small))*m_dot_bypass


 "discharge"
Velocity_small_D = (m_dot_bypass/(rho[2]*A_cross_small))*
    convert(m/h, ft/min)
Velocity_med_D = (m_dot_bypass/(rho[2]*A_cross_med))*convert(
    m/h, ft/min)
Velocity_large_D = (m_dot_bypass/(rho[2]*A_cross_large))*
    convert(m/h, ft/min)

velocity_largemed = (m_dot_largemed/(rho[2]*A_cross_large))*
    convert(m/h, ft/min)
velocity_medlarge = (m_dot_medlarge/(rho[2]*A_cross_med))*
    convert(m/h, ft/min)

velocity_smallmed = (m_dot_smallmed/(rho[2]*A_cross_small))*
    convert(m/h, ft/min)
velocity_medsmall = (m_dot_medsmall/(rho[2]*A_cross_med))*
    convert(m/h, ft/min)

velocity_smalllarge = (m_dot_smalllarge/(rho[2]*A_cross_small
    ))*convert(m/h, ft/min)
velocity_largesmall = (m_dot_largesmall/(rho[2]*A_cross_large
    ))*convert(m/h, ft/min)

velocity_three = (m_dot_three_s/(rho[2]*A_cross_small))*
    convert(m/h, ft/min)



"suction"
Velocity_small_S = (m_dot_tot/(rho[1]*A_cross_small))*convert
    (m/h, ft/min)
Velocity_med_S = (m_dot_tot/(rho[1]*A_cross_med))*convert(m/h
    , ft/min)
```

```
Velocity_large_S = (m_dot_tot/(rho[1]*A_cross_large))*convert
    (m/h,ft/min)

{velocity_largemed = (m_dot_largemed/(rho[1]*A_cross_large))*
    convert(m/h,ft/min)
velocity_medlarge = (m_dot_medlarge/(rho[1]*A_cross_med))*
    convert(m/h,ft/min)

velocity_smallmed = (m_dot_smallmed/(rho[1]*A_cross_small))*
    convert(m/h,ft/min)
velocity_medsmall = (m_dot_medsmall/(rho[1]*A_cross_med))*
    convert(m/h,ft/min)

velocity_smalllarge = (m_dot_smalllarge/(rho[1]*A_cross_small
    ))*convert(m/h,ft/min)
velocity_largesmall = (m_dot_largesmall/(rho[1]*A_cross_large
    ))*convert(m/h,ft/min)

velocity_three = (m_dot_three/(rho[1]*A_cross_small))*convert
    (m/h,ft/min)}

"liquid"
Velocity_small_L = (m_dot_c/(rho[5]*A_cross_small))*convert(m
    /h,ft/min)
Velocity_med_L = (m_dot_c/(rho[5]*A_cross_med))*convert(m/h,
    ft/min)
Velocity_large_L = (m_dot_c/(rho[5]*A_cross_large))*convert(m
    /h,ft/min)

{velocity_largemed = (m_dot_largemed/(rho[5]*A_cross_large))*
    convert(m/h,ft/min)
velocity_medlarge = (m_dot_medlarge/(rho[5]*A_cross_med))*
    convert(m/h,ft/min)

velocity_smallmed = (m_dot_smallmed/(rho[5]*A_cross_small))*
    convert(m/h,ft/min)
velocity_medsmall = (m_dot_medsmall/(rho[5]*A_cross_med))*
    convert(m/h,ft/min)

velocity_smalllarge = (m_dot_smalllarge/(rho[5]*A_cross_small
    ))*convert(m/h,ft/min)
velocity_largesmall = (m_dot_largesmall/(rho[5]*A_cross_large
    ))*convert(m/h,ft/min)

velocity_three = (m_dot_three/(rho[5]*A_cross_small))*convert
```

(m/h , ft /min) }

APPENDIX G

EES If statement code

```
Procedure cycle(type$,type2$,R$,CP,CT,T_sup,T_sub,ETA_comp,
   T_evap,T_cond,P_gc,P_anchor,T_anchor:T[1..6],P[1..6],h
   [1..6],h_s[2],s[1..6],rho[1..6])
{Procedure to calculate the state points of a transcritical
   or subcritical refrigeration system}

$UnitSystem SI C bar kJ
{Sets the unit system for this procedure}

 If (type$='transcritical') or (T_cond>CT) Then
 {if statement to calculate the state points based on whether
    it is transcritical or subcritical}

        T_gc = T_cond                {sets the gas cooler
           exit temp equal to the condensing temperature}

        If (type2$='throttled') Then
        {if statement to determine a throttled transcritical
           cycle or a normal transcritical cycle}

            "Compressor"
            T[1]= T_evap + T_sup
            P[1]=pressure(R$,T=T_evap,x=1)
            h[1]=enthalpy(R$,T=T[1],P=P[1])
            s[1]=entropy(R$,T=T[1],P=P[1])
            rho[1]=density(R$,T=T[1],P=P[1])

            P[2]=P_gc
            h_s[2]=enthalpy(R$,P=P[2],s=s[1])
            h[2]=(h_s[2]-(h[1]-ETA_comp*h[1]))/ETA_comp
            T[2]=temperature(R$,P=P[2],h=h[2])
            s[2]=entropy(R$,T=T[2],P=P[2])
            rho[2]=density(R$,T=T[2],P=P[2])

            "Throttling"
            P[3]=P_anchor
            h[3]=h[2]
```

```
        T[3]=temperature(R$,P=P[3],h=h[3])
        s[3]=entropy(R$,P=P[3],h=h[3])
        rho[3]=density(R$,P=P[3],h=h[3])

        "Bypass Valve"
        h[4]=h[2]
        P[4]=P[1]
        T[4]=temperature(R$,P=P[4],h=h[4])
        s[4]=entropy(R$,P=P[4],h=h[4])
        rho[4]=density(R$,P=P[4],h=h[4])

        "Condenser"
        T[5]=T_anchor-T_sub
        P[5]=pressure(R$,T=T_anchor,x=0)
        h[5]=enthalpy(R$,T=T[5],P=P[5])
        s[5]=entropy(R$,T=T[5],P=P[5])
        rho[5]=density(R$,T=T[5],P=P[5])

        "Liquid expansion valve"
        h[6]=h[5]
        P[6]=P[1]
        T[6]=temperature(R$,P=P[6],h=h[6])
        s[6]=entropy(R$,P=P[6],h=h[6])
        rho[6]=density(R$,P=P[6],h=h[6])

Else {normal transcritical cycle}

        "Compressor"
        T[1]= T_evap + T_sup
        P[1]=pressure(R$,T=T_evap,x=1)
        h[1]=enthalpy(R$,T=T[1],P=P[1])
        s[1]=entropy(R$,T=T[1],P=P[1])
        rho[1]=density(R$,T=T[1],P=P[1])

        P[2]=P_gc
        h_s[2]=enthalpy(R$,P=P[2],s=s[1])
        h[2]=(h_s[2]-(h[1]-ETA_comp*h[1]))/ETA_comp
        T[2]=temperature(R$,P=P[2],h=h[2])
        s[2]=entropy(R$,T=T[2],P=P[2])
        rho[2]=density(R$,T=T[2],P=P[2])

        "Extra output to have six outputs"
        P[3]=P[2]
        h[3]=h[2]
        T[3]=T[2]
```

```
        s[3]=s[2]
        rho[3]=rho[2]

        "Bypass Valve"
        h[4]=h[2]
        P[4]=P[1]
        T[4]=temperature(R$,P=P[4],h=h[4])
        s[4]=entropy(R$,P=P[4],h=h[4])
        rho[4]=density(R$,P=P[4],h=h[4])

        "Gas Cooler"
        T[5]=T_gc
        P[5]=P[2]
        h[5]=enthalpy(R$,T=T[5],P=P[5])
        s[5]=entropy(R$,T=T[5],P=P[5])
        rho[5]=density(R$,T=T[5],P=P[5])

        "Liquid expansion valve"
        h[6]=h[5]
        P[6]=P[1]
        T[6]=temperature(R$,P=P[6],h=h[6])
        s[6]=entropy(R$,P=P[6],h=h[6])
        rho[6]=density(R$,P=P[6],h=h[6])

    Endif

Else {subcritical cycle}


    "Compressor"
    T[1]= T_evap + T_sup
    P[1]=pressure(R$,T=T_evap,x=1)
    h[1]=enthalpy(R$,T=T[1],P=P[1])
    s[1]=entropy(R$,T=T[1],P=P[1])
    rho[1]=density(R$,T=T[1],P=P[1])

    P[2]=pressure(R$,T=T_cond,x=0)
    h_s[2]=enthalpy(R$,P=P[2],s=s[1])
    h[2]=(h_s[2]-(h[1]-ETA_comp*h[1]))/ETA_comp
    T[2]=temperature(R$,P=P[2],h=h[2])
    s[2]=entropy(R$,T=T[2],P=P[2])
    rho[2]=density(R$,T=T[2],P=P[2])

    "Extra output to have six outputs"
    P[3]=P[2]
```

```
h[3]=h[2]
T[3]=T[2]
s[3]=s[2]
rho[3]=rho[2]

"Bypass Valve"
h[4]=h[2]
P[4]=P[1]
T[4]=temperature(R$,P=P[4],h=h[4])
s[4]=entropy(R$,P=P[4],h=h[4])
rho[4]=density(R$,P=P[4],h=h[4])

"Condenser"
T[5]=T_cond-T_sub
P[5]=pressure(R$,T=T_cond,x=0)
h[5]=enthalpy(R$,T=T[5],P=P[5])
s[5]=entropy(R$,T=T[5],P=P[5])
rho[5]=density(R$,T=T[5],P=P[5])

"Liquid expansion valve"
h[6]=h[5]
P[6]=P[1]
T[6]=temperature(R$,P=P[6],h=h[6])
s[6]=entropy(R$,P=P[6],h=h[6])
rho[6]=density(R$,P=P[6],h=h[6])
```

```
 Endif

End

type$=if$(P_gc,CP,'subcritical','critical','transcritical')
          {if statement to determine the type of cycle}
$ifnot ParametricTable='CO2, Volume displacement, Condensing
   Temp.'
type2$='throttled'
                                                          {
   input 'throttled' or 'normal' to determine type of
```

```
   transcritical cycle}
$endif



"System"
$ifnot Parametric{Table='R134a, Volume displacement,
   Condensing Temp.' }
R$='R744'                          {refrigerant being used in
   system}
$endif
CP=p_crit(R$)                     {critical pressure of the
   refrigerant}
CT=t_crit(R$)                      {critical temperature of the
   refrigerant}
T_sup= 10[C]                      {superheat}
T_sub= 10[C]                      {subcooling}
ETA_comp=0.7                    {assumed compressor effeciency}
ETA_vol=0.9                       {assumed volumetric effeciency}

 "Variables"
T_evap= 5[C]                         {evaporating temperature}
Q_dot_cc= 22.3 [kW]             {given compressor cooling
   capacity}
n=3550 [rev/min]                        {compressor speed}
$ifnot Parametric
V_displ=54.5[cm^3/rev]              {volumetric displacement}
T_cond = 40[C]                       {condensing temperature}
$endif

"Transcritical Specific Variables"
$ifnot Parametric
P_gc = 100 [bar]                                {gas cooler pressure
   }
$endif
P_anchor = pressure(R$,T=T_anchor,x=0)
   {intermediate pressure at given condensing temp}
T_anchor = 10 [C]
                                                        {
   intermediate condensing temperatue}


Call cycle(type$,type2$,R$,CP,CT,T_sup,T_sub,ETA_comp,T_evap,
   T_cond,P_gc,P_anchor,T_anchor:T[1..6],P[1..6],h[1..6],h_s
   [2],s[1..6],rho[1..6])
```

```
{calls the procedure cycle to output the statepoints with the
    given inputs}

"Volume flow rate"
V_dot=n*V_displ*convert(cm^3/min,m^3/h)

"mass flow rate"
{m_dot = abs(Q_dot_cc/(h[6]-h[1]))*convert(kg/s,kg/h)}
m_dot_tot=V_dot*rho[1]*ETA_vol

"heat rejection"
Q_dot_hr = abs(m_dot_c*(h[5]-h[3])*convert(kJ/h,kW))

"Compressor Power"
W_dot_cp = m_dot_tot*(h[2]-h[1])*convert(kJ/h,kW)

"Energy Balance"
m_dot_bypass*h[4] + m_dot_c*h[6] = m_dot_tot*h[1]

m_dot_bypass = m_dot_tot-m_dot_c

"Cooling Capacity"
Q_dot_cool = m_dot_tot*(h[1]-h[6])*convert('kJ/hr','tons')

"Discharge and Suction Volumetric Flow"
V_dot_discharge = m_dot_tot/rho[2]
V_dot_suction = m_dot_tot/rho[1]

{"Finding heat rejection for just the condenser"
h[7] = enthalpy(R$, T=T_cond, x=0)
Q_dot_hr_cond = abs(m_dot_c*(h[7]-h[3])*convert(kJ/h, kW))}

"Efficiency"
ETA_is=(h_s[2]-h[1])/(h[2]-h[1])
```

VITA

Drew D. Schmidt

Candidate for the Degree of

Master of Science

Thesis: DEVELOPMENT OF A LIGHT-COMMERCIAL COMPRESSOR LOAD STAND TO MEASURE COMPRESSOR PERFORMANCE USING LOW-GWP REFRIGERANTS

Major Field: Mechanical Engineering

Biographical:

Education:

Completed the requirements for the Master of Science in Mechanical Engineering at Oklahoma State University, Stillwater, Oklahoma in December, 2018.

Completed the requirements for the Bachelor of Science in Mechanical Engineering at Oklahoma State University, Stillwater, Oklahoma in 2016.

Professional Affiliations:

ASHRAE Student Member